Defining the Relationship between the Bioactivation of Lapatinib by CYP3A and Lapatinib-Induced Hepatotoxicity

Michelle Diane Wahlin

A dissertation

submitted in partial fulfillment of the

requirements for the degree

Doctorate of Philosophy

University of Washington

2014

Reading Committee:

Dr. Thomas Baillie, Chair

Dr. Allan Rettie

Dr. Rheem Totah

Program Authorized to Offer Degree:

Medicinal Chemistry

University of Washington

Abstract

Defining the Relationship between the Bioactivation of Lapatinib by CYP3A

and Lapatinib-Induced Hepatotoxicity

Michelle Diane Wahlin

Chair of the Supervisory Committee:

Dr. Thomas Baillie

Dean, School of Pharmacy

Lapatinib was the first orally active dual tyrosine kinase inhibitor (TKI) of the epidermal growth factor receptor (EGFR, ErbB1) and human epidermal receptor 2 (HER2, ErbB2) to be approved by the US Food and Drug Administration (FDA). In 2008, the FDA issued a black-box warning for lapatinib idiosyncratic hepatotoxicity, which was observed in a small proportion of patients (<1%) in clinical trials and during post-market surveillance. In combination with other factors, metabolic activation has been suggested to play an important role in lapatinib hepatotoxicity. Lapatinib is metabolized by both cytochrome P450 3A4 and 3A5 to yield an *O*-debenzylated metabolite (LAP-OH), which can be further oxidized to a reactive quinoneimine that is captured by glutathione. The effect of pharmacogenetic polymorphisms of CYP3A5 on lapatinib metabolism in human liver microsomes was investigated and it was determined that a high-activity CYP3A5 genotype resulted in increased formation of the reactive metabolite glutathione conjugate *in vitro*. This suggests that genetic polymorphisms of CYP3A5 could affect the pharmacokinetics of lapatinib and impact the incidence of hepatotoxicity *in*

vivo. HepaRG cells were established as a cellular model to study lapatinib hepatotoxicity. Pretreatment of cells with dexamethasone and rifampicin (CYP3A4 inducers) markedly enhanced the cytotoxicity of lapatinib and resulted in an increase in formation of LAP-OH, as well as glutathione and cysteine adducts of the reactive metabolite. A lapatinib analog deuterated at the site of oxidative debenzylation produced less debenzylated metabolite and glutathione conjugates than lapatinib itself. This decrease also corresponded to reduced lapatinib cytotoxicity in HepaRG cells. Finally, a CYP3A4 mutant with a single point mutation at position 108 (F108L) shifted the metabolic profile of lapatinib to one more similar to that of CYP3A5, thus demonstrating the importance of this CYP3A5 amino acid for the orientation of lapatinib in the enzyme active site. Taken together, these studies highlight the importance of metabolic activation of lapatinib by CYP3A4 and CYP3A5 to the hepatotoxicity of the drug. The use of analogs of lapatinib whose metabolism to LAP-OH is blocked by structural modification, or genotyping patients for expression levels of CYP3A5, may lead to a decrease in incidences of idiosyncratic hepatotoxicity with lapatinib treatment and should be further explored.

Table of Contents

List of Figures

DEDICATION

This dissertation is dedicated to the memory of Sidney D Nelson.

Sid was patient, kind, brilliant, funny, and humble.

In the middle of chemistry demonstrations in his granddaughter's 4th grade classroom,

I overheard a classmate say to her, "You're **so** lucky he's your grandpa!"

I feel the same way, Sid. I'm so lucky you were my advisor.

Chapter 1: Introduction

1.1 The functional role of the liver and its susceptibility to drug toxicity

The liver is the largest visceral organ in the human body and consists of two lobes that are further divided by connective tissue into thousands of liver lobules: the basic functional units of the liver. The major cell type present in the liver is the hepatic parenchymal cells, or hepatocytes, which form a series of irregular plates arranged like the spokes of a wheel (Figure 1.1). Other cells include sinusoidal cells, which create a permeable barrier between hepatocytes and the blood transferred by the sinusoidal capillary network. While they block the entry of red blood cells, these fenestrated endothelial cells allow for rapid diffusion of small molecules such as hormones and xenobiotics, unlike in the brain where such diffusion is prohibited by tight junctions. In addition to these typical endothelial cells, the sinusoidal lining also includes a large number of Kupffer cells, which are macrophages found specifically in the liver that act as the liver's host defense by releasing inflammatory mediators such as free radicals, cytokines, eicosanoids, and lysosomal enzymes. They can also engulf pathogens, cell debris, and damaged blood cells. This response is beneficial for their role in host defense, but can be deleterious in certain cases of liver disease (Kolios, 2006; Roberts, 2007).

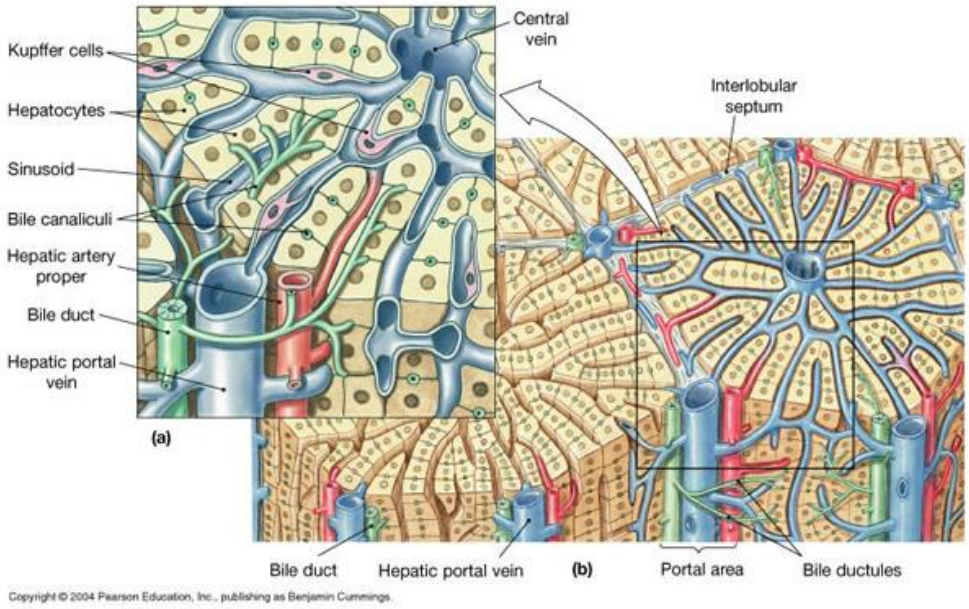

Figure 1.1 ***Basic histology of the liver,*** *showing (a) a single liver lobule and its cellular components and (b) a diagrammatic view of liver structure and relationships among lobules. (Figure from Pearson Education, Inc.; Silverthorn, 2004.)*

The liver is responsible for four primary physiological functions. The first is the synthesis and secretion of bile acids. The second is the synthesis of proteins such as albumin, transferrin, prothrombin, fibrinogen, and lipoproteins. The third is the maintenance of blood glucose levels by storage or synthesis of glucose in response to insulin and glucagon levels. And finally, the liver contains enzymes and transporters that are responsible for the metabolism of xenobiotics into hydrophilic metabolites to facilitate their excretion. This metabolism can be divided into three phases: oxidation (Phase I), conjugation of hydrophilic groups to the xenobiotic scaffold (Phase II), and uptake and excretion of the xenobiotic or metabolite (Phase III).

The susceptibility of the liver to toxicity is a result of being the first organ encountered by orally absorbed small molecules, it is exposed to a large volume of blood per unit time, and its biological function involves metabolism of xenobiotics by a multitude of enzymes, including Cytochromes P450

(P450s). Although the metabolic pathway typically facilitates excretion of the xenobiotics and prevents the accumulation of toxic, hydrophobic molecules, it can also lead to bioactivation of chemically stable xenobiotics into more reactive metabolites that impair cellular function.

1.2 Drug induced liver injury

Drug induced liver injury, or DILI, is impairment in liver function due to the use of a drug. It is the primary cause for the termination of a drug in clinical trials and withdrawal of a drug once it is on the market (Ballet, 1997; Temple and Himmel, 2002). Over half of the cases of acute liver failure in the US are drug-induced (Ostapowicz et al., 2002) and such failure in trials or during post-marketing can have drastic economic implications because of the enormous cost of drug discovery and development. Over 1000 drugs are associated with liver injury (Zimmerman, 1999) and half of the drugs listed in the Physician's Desk Reference (PDR) cause some degree of liver toxicity (Lewis, 2002).

DILI can be separated into two categories, primarily based on predictability. Predictable hepatotoxicity, or Type A reactions, occur after short exposure to the drug, are dose-dependent, and have a similar impact on all individuals. The mechanisms of these reactions are often well understood, and animal models have been developed to reproduce the human toxicity. Unpredictable hepatotoxicity, also called Type B reactions or idiosyncratic drug reactions (IDRs), occur rarely, do not exhibit time- or dose-dependency, and typically have poorly understood mechanisms (Uetrecht, 2008). Only about 10% of overall DILI cases are due to IDRs (Kaplowitz, 2005), but this is largely due to the fact that the primary cause of DILI, acetaminophen, exhibits predictable hepatotoxicity (Oztapowitz, 2002). Most drugs that result in hepatotoxicity are considered idiosyncratic (Kaplowitz, 2001).

Clinically, DILI can manifest itself in different ways. It can mimic various forms of naturally-occurring liver disease such as hemochromatosis or Wilson's disease (Navarro and Senior, 2006), can result in non-specific symptoms such as fatigue, and often occurs in patients with other confounding medical conditions. DILI is primarily assessed using non-invasive quantification of blood biomarkers such as alanine aminotransferase (ALT) and aspartate aminotransferase (AST). These, however, are indicators of liver injury rather than abnormal liver function (Antoine et al., 2008), and a liver biopsy must be performed to definitively diagnose DILI. No specific non-invasive diagnosis, treatment, or prevention of DILI exists.

1.3 Idiosyncratic hepatotoxicity: the current understanding

An idiosyncratic drug reaction (IDR), or Type B reaction, is a rare adverse response to a drug that is unrelated to the pharmacological activity of the drug (Uetrecht, 2008). Such reactions are unpredictable in terms of which patients will experience a response and when such a response will occur (Walgren, 2005). While most patients will not experience an IDR at any dose of the drug, susceptible individuals can be affected within the therapeutic dose range (Uetrecht, 2000). IDRs are particularly problematic because they are difficult to accurately predict for drugs in development and are often not detected until the drug has been used widely in a large patient population. This is due to their low frequency of occurrence (0.0001% to 0.00001%), the relatively small size of clinical trial populations, and a delayed onset of weeks to months following initial exposure to the drug (Uetrecht, 1999).

Historically, IDRs have been classified as either immune or metabolically mediated. Immune mediated toxicity is associated with clinical factors such as fever and rash, eosinophilia, the development of

autoantibodies, and a relapse of toxicity upon readministration of the drug (Zimmerman, 1976). A proposed mechanism of immune-mediated toxicity is the hapten hypothesis (Park et al., 1998; Uetrecht, 1999; Ju and Uetrecht, 2002), which suggests that small molecules are not immunogenic on their own, but rather require binding to proteins or other cellular macromolecules to produce an immune response. The resulting chemical species, called a hapten, is recognized as foreign and induces autoantibody production. The anesthetic halothane, for example, is oxidized by cytochrome P450s to trifluoroacetyl chloride, a reactive metabolite that binds to proteins and elicits an immune response (Njoku et al., 1997). While halothane is often used as a model drug for the hapten hypothesis, it is in fact a classic example that links reactive metabolite formation with the hapten hypothesis. Metabolically-mediated IDRs, or metabolic idiosyncracy, refers to injury in the absence of the characteristic clinical signs of immune-mediated IDRs (Zimmerman, 1999) and often has a long lag time between initiation of the drug and the onset of toxicity (Zimmerman, 1976). Isoniazid is an example of a drug that is associated with metabolic idiosyncracy. It is metabolized by *N*-acetyltransferase (NAT) and CYP2E1 into reactive intermediates and genetic variation leading to changes in these enzyme activities have been associated with a higher incidence of isoniazid hepatotoxicity (Huang et al., 2002; Vuilleumier et al., 2006). While these genetic variations appear to be risk factors for the IDR caused by isoniazid, there are no examples where a known variation is sufficient to completely explain the idiosyncratic nature of the liver toxicity (Uetrecht, 2008).

The danger hypothesis, first proposed in 1994, suggests that formation of reactive metabolites or the production of antibodies against drug-protein adducts are not sufficient, on their own, to elicit an immune response. A second signal, called the “danger signal,” is necessary (Matzinger, 1994; Uetrecht, 1999). The presentation of an antigen to the T cells by antigen presenting cells (APCs) is known as signal 1. When haptenized proteins are formed through the bioactivation of halothane,

signal 1 is generated. Signal 2 is the receptor binding of T cells to costimulatory receptors on APCs. These costimulatory receptors are induced by the danger signals, and in the absence of this induction, immune tolerance occurs instead of DILI (Uetrecht, 2008). This hypothesis is summarized in Figure 1.2. The origin of signal 2 is not clear, but may be the result of cell damage caused by the drug or a reactive metabolite. This cell damage can come in the form of enzyme inhibition, decreased thiol levels, or an existing infection (Park et al., 2000; Ganey and Roth, 2001). In patients who take halothane and anesthesiologists who are exposed to halothane, protein alkylation and autoantibodies are often detected but a very small percentage of the individuals actually develop DILI (Njoku et al., 2002). This can be explained by the absence of a danger signal, as well as other factors including inflammation and mitochondrial abnormalities.

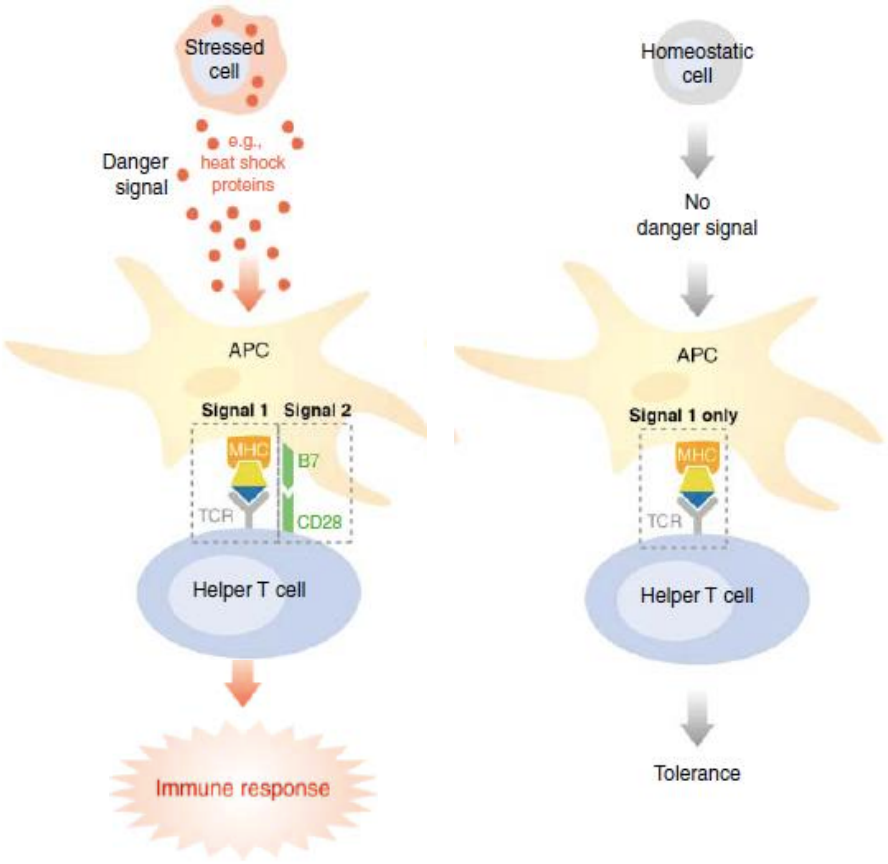

Figure 1.2 ***Danger hypothesis.*** *Two signals are required to elicit an immune response. Signal 1: a drug or its metabolite (hapten) covalently binds to proteins, which are recognized, processed, and displayed to T cells by*

antigen presenting cells (APCs). Signal 2 (the danger signal): initiated by cell stress factors that induce the expression of costimulatory receptors on the surface of APCs, such as B7. These costimulatory receptors bind to the helper T cells and initiate an immune response. (Figure from Uetrecht J, 2007.)

The metabolic and immune hypotheses for IDRs, even with the added factor of the danger signals, are generally recognized on their own to be insufficient explanations for the varied, infrequent, and complex manifestations of idiosyncratic DILIs. In the case of isoniazid, for example, known polymorphisms in the drug metabolizing enzymes are not rare enough to explain the idiosyncracy (Uetrecht, 2008). The multiple determinant hypotheses suggest that there are different steps or factors that contribute to the development of an IDR. These include chemical properties, exposure levels, environmental factors, and genetic factors (Li, 2002), as well as underlying disease states, nutrition, age, physical activity, co-medications, and the innate immune system (Boelsterli 2003b; Roth et al., 2003; Ulrich, 2007). The idiosyncratic nature of IDRs may be a function of the low probability that any of these adverse events occurs in a given individual at a given time, as illustrated in Figure 1.3.

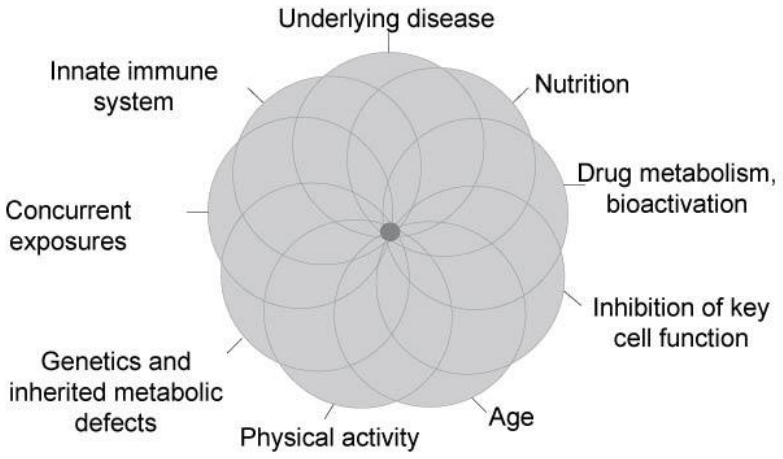

Ulrich RG. 2007.
Annu. Rev. Med. 58:17–34

Figure 1.3 ***Risk factors of idiosyncratic toxicity.*** *The low incidence of idiosyncratic drug reactions may be a function of the rare occurrence of multiple risk factors converging in a particular combination that results in drug toxicity. The infrequent occurrence of such a combination in the general patient population explains the typical safety of these drugs. (Figure from Ulrich RG, 2007.)*

The inflammagen hypothesis connects idiosyncratic hepatotoxicity with episodic bouts of inflammation in the liver. Disturbances in the gastrointestinal tract from infection, alcohol consumption, stress, and surgery can permit release of inflammagens such as lipopolysaccharide (LPS), a component of the cell walls of Gram-negative bacteria in the gut. The exposure to LPS initiates transcriptional changes in the Kupffer and other inflammatory cells, resulting in elevated expression of cytokines, proteases, and enzymes that promote formation of reactive oxygen species (ROS), (Spolarics, 1998; Beutler, 2000). These events are often mild and do not directly damage the liver, but concurrence of such an inflammation episode with the administration of a particular drug could lower the threshold of hepatotoxicity and result in DILI from an otherwise safe drug (Figure 1.4; Roth et al., 2003). This hypothesis has been validated in rat models, which demonstrate hepatotoxicity to known idiosyncratic hepatotoxicants such as trovafloxacin, diclofenac, chlorpromazine, and ranitidine only upon coadministration of the drug and LPS (Buchweitz et al., 2002; Luyendyk et al., 2003; Deng et al., 2006; Waring et al., 2006). It is noted that this mechanism likely does not explain most IDRs because most have a characteristic time to onset, while this model would predict a more random pattern (Uetrecht, 2008). Environmental factors, such as those suggested here, do likely play some role, and this inflammatory response could be related to mitochondrial damage, as well as other protein modifications.

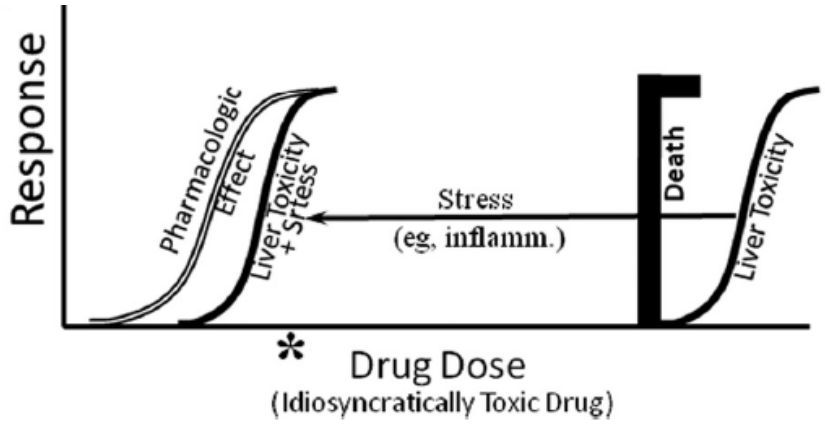

Figure 1.4 ***Inflammagen hypothesis.*** *The toxicity threshold for a given drug is not constant and can be lowered, for example, by an inflammatory response or other causes. The shifted threshold would result in lower doses of the drug leading to toxicity. (Figure from Roth and Ganey, 2010.)*

An additional sensitizing risk factor for idiosyncratic hepatotoxicity is mitochondrial abnormalities. The mitochondrion, a critical organelle for cell survival and cell death, provides the cell with energy in the form of adenosine triphosphate (ATP) through oxidative phosphorylation. The mitochondria is also capable of generating reactive oxygen species (ROS) from electron uncoupling in the electron transport chain (ETC) and can release high levels of apoptosis initiators if the mitochondrial membrane permeability is impaired. All cells contain some mixture of normal and mutated mitochondria, a natural phenomenon called heteroplasmy. A small percentage of mutated mitochondria is not typically problematic, since a cell contains hundreds to thousands of mitochondria (Boelsterli and Lim, 2007). In addition, cells are able to compensate for mitochondrial mutations (and resulting low ATP levels) by promoting mitochondrial proliferation independent of the cell cycle (Boelsterli and Lim, 2007). There is a threshold for this ability to adapt, though, and when too many mitochondria are mutated the cell may no longer be able to generate enough ATP to survive. This means that mitochondrial abnormalities often go unnoticed until they reach the threshold, when resulting cell death is rapid. Drugs and their reactive metabolites have the ability to shift the balance of normal and

mutated mitochondria through various mechanisms (Feng et al., 2001; Lewis et al., 2003). Individuals with clinically silent mitochondrial abnormalities who receive a drug with an intrinsic risk for further impairing mitochondrial function may be at an increased risk of DILI (Boelsterli and Lim, 2007). The prevalence of mitochondrial abnormalities is estimated to be 1 in every 5,000 individuals (Taylor and Turnbull, 2005), which could, at least in part, explain the low incidence of IDRs.

A factor that seems to be important in all hypotheses for IDRs is the drug's ability to damage hepatocytes to a degree that results in liver injury. In order to relate the IDR to the chemical properties of the particular drug that results in liver toxicity, it is necessary to consider the drug's ability to form reactive intermediates and impair hepatocyte function.

1.4 Metabolic activation in drug-induced liver injury

Metabolic activation, or bioactivation, of drugs can lead to the formation of metabolites with intrinsic chemical reactivity. The generation of these reactive metabolites from inert chemicals can initiate serious adverse drug reactions (Park et al., 2011; Stachulski et al., 2013) and can be considered the rate-determining step in some DILI (Leung et al., 2012). Upon generation, electrophilic metabolites can react with nucleophilic amino acid residues at the enzyme active site, leading to mechanism-based enzyme inactivation. If they diffuse from the enzyme active site before adducting, they can be deactivated through reaction with water or reduced glutathione (GSH). If reaction with water or other small nucleophiles is evaded, the metabolites can react with proteins or nucleic acids in other parts of the cells or in other cells and tissues altogether, potentially resulting in toxicity.

Cytochrome P450s play a major role in drug metabolism and bioactivation. The CYP3A subfamily, specifically, has very broad substrate selectivity and CYP3A4 is responsible for the metabolism of over

one third of all clinically used drugs (Kashuba and Bertino, 2001). In the P450 catalytic cycle, the substrate first binds to the active site of the P450. The ferric heme iron is reduced to its ferrous state and molecular oxygen binds. The iron-oxo intermediate (compound I) is formed through a second one-electron transfer and two-step protonation. Catalysis occurs through eventual insertion of an oxygen atom into the substrate (Ortiz de Montellano, 2005).

Chemical moieties within a drug that are subject to metabolic activation to reactive metabolites are often called structural alerts. In the absence of well-understood mechanisms and reliable animal models, a pragmatic approach to minimizing metabolic activation in drugs is by identifying such substituents during development and replacing them with alternative functional groups that retain the desired pharmacology and pharmacokinetics of the drug (Evans et al., 2004; Kalgutkar and Soglia, 2005; Uetrecht, 2008; Stepan et al., 2011). Complete avoidance of such alerts, however, is problematic for two reasons. First, it is impossible to avoid potentially bioactivated structures that have not yet been identified, and thus the avoidance approach will always be insufficient. Second, not all functional groups that can undergo metabolic activation will in all situations. For example, methylenedioxyphenyl is a well-established structural alert that can be bioactivated to reactive carbene and quinoid structures. Paroxetine, a highly successful antidepressant, contains this structural alert but has not been shown to have any serious direct safety problems beyond those associated with its pharmacology (Stachulski et al., 2013), although coadministration with thioridazine is contraindicated (Paxil, 2012). Complete avoidance of this structural alert, as well as others, would result in the loss of useful and relatively safe therapeutic agents. If the structural alert can be removed without sacrificing the desired pharmacology and pharmacokinetic properties, then this should be considered. In other situations, additional information such as dose, use pattern, and severity of the unmet medical need must be taken into account (Stachulski et al., 2013).

Examples of well-established structural alerts are listed in Table 1.1. A specific quinone reactive metabolite that will be discussed in this thesis is a quinoneimine, which is formed by P450-mediated two-electron oxidation of *ortho*- and *para*-aminophenols. This bioactivation pathway occurs in amodiaquine, which was withdrawn from clinical use due to hepatotoxicity and agranulocytosis (Maggs et al., 1988) and acetaminophen, which is a dose-dependent hepatotoxin in animals and human (Dahlin et al., 1984). Other examples include diclofenac, an idiosyncratic hepatotoxin, which can be metabolized to a quinoneimine in a two-step P450-mediated process (Tang et al., 1999; Miyamoto et al., 1997). The idiosyncratic hepatotoxin, indomethacin, requires three metabolic steps including CYP2C9-catalyzed *O*-demethylation to form a quinoneimine (Ju and Uetrecht, 1998). Nefazodone, a hepatotoxic antidepressant, can be bioactivated by P450 aromatic hydroxylation followed by two-electron oxidation to generate a quinoneimine metabolite (Kalgutkar et al., 2005a).

Precursor	Reactive metabolite
Alkene	Epoxide
Alkyne	Ketene
Polycyclic arene	Epoxide
o-, or *p*-Dialkoxyarene	Quinone
Furan	α,β-Unsaturated aldehyde
Thiophene	*S*-Oxide or 2,3-epoxide
Methylenedioxyphenyl	*o*-Quinone
2-Aminothiazole	Thiourea *S*-oxide
3-Alkylindole	α,β-Unsaturated imine
Haloalkane	Acyl halide

Table 1.1 ***A list of common structural alerts associated with reactive metabolites and toxicity. (****Table from Stachulski et al., 2013.)*

The structure of potential reactive metabolites can be inferred through characterization of their glutathione (GSH) conjugates in mass spectrometry-based electrophile trapping assays (Chen et al.,

2001; Samuel et al., 2003). The endogenous antioxidant, GSH, is conjugated via its nucleophilic thiol group to the electrophilic center of the reactive metabolite, forming a stable sulfhydryl conjugate that can provide mechanistic insight into the bioactivation pathway and possible mechanisms of toxicity. In such trapping experiments, the test compound is incubated with human liver microsomes (HLMs), nicotinamide adenine dinucleotide phosphate (NADPH) or an NADPH-regenerating system, and reduced GSH. The incubation is analyzed using neutral loss scanning on a tandem mass spectrometer (LC-MS/MS) for a 129-Da neutral loss from the parent ion, which corresponds to the loss of glutamic acid. This is taken as indirect evidence that metabolism of the compound *in vivo* may result in a reactive metabolite capable of being trapped by GSH.

1.5 Acetaminophen: an example of metabolic activation and the quinoneimine structural alert

Acetaminophen (APAP) poisoning is a hallmark example of hepatotoxicity and has been widely studied as a model of metabolic activation. One third to one half of the US and UK cases of drug-induced liver failure result from acetaminophen overdose (Ostapowicz et al., 2002; Bernal et al., 2009; Russo et al., 2004). The main route of clearance for APAP is through Phase II glucuronidation and sulfation followed by excretion in the urine (Figure 1.5). A portion of the drug, however, is bioactivated by CYP2E1, CYP1A2, and CYP3A4 to *N*-acetyl-*p*-benzoquinoneimine (NAPQI), a reactive metabolite (Raucy et al., 1989). At therapeutic doses of acetaminophen, the NAPQI produced can be detoxified by GSH conjugation, but in overdose situations GSH stores are depleted and an accumulation of NAPQI results in oxidative stress and covalent binding.

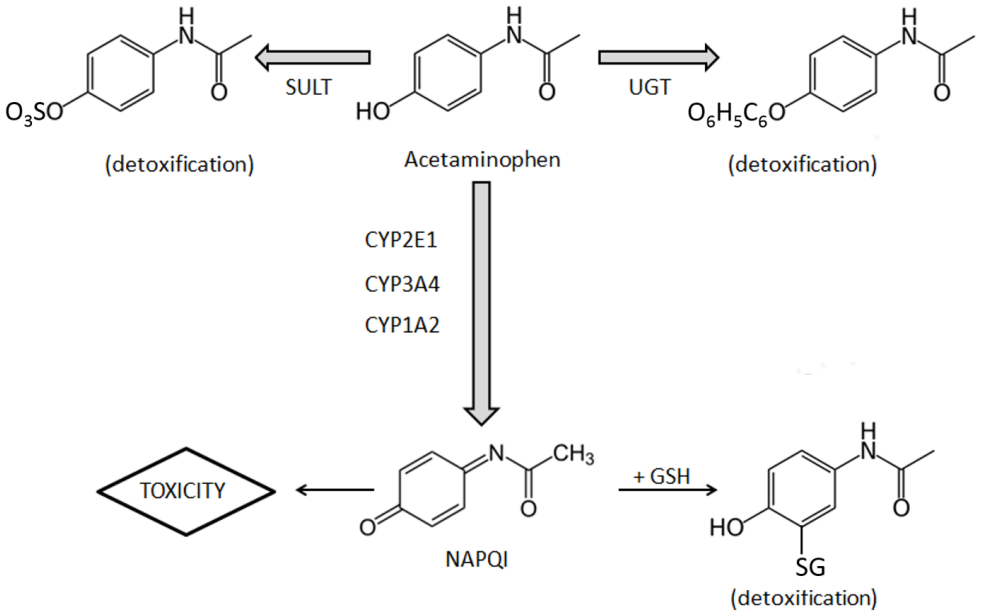

Figure 1.5 ***Metabolic activation of APAP.*** *APAP is primarily detoxified by glucuronidation and sulfation in the liver. APAP can also be metabolized by P450s to the reactive metabolite NAPQI. NAPQI can be inactivated through GSH conjugation, but in the absence of GSH NAPQI can oxidize and covalently modify proteins, resulting in hepatotoxicity.*

The mechanism of hepatotoxicity of acetaminophen occurs through the reactive metabolite NAPQI, which induces "chemical stress" and leads to a complex series of structural and functional changes within the liver cell (Stachulski et al., 2013).

1.6 Lapatinib: an idiosyncratic hepatotoxicant

1.6.1 Pharmacology of LAP

Lapatinib (LAP; Figure 1.6) was the first orally active dual tyrosine kinase inhibitor (TKI) of the epidermal growth factor receptor (EGFR, ErbB1) and human epidermal receptor 2 (HER2, ErbB2) to be approved by the FDA (Rusnak et al., 2001; Moy et al., 2007). Inhibition of EGFR and HER2 is

reversible, but with a slow dissociation rate (half-life ≥ 300 minutes) (European Medicines Agency, 2008). The HER and ErbB family of receptors are partially homologous transmembrane tyrosine kinases that are important in the regulation of cell growth, proliferation, and survival (Yarden, 2001). Following ligand binding, the tyrosine kinases dimerize and activate a signal-transduction cascade through the RAS-MAPK pathway that inhibits cell death (Yarden and Sliwkowski, 2001). HER2 can also dimerize in the absence of a ligand (Cho et al., 2003) or when overexpressed (Brennan et al., 2000). Overexpression and activation of HER2 is reported in about 20% of human breast cancers and, prior to the development of HER2-targeted therapies, was associated with an inferior clinical outcome and a higher risk of breast cancer recurrence (Slamon et al., 1987; Slamon et al., 1989). EGFR is also frequently overactive in solid tumors (Khazaie et al., 2002). Lapatinib inhibits by reversibly binding to the intracellular ATP-binding site, thus blocking dimerization and phosphorylation and preventing the downstream effects of the kinases such as cell proliferation and survival, and inducing apoptosis (Figure 1.7).

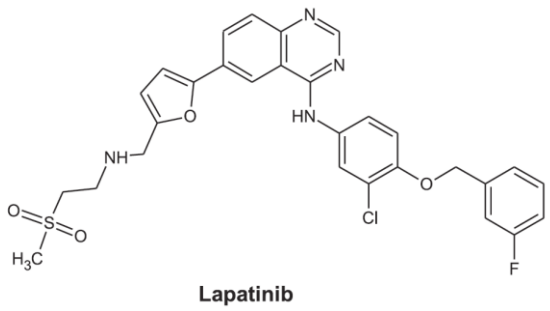

Figure 1.6 ***Chemical structure of lapatinib.*** *Molecular formula = $C_{29}H_{26}ClFN_4O_4S$; monoisotopic mass = 580.134731 Da.*

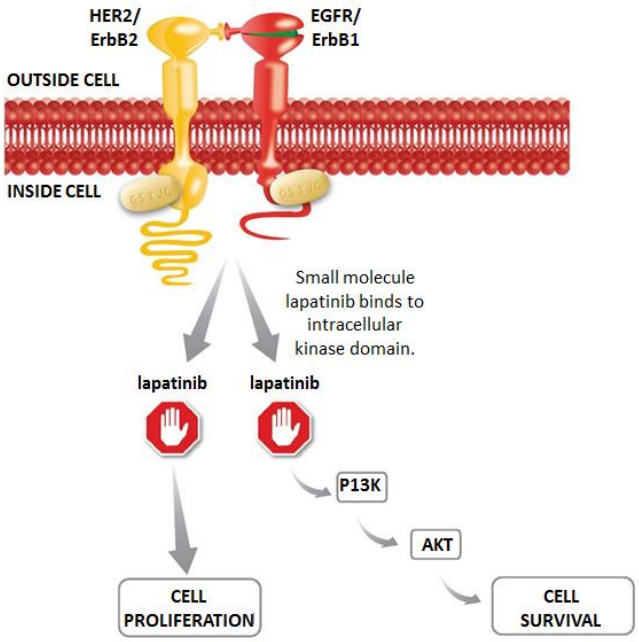

Figure 1.7 ***Lapatinib mechanism of action.*** *Figure modified from http://hcp.gsk.co.uk.*

Lapatinib (TYKERB®, GlaxoSmithKline) was first approved in 2007 for use in combination with capecitabine (Her2-positive metastatic breast cancer indication) at 1250 mg/day in patients who had received prior therapy with anthracycline, a taxane, and trastuzumab (Lapatinib product monograph; Geyer et al., 2006; Kroep et al., 2010). Lapatinib has been shown to reduce disease progression by 51% and increase survival (Geyer et al., 2006; Cameron et al., 2008). In 2010, Lapatinib was approved for first-line combination therapy with letrozole (hormone receptor positive, HER2-positive breast cancer indication) at 1500 mg/day (Lapatinib product monograph). Due to its clinical efficacy, lapatinib is being evaluated clinically for broader applications in cancer therapy. The ALTTO (Adjuvant Lapatinib and/or Trastuzumab Treatment Optimization) trial is an international multicenter Phase III trial sponsored by the National Cancer Institute and GlaxoSmithKline to directly compare lapatinib with trastuzumab for the first-line treatment of metastatic breast cancer (Jelovac and Wolff, 2012). While the lapatinib-alone arm has been closed, ongoing studies are focused on patients taking a combination of lapatinib and trastuzumab, either concurrently or in sequence with a washout period

in between. A recent adjuvant randomized trial called TEACH (Tykerb Evaluation After Chemotherapy) looked at women who had completed therapy and were disease-free. The women received either lapatinib or placebo for 12 months. Four years later, the outcome was better for patients who had received lapatinib (Goss et al., 2013), but the difference was not great enough to meet the pre-specified success criteria. In NeoALTTO, another phase III trial, patients who were given a therapy that included lapatinib, trastuzumab, and paclitaxel had significantly higher pathological complete response (pCR) than patients who had been given only trastuzumab and paclitaxel (Baselga et al., 2012). In addition, there are currently 139 clinical trials in progress related to a wide range of lapatinib indications including gastric, thyroid, and prostate cancers (www.cancer.gov; accessed April 15, 2014).

1.6.2 Idiosyncratic hepatotoxicity of LAP

At the time of initial clinical trials and approval, lapatinib's safety profile was acceptable for the treatment of breast cancer (Bence et al., 2005; Geyer et al., 2006). Following approval, however, incidences of severe and even fatal cases of liver injury began to be reported with lapatinib use (Moy et al., 2009; Cristofanilli et al., 2013). In 2008, the US Food and Drug Administration issued a black-box warning for lapatinib idiosyncratic hepatotoxicity, which was observed in a small proportion of patients (<1%) in clinical trials and post-market surveillance (Gomez et al., 2008). The hepatotoxicity of lapatinib is associated with a 6-8 week delayed onset of occurrence following the initiation of therapy (Teo et al., 2012). In addition to the rare high-grade toxicity, approximately 10% of the population taking lapatinib may experience transient transaminitis (Azim et al., 2013). The severe hepatotoxicity associated with lapatinib bears the classical features of idiosyncratic toxicity. It occurs rarely and does not appear to be linked to the mechanism of action for the drug as trastuzumab, an anti-HER2 monoclonal antibody, does not exhibit similar toxicity. Other tyrosine kinase inhibitors,

though, such as imatinib, do exhibit hepatotoxicity. Metabolic activation has been suggested as an underlying factor in these cases (Loriot et al., 2008; Duckett and Cameron, 2010).

Recent pharmacogenetic investigations of patients taking lapatinib for the treatment of metastatic breast cancer found that the human leukocyte antigen (HLA) allelic variants *DQA1*02:01, DRB1*07:01, DBQ1*02:02,* and *TNXBrs12153855* were associated with increased hepatotoxicity risk (Spraggs et al., 2012; Spraggs et al., 2013; Schaid et al., 2014). HLA is the human version of the major histocompatibility complex (MHC); thus it is the molecule involved in antigen presentation. There are several examples of associations between HLA genotypes and IDRs, and the presence of this association suggests an immune mechanism. Patients taking abacavir, for example, who had the *HLA-B*5701* allele were found to be at a higher risk for a hypersensitivity reaction (Martin et al., 2004). In Han Chinese, there is a strong association between *HLA-B*1502* and carbamazepine-induced toxic epidermal necrolysis (Chung et al., 2004). Interestingly, that association is not observed in a European population (Lonjou et al., 2006). An association between *HLA-B*5801* and allopurinol-induced toxic epidermal necrolysis was also observed in a Han Chinese population (Hung et al., 2005). Other associations between DILI and specific HLA polymorphisms include those with amoxicillin-clavulanate, flucloxacillin, ximelagatran, and ticlopidine (Russmann, 2010).

The association of hepatotoxicity with an HLA allele suggests that lapatinib-related liver injury involves activation of the adaptive immune system, which may be triggered by the chemically reactive quinoneimine metabolite of lapatinib (Spraggs et al., 2011).

1.6.3 Metabolic activation in lapatinib-induced hepatotoxicity

Lapatinib is extensively metabolized by CYP3A4/5 with minor contributions from CYP2C19 and CYP2C8 (GlaxoSmithKline, 2007). The three primary metabolic pathways are *O*-dealkylation, *N*-dealkylation, and *N*-hydroxylation (Figure 1.8; Takakusa et al., 2011; Castellino et al., 2012). The metabolite formed from *O*-dealkylation (LAP-OH) accounted for 3.9% of the dose in human fecal homogenates, with a range of below the limit of quantification (BLQ) to 19.2%. Another metabolite that is dealkylated and also hydroxylated on the quinazoline moiety, constituted 3.3% of the dose with a range of BQL to 17.8% (Castellino, et al., 2012). Further oxidation of the *O*-dealkylated phenolic metabolite results in the formation of a reactive quinoneimine intermediate (Teng et al., 2010), which is analogous to NAPQI, an electrophilic metabolite of acetaminophen. As mentioned earlier, quinoneimines can readily adduct proteins and other cellular nucleophiles and lead to direct cell stress or activation of immune-mediated reactions (Park et al., 2005; Park et al., 2011; Stachulski et al., 2013). *In vivo* studies in preclinical species and *in vitro* investigations in humans suggest that LAP-OH is extensively glucuronidated and sulfated (Castellino et al., 2012).

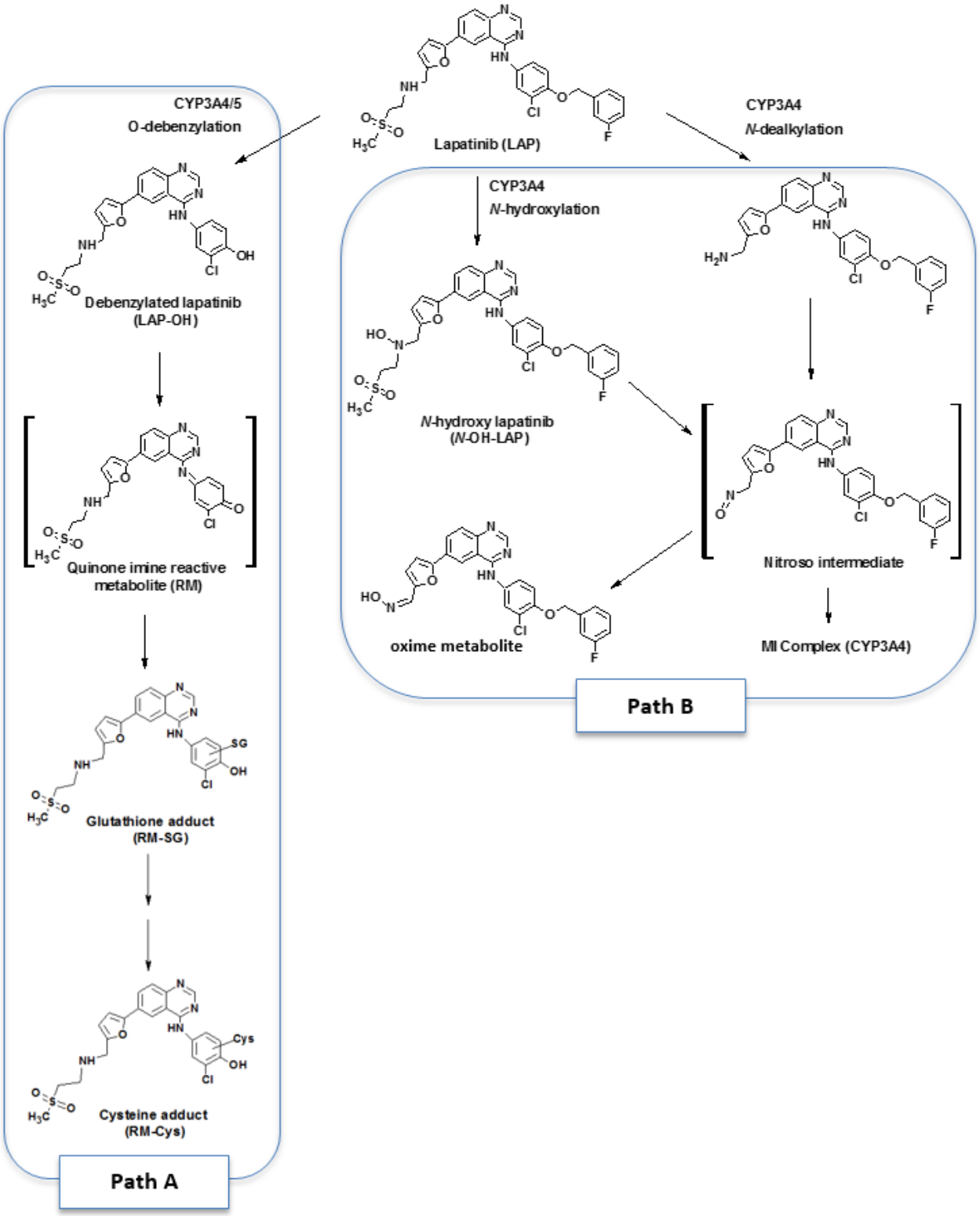

Figure 1.8 ***Proposed in vitro metabolic scheme of lapatinib.***

1.6.4 Mechanism-Based Inactivation (MBI)

A mechanism-based inactivator is a compound that is converted, during the course of enzymatic catalysis, to a reactive species that then inactivates the same enzyme. Clinical observations with lapatinib suggest that the drug may be a mechanism-based inactivator of the enzymes that oxidize it. Continuous dosing of the drug leads to an increase in the half-life from 6 to 14 hours and an increase in plasma concentrations (C_{max} and area-under-the-curve, AUC) at a rate that is more than dose-proportional (European Medicines Agency, 2008; GlaxoSmithKline). This can be explained by autoinhibition of metabolism, possibly by inactivation of one of the enzymes responsible for metabolism. A set of seven criteria for MBI have been established, which include that inactivation must be dependent on catalytic turnover, time-dependent, and irreversible or at least quasi-irreversible. In addition, the inactivation must exhibit saturation kinetics and occur prior to release of the reactive species from the active site of the enzyme. The enzyme must be protected from inactivation through the addition of an alternate substrate and only one inactivator molecule can be attached to each molecule of inactivated enzyme (Silverman, 1995).

Lapatinib has been established as an MBI in accordance with these criteria (Teng et al., 2010). This group proposed that the inactivation was due to covalent modification of the CYP3A4 apoprotein and/or heme moiety by the reactive quinoneimine species formed from debenzylated lapatinib. Further studies in our lab, however, demonstrated that MBI of CYP3A4 by lapatinib is quasi-irreversible and not a result of adduction of a reactive metabolite to P450 apoprotein or heme (Takakusa et al., 2011). Quasi-irreversible inactivation is caused by formation of a coordinate covalent bond between lapatinib and the heme iron, and the coordination complex is referred to as a metabolic intermediate complex (MI complex). MI complex formation was observed between lapatinib and CYP3A4, as demonstrated by the presence of a signature Soret absorbance at approximately 455 nm

(Franklin, 1974). The absorbance of CYP3A4 at 455 nm increased in a time-dependent manner after the addition of NADPH in the presence of lapatinib (Takakusa et al., 2011).

MI complex formation by lapatinib is hypothesized to occur via sequential metabolism of the secondary amine located between the furan and methanesulfonyl moieties to a reactive nitroso intermediate (Figure 1.8; Takakusa et al., 2011). Nitroso-iron MI complexes have been previously identified (Lin and Lu, 1998). Although P450 enzymes can be reactivated by chemical oxidation of the heme iron, these complexes are stable enough *in vivo* that quasi-irreversible inactivators might cause significant drug-drug interactions (DDIs) (Mayhew et al., 2000). Mechanism-based inactivation of CYP3A4 by lapatinib is considered clinically important because of DDIs that may occur upon coadministration with other drugs that are CYP3A4 substrates.

1.6.5 Genetic Factors (CYP3A4 and CYP3A5)

Lapatinib's extensive metabolism in the liver is primarily mediated by CYP3A4 and CYP3A5 (GlaxoSmithKline, 2007). Because CYP3A4 is the major P450 expressed in the human intestines and liver (Guengerich, 1999) and has broad substrate selectivity, it is often the focus of DDIs interactions and metabolic activation. The importance of CYP3A5, however, should also be considered. CYP3A5 is highly polymorphic (Kuehl et al., 2001; Lamba et al., 2002) and its expression is dependent on which alleles are carried by an individual. Several low-expression variants have been identified for CYP3A5. The most common is the *CYP3A5*3* variant allele, which contains a single nucleotide polymorphism (SNP), 6896 A → G within intron 3, which causes alternative splicing and protein truncation and results in the absence of functional CYP3A5 in the liver and intestines (Kuehl et al., 2001). Individuals with the *CYP3A5*1* allele express high levels of the functional protein, whereas the *CYP3A5*3* variant allele

results in low to undetectable levels of CYP3A5. The frequency of the reference *CYP3A5*1* allele varies, with 10-30% of Caucasians, 30-40% of Asians of different ethnic groups, and 50-70% of African Americans expressing at least one allele (Kuehl et al., 2001; Lamba et al., 2002). When at least one *CYP3A5*1* allele is expressed, CYP3A5 may represent up to 50% of the total CYP3A content and contribute significantly to the overall CYP3A catalytic activity (Kuehl et al., 2001; Saeki et al., 2003).

There are several examples of drugs for which variable CYP3A5 activity alters pharmacokinetics. Midazolam clearance is significantly higher in *CYP3A5*1*1* and *CYP3A5*1*3* subjects than in *CYP3A5*3*3* subjects *in vitro* and *in vivo* (Kuehl et al., 2001; Lin et al., 2002; Wong et al., 2004). In a population of Chinese patients who had just undergone renal transplantation, the necessary dose of cyclosporine (a calcineurin inhibitor) was significantly higher in subjects carrying the *CYP3A5*1*1* genotype than in patients with the *CYP3A5*3*3* genotype (Hu et al., 2006). The chemotherapeutic agent vincristine is metabolized by CYP3A5 with a 9- to 14-fold higher intrinsic clearance than CYP3A4 in a cDNA-expressed enzyme system (Dennison et al., 2006). In human liver microsomes (HLMs) from CYP3A5 high expressers, the contribution of CYP3A5 to vincristine metabolism was 54-95% of the total activity and the estimated hepatic clearances were 5-fold higher than for low expressers (Dennison et al., 2007). Metabolism of tamoxifen, an antiestrogen used in the prevention and treatment of breast cancer, to *N*-desmethyltamoxifen is approximately 3-fold lower by HLM with CYP3A5*3/*3 alleles than for HLM expressing CYP3A5*1/*1 (Mugundu et al., 2012).

CYP3A4 and CYP3A5 share 85% sequence homology and display overlap in substrate specificity (Thummel and Wilkinson, 1998); however they differ in product regioselectivity (Huang et al., 2004). Substrate-dependent differences in the extent and mechanism of inhibition of CYP3A4 and CYP3A5 have been observed. Verapamil, a calcium channel blocker, is metabolized by CYP3A4 and CYP3A5 to

form two *N*-dealkylated products. CYP3A4 is much more active than CYP3A5 and the two enzymes exhibit different enantioselectivity (Shen et al., 2004). Verapamil and one major metabolite, norverapamil, are mechanism-based inactivators of CYP3A4, but inactivate CYP3A5 to a much lesser extent. This indicates that variability in CYP3A5/CYP3A4 expression in the liver may play a role in interindividual variability in drug interaction associated with verapamil (Wang et al., 2005).

Some work has been done on the metabolism of lapatinib by CYP3A5. Lapatinib does not form an MI complex with CYP3A5 like it does with CYP3A4 (Takakusa et al., 2011). Formation of the *N*-hydroxy-lapatinib metabolite, the putative precursor for MI complex formation with CYP3A4, was more than 10-fold lower in CYP3A5 incubations than in CYP3A4 incubations (Takakusa et al., 2011). Inactivation of CYP3A5 by lapatinib appears to be substrate-specific, as midazolam hydroxylation activity was not significantly inactivated by lapatinib in incubations with CYP3A5 Supersomes™ (Takakusa et al., 2011; Chan et al., 2012), while testosterone 6β-hydroxylation was inactivated by lapatinib in a time- and concentration-dependent manner (Chan et al., 2012). This could be a result of the large active site of CYP3A5 and the multiple modes of substrate binding (Ekins et al., 2003) and may lead to only a subset of drugs eliminated by CYP3A5 resulting in DDIs.

A link between idiosyncratic hepatotoxicity and polymorphic gene expression has been identified in the mechanisms of DILI (Corsini and Bortolini, 2013). The wide variation in expression levels of CYP3A5 in the human population provides the scientific rationale for understanding the role of CYP3A5 in the metabolism and idiosyncratic hepatotoxicity of lapatinib.

1.7 Scope of Work:

The overall goal of the research described herein is to evaluate the metabolic bioactivation of lapatinib by cytochrome P450 enzymes and correlate this process with the hepatotoxicity of the drug. It is hypothesized that CYP3A4 and CYP3A5 metabolize lapatinib to an *O*-debenzylated lapatinib metabolite that is further oxidized to a reactive quinoneimine, and that this pathway is implicated in the observed hepatotoxicity. Studies examining the formation and further metabolism of the *O*-debenzylated lapatinib metabolite in various *in vitro* systems will yield important insights towards understanding the mechanism of hepatotoxicity of lapatinib *in vivo*.

The specific aims of this dissertation research are as follows:

1. Characterize the metabolism of lapatinib by CYP3A and establish the role of CYP3A5 relative to CYP3A4 in the formation and further metabolism of debenzylated lapatinib.
2. Use HepaRG cells as a model to characterize the role of CYP3A4-mediated metabolic activation in lapatinib-induced hepatotoxicity.
3. Understand the molecular interaction in the lapatinib/CYP3A system through analysis of a deuterium-substituted lapatinib analog and a CYP3A4 mutant enzyme.

Chapter 2: The Formation and Fate of Debenzylated Lapatinib *in vitro*

Objective: The objective of this investigation was to characterize the metabolism of lapatinib by cytochrome P450s in CYP3A4 and CYP3A5 Supersome™ systems, human liver microsomes, and CYP3A5-genotyped human liver microsomes. An important aim was to establish the role of CYP3A5 relative to CYP3A4 in the formation and further metabolism of debenzylated lapatinib.

Introduction:

Quantitative comparisons of the catalytic efficiencies of CYP3A4 and CYP3A5 in the formation of the *O*-debenzylated metabolite and reactive metabolite glutathione conjugates of lapatinib have not been carried out. The expression of CYP3A5 is typically low compared to CYP3A4, but because it is polymorphically expressed, its contribution to total hepatic CYP3A content can be up to 50% for some individuals (Kuehl et al., 2001). The most common variant is the *CYP3A5*3* allele, which results in a loss of enzyme activity relative to the wild type (*CYP3A5*1*). The frequency of individuals that are homozygous for the *CYP3A5*3* allele, and thus do not express active CYP3A5, is 70-90% in Caucasians, 60-70% in Asians of different ethnic groups, and 30-50% in African Americans (Kuehl et al., 2001; Lamba et al., 2002). Numerous studies have demonstrated an association between *CYP3A5*3* genotype and the metabolism and pharmacokinetics of various drugs, including midazolam, cyclosporine, vincristine, tamoxifen, tacrolimus, and vardenafil (Kuehl et al., 2001; Lin et al., 2002; Wong et al., 2004; Hu et al., 2006; Dennison et al., 2006; Mugundu et al., 2012; Thervet et al., 2003; Ku et al., 2008). The potential impact of variable expression of CYP3A5 on the metabolism of lapatinib via the *O*-debenzylation pathway remains to be investigated. This is important, given the pharmacological and toxicological effects of the metabolites formed. Therefore, the catalytic efficiencies of CYP3A4 and CYP3A5 in the formation of *O*-debenzylated lapatinib and a glutathione

conjugate thereof were compared using *in vitro* methods and the impact of CYP3A5 polymorphisms on these reactions was assessed.

Materials and Methods:

Materials

Lapatinib (free base) was purchased from LC Laboratories (Woburn, MA). A deuterium-labeled analog of debenzylated lapatinib ([D_4]-debenzylated lapatinib, D_4-LAP-OH, Figure 2.1) and the *N*-dealkylated lapatinib metabolites were supplied by Concert Pharmaceuticals Inc® (Lexington, MA). Stock solutions of lapatinib and lapatinib metabolites were prepared in dimethyl sulfoxide (DMSO). Glutathione (reduced) and ammonium acetate were purchased from Sigma Aldrich (St. Louis, MO). Optima LC-MS-grade water, Optima LC-MS-grade acetonitrile, and HPLC-grade acetonitrile were purchased from Fisher Scientific (Pittsburgh, PA). Human CYP3A4 and CYP3A5 Supersomes™ expressing P450 reductase and cytochrome b_5 and pooled human liver microsomes were purchased from BD Biosciences (San Jose, CA). HepaRG cells were purchased from ABC (xyz). All other chemicals and reagents were of analytical grade and were purchased from commercial sources.

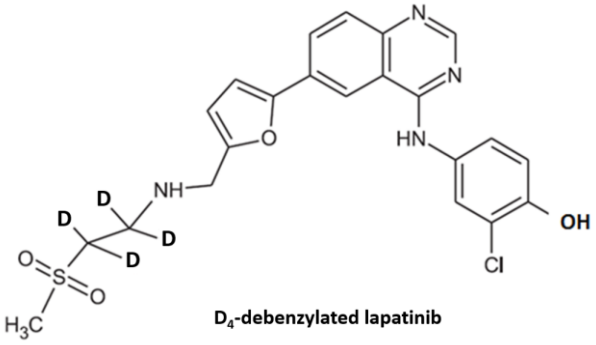

Figure 2.1 – ***Chemical structure of D_4-debenzylated lapatinib (D_4-LAP-OH).***

Synthesis of Debenzylated Lapatinib

Lapatinib (20 mg) was dissolved in 30 mL of a 1:1 mixture of trifluoroacetic acid (TFA) and toluene. The solution was yellow in color. The mixture was refluxed at 72°C for 18 hr with constant stirring. At termination, the mixture was evaporated under a stream of nitrogen, and then dissolved in methanol. Purification was performed using an Ultrasphere C18 prep column (10 µm, 10 mm x 25 cm, Beckman Coulter, Brea, CA) and a Shimadzu LC-10AD VP HPLC-UV system (Shimadzu Scientific Instruments Inc., Columbia, MD) at a flow rate of 0.3 mL/min. Solvents A and B were HPLC-grade acetonitrile and 0.1 M ammonium acetate (pH = 5.4), respectively. The gradient used for purification was as follows: isocratic at 10% B (0-2 min), linear gradient from 10% to 50% B (2-6 min), isocratic at 50% B (6-12 min), linear gradient from 50% to 80% B (12-14 min), isocratic at 80% B (14-15 min), returned to 10% B (15-15.1 min), and isocratic at 10% B (15.1-17 min). After 50 µL injections, the material between 10.3 and 11.5 min was detected by UV at 254 nm and collected and the combined collections were dried under a stream of nitrogen and analyzed by LC-MS and NMR.

Detection and Identification of Lapatinib Metabolites

Lapatinib and its metabolites were detected and identified from 24 hr HepaRG cell incubations with lapatinib (100 µM) (see Chapter 3 for cell culture details). The samples were analyzed using an HPLC system consisting of two Shimadzu LC-10AD pumps with a gradient controller and a Shimadzu SIL-10ADvp autoinjector coupled to a Waters Micromass Quattro Micro II triple quadrupole mass spectrometer (Waters Corporation, Milford, MA), as described previously (Takakusa et al., 2011). A 30 µL aliquot of each sample was injected into the equilibrated HPLC. Solvents A and B were Optima LC-MS-grade water with 0.1% (v/v) TFA and Optima LC-MS-grade acetonitrile with 0.1% (v/v) TFA, respectively. Analyte separation was achieved with an Agilent Zorbax SB-C_{18} column (5 µm, 2.1 mm x 150 mm; Agilent Technologies, Santa Clara, CA) at a flow rate of 0.3 mL/min. The gradient program

for analysis of lapatinib (LAP) and debenzylated lapatinib (LAP-OH) was as follows: isocratic at 15% B (0-1 min), linear gradient from 15 to 95% B (1-4.5 min), isocratic at 95% B (4.5-7 min), returned to 15% B (7-7.1 min), and isocratic at 15% B (7.1-8 min). For analysis of GSH adducts, the following gradient program was used: isocratic at 15% B (0-1.5 min), linear gradient from 15 to 95% B (1.5-5 min), isocratic at 95% B (5-7 min), returned to 15% B (7-7.1 min), and isocratic at 15% B (7.1-9.1 min). The effluent was introduced directly into the mass spectrometer that was operated in the electrospray ionization mode with positive ion detection (ESI+). The MS conditions were as follows: capillary voltage, 3.5 kV; cone voltage, 60 V; source temperature, 120°C; desolvation temperature, 350°C; and analyzer, V mode.

Product Ion Analysis: Product ion analysis utilizing collision-induced dissociation was carried out to determine the major product ions of LAP and LAP metabolites for subsequent method development. A collision energy of 30 V was used to generate MS/MS spectra for each analyte.

Multiple Reaction Monitoring (MRM) Analysis: LAP and LAP metabolites were selectively detected and quantified by LC-MS/MS utilizing a collision energy of 30 V. The following precursor to product MRM transitions were used for the detection of LAP and LAP metabolites based on structurally specific fragmentation obtained from collision-induced dissociation of the respective MH^+ ions: *m/z* 581 → 365 for LAP, *m/z* 473 → 350 for LAP-OH; *m/z* 475 → 366 for *N*-dealkyl lapatinib (*N*-dealkyl-LAP), and *m/z* 597 → 458 for *N*-hydroxy lapatinib (*N*-OH-LAP). D_4-LAP-OH, which was detected using the MRM transition m/z 477 → 352, was used as the internal standard for quantitation. Relative quantitation of GSH adducts was carried out by LC-MS/MS monitoring the transition *m/z* 778 → 655. The MS spectral data were analyzed and deconvoluted using MassLynx version 4.1 (Waters Corporation, Milford, MA).

Contributions of CYP3A4 and CYP3A5 Isoforms to Lapatinib Metabolism

Incubation solutions containing 20 nM P450 enzyme (Supersome™), 0.1 M KPi buffer (pH = 7.4), and 50 µM LAP were prepared and pre-incubated at 37°C for 3 min. Incubation reactions were initiated by the addition of 10 µL of a 10 mM solution of NADPH in H_2O (final concentration, 1.0 mM) or H_2O as a negative control. The total volume of each preincubation solution was 100 µL, and the final organic solvent concentration was 1.0% (v/v) acetonitrile. Following the 30 min incubation at 37°C, reactions were quenched with 200 µL of ice-cold acetonitrile containing D_4-LAP-OH (0.1 ng/µL) as the internal standard and cooled on ice. Samples were cooled and centrifuged at 6600 g for 3 min, and the supernatants were transferred to new tubes and kept at -80°C until LC-MS analysis. Samples were analyzed using the same HPLC system as described above. Analyte separation was achieved using a Zorbax SB-C_{18} column (150 mm x 2.1 mm, 5 µm particle size; Agilent Technologies, Santa Clara, CA) at a flow rate of 0.3 mL/min. Solvents A and B were nanopure H_2O with 0.1% (v/v) TFA and LC-MS-grade acetonitrile with 0.1% (v/v) TFA, respectively. The gradient program was as follows: isocratic at 25% B (0-3 min), linear gradient from 25 to 65% B (3-7 min), linear gradient from 65 to 95% B (7-10 min), and isocratic at 95% B (10-11 min). The effluent was introduced directly into the mass spectrometer which was operated in the electrospray ionization mode with positive ion detection (ESI+). The MS conditions were as follows: capillary voltage, 3.5 kV; cone voltage, 25 V; source temperature, 120°C; desolvation temperature, 300°C; and analyzer, V mode. The data were acquired in MRM mode monitoring the *m/z* transitions described in the previous section. The *m/z* value for the internal standard, 11α-hydroxyprogesterone, was 331. The MS spectral data were analyzed and deconvoluted using MassLynx software version 4.1 and the peak area of each metabolite was normalized to that of the internal standard. Then, the ratio of metabolite formation (3A5/3A4) was calculated from the normalized peak area of each metabolite.

Time-course for Formation of LAP-OH

LAP (5 µM) was incubated with CYP3A4 or CYP3A5 Supersomes™ (20 nM) in 0.1 M potassium phosphate buffer (pH = 7.4) fortified with an NADPH-regenerating system (glucose 6-phosphate, $NADP^+$, and glucose 6-phosphate dehydrogenase) and allowed to proceed for various times (0.5, 1, 2, 5, 10, 20, 30 min). The total incubation volume was 1 mL. Following the set incubation period, aliquots (100 µL) were removed, combined with an equal volume of ice-cold acetonitrile (containing 1 ng/µL D_4-LAP-OH), and centrifuged at 16,000 g for 10 min at 4°C to remove precipitated proteins. The supernatant from metabolic incubations was analyzed by LC-MS analysis with MRM and compared to standard curves prepared with an authentic chemical standard to quantify levels of LAP-OH.

Formation of LAP-OH and RM-SG Adducts by Individual CYP Isoforms

Next, studies were carried out to determine the relative contribution of individual P450 isoforms to formation of LAP-OH and GSH adducts of the putative quinoneimine reactive metabolite of lapatinib. Initial experiments were conducted to determine the linearity of LAP-OH and GSH adduct formation with respect to incubation time and protein concentration. The formation of LAP-OH was examined by incubation of LAP (5 µM) with individual P450 Supersomes™ (20 nM) fortified with 1 mM NADPH for 2 min. To evaluate the formation of reactive metabolite GSH adducts, LAP or LAP-OH (5 µM) were incubated with P450 Supersomes™ (20 nM) supplemented with GSH (5 mM) and an NADPH regenerating system for 20 min at 37°C. Relative levels of LAP-OH and GSH adducts were measured by LC-MS analysis with MRM.

Kinetic Experiments for the Formation of LAP-OH and RM-SG in HLM and Recombinant CYP3A4 and CYP3A5

Incubations with CYP Supersomes™: Preliminary incubations were performed in CYP3A4 and CYP3A5 Supersomes™ with 5 µM LAP to determine microsomal metabolite formation under linear conditions with respect to protein concentration and time of incubation. To determine Michaelis-Menten parameters of LAP-OH formation, LAP (0.1 – 50 µM) was incubated with CYP3A4 and CYP3A5 Supersomes™ (20 nM) in 100 mM potassium phosphate buffer (pH = 7.4). The reaction mixture was pre-incubated for 5 min at 37°C. Reactions were initiated by the addition of 10 µL of a 20 mM solution of NADPH (final concentration, 1 mM) incubated at 37°C for a period of 2 min at a final volume of 200 µL in a 96-well plate. The final concentration of organic solvent in the incubation was 1% (0.1% DMSO and 0.9% acetonitrile). The reactions were quenched by addition of an equal volume of ice-cold acetonitrile (containing 1 ng/µL D_4-LAP-OH) and centrifuged at 16,000 g for 10 min at 4°C to remove proteins. The supernatant was transferred to LC-MS vials for LC-MS analysis with MRM. Assays were conducted in triplicate.

Incubations with pooled human liver microsomes (HLM): Pooled human liver microsomes (BD UltraPool™ HLM 150-donor) were purchased from BD Biosciences (San Jose, CA). Preliminary incubations were performed with LAP (5 µM) to determine microsomal metabolite formation under linear conditions with respect to protein concentration and time of incubation. After assay optimization, LAP (0.1 - 50 µM) was incubated with pooled HLM (0.1 mg of protein/mL) in 100 mM potassium phosphate buffer (pH = 7.4). The reaction mixture was incubated for 5 min at 37°C before the addition of 10 µL a 20 mM solution of NADPH (final concentration, 1 mM) or potassium phosphate buffer as a control. Reactions were incubated at 37°C for a period of 5 min at a final volume of 200 µl in a 96-well plate. The final concentration of organic solvent in the incubation was 1% (0.1% DMSO and 0.9% acetonitrile). Following the incubation, reactions were quenched with 200 µL of ice-cold acetonitrile containing 0.1 ng/µL of D_4-LAP-OH as the internal standard and cooled on ice. Reactions

were then centrifuged at 1300 g for 20 min at 4°C to remove proteins. The supernatant was transferred to LC-MS vials for LC-MS analysis with MRM. Assays were conducted in triplicate.

Standard curve for LAP-OH: For quantitation of LAP-OH formation, a standard curve was generated over a range of concentrations (0.005 - 1.0 ng/μL) of LAP-OH with peak area ratios calculated against D_4-LAP-OH (0.1 ng/μL) as the internal standard. Standard incubations were carried out under the same experimental conditions as described above except using heat-inactivated enzyme without NADPH to calculate the concentration of metabolite formation.

GSH Adduct Formation: For kinetic analysis of formation of GSH adducts, LAP (0.1-100 μM) was incubated with CYP3A4 or CYP3A5 Supersomes™ (20 nM) supplemented with 5 mM GSH for 20 min. Samples were run in duplicate. Control incubations were carried out in the absence of NADPH or GSH. Relative levels of GSH adducts were determined by LC-MS analysis with MRM.

Formation of RM-SG Adducts from LAP-OH in CYP3A5 Genotyped HLMs

Metabolism studies were performed using individual genotyped human liver microsomal preparations, which were obtained from the University of Washington, School of Pharmacy Human Liver Bank. Immunoquantification of CYP3A4 and CYP3A5 specific protein content in human liver microsomal preparations was previously reported by Lin et al., (2002). Donor liver microsomal preparations (0.1 mg protein/mL) were incubated for 20 min with LAP-OH (5 μM) and GSH (50 mM). Incubations were supplemented with an NADPH regenerating system for P450 enzyme activity. Formation of RM-SG was measured by LC-MS analysis with MRM.

Results:

Synthesis, Detection, and Identification of Lapatinib Metabolites

<u>*O*-Debenzylated lapatinib (LAP-OH)</u>: The debenzylated metabolite was synthesized and purified as a reference standard for subsequent experiments. NMR analysis confirmed the structure of the product. Purified product was obtained as a yellow solid in 48% yield. ^{1}H NMR (acetone-d_6): 1.96 ppm (1 H, s, NH), 3.02 ppm (3 H, s, CH_3), 3.08 ppm (1 H, s, NH), 3.18 ppm (2 H, t, CH_2, J = 1.5 Hz), 3.29 ppm (2 H, t, CH_2, J = 1.5 Hz), 3.92 ppm (2 H, s, CH_2), 6.45 ppm (1 H, d, aromatic-CH, J = 3.5 Hz), 6.95 ppm (1 H, d, aromatic-CH, J = 3.5 Hz), 7.05 ppm (1 H, d, aromatic-CH, J = 9 Hz), 7.64 ppm (1 H, dd, aromatic-CH, J_L = 8.5 Hz, J_S = 2.5 Hz), 7.82 ppm (1 H, d, aromatic-CH, J = 8.5 Hz), 8.02 ppm (1 H, dd, aromatic-CH, J_L = 6 Hz, J_S = 2.5 Hz), 8.16 ppm (1 H, dd, aromatic-CH, J_L = 9 Hz, J_S = 2 Hz), 8.57 ppm (1 H, s, aromatic-CH), 8.66 ppm (1 H, d, aromatic-CH, J = 1.5 Hz), 9.15 ppm (1 H, s, OH). The NMR spectrum of the debenzylated metabolite was comparable to that of lapatinib itself, but lacked four signals in the aromatic region as well as the signal for the two benzylic protons at 5.27 ppm.

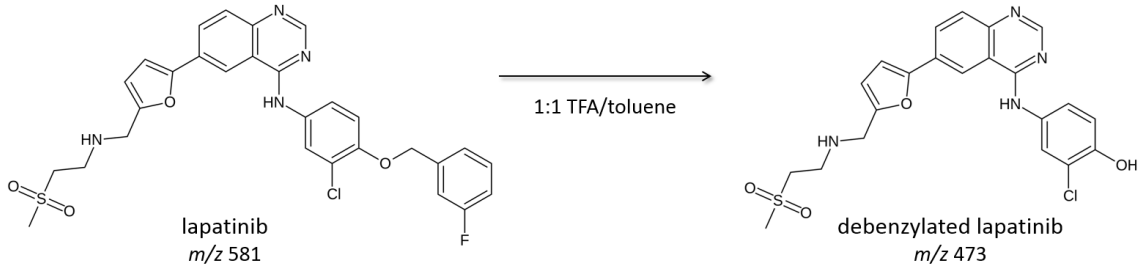

Scheme 2.1 – ***Synthesis of debenzylated lapatinib.*** Debenzylated lapatinib (LAP-OH) was synthesized from lapatinib and then purified using HPLC and analyzed by NMR.

The generation of lapatinib metabolites was investigated to better characterize the bioactivation pathways of lapatinib. Mass spectrometry product ion and MRM methods were developed to detect and identify lapatinib and each of the metabolites of interest.

Lapatinib (LAP): The MH^+ ion of LAP appears at *m/z* 581. Collision-induced dissociation of this ion yielded fragmentation with neutral loss of 217 atomic mass units (amu) that yielded the major product ion *m/z* 365 $[M + H - 217]^+$. This corresponds to fragmentation of lapatinib at two locations. Figure 2.2 shows a representative LC-MS/MS chromatogram of lapatinib, monitoring the precursor to product transition *m/z* 581 → 365 (retention time 6.79 min).

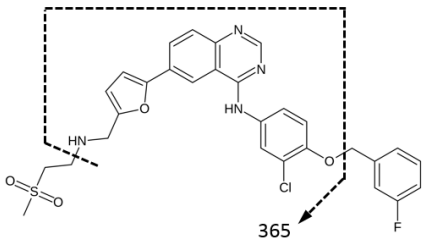

lapatinib: *m/z* 581

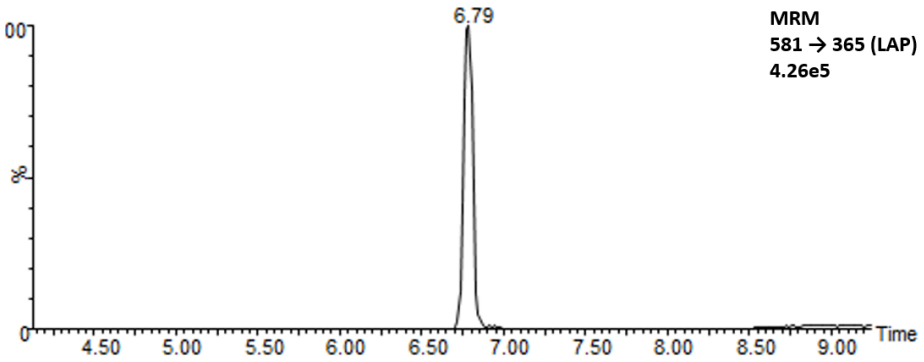

Figure 2.2 – ***LC-MS/MS analysis of lapatinib (LAP).*** *Representative LC-MS/MS chromatogram of lapatinib monitoring the precursor to product transition m/z 581 → 365.*

Debenzylated Lapatinib (LAP-OH): LAP-OH was identified following treatment of HepaRG cells with LAP (100 µM) for 24 hr and analyzed using LC-MS/MS. The MH^+ ion of LAP-OH appears at *m/z* 473. Figure 2.3B shows the enhanced product ion spectrum of LAP-OH (*m/z* 473), which exhibited a neutral

loss of 123 amu, yielding the product ion *m/z* 350, $[M + H - 123]^+$. This corresponds to fragmentation adjacent to the secondary amine moiety of lapatinib. Figure 2.3A shows a representative LC-MS/MS chromatogram of LAP-OH, monitoring the precursor to product transition *m/z* 473 → 350 (retention time 5.16 min).

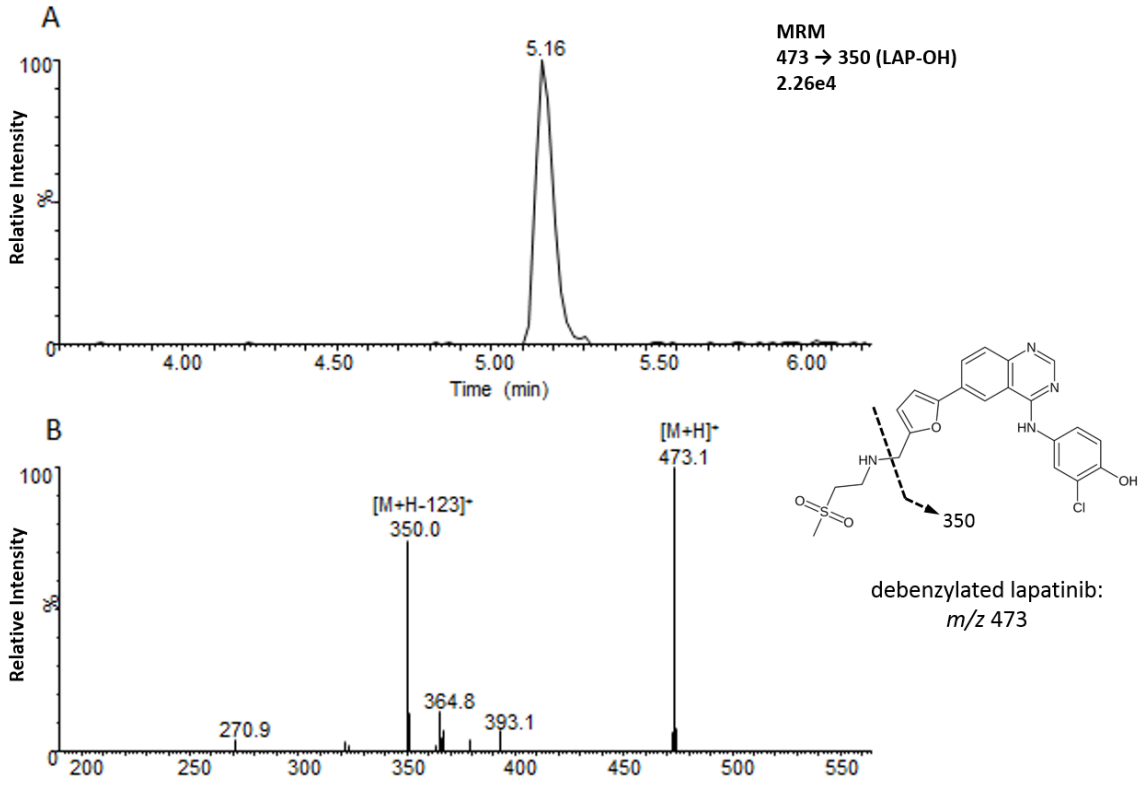

Figure 2.3 – ***LC-MS/MS analysis of the O-debenzylated metabolite of lapatinib (LAP-OH).*** *HepaRG cells were treated with LAP (100 µM) for 24 hr. (A) Representative LC-MS/MS chromatogram of LAP-OH, monitoring the precursor to product transition m/z 473 → 350. (B) Product ion scans of the MH^+ precursor ion m/z 473 obtained by collision induced dissociation in ESI+ mode.*

<u>*N*-Dealkyl Lapatinib</u>: *N*-Dealkyl-LAP was identified following treatment of HepaRG cells with LAP (100 µM) for 24 hr and analyzed using LC-MS/MS. The MH^+ ion of *N*-dealkyl-LAP appears at *m/z* 475. Figure 2.4B shows the enhanced product ion spectrum of *N*-dealkyl-LAP (*m/z* 475), which exhibited a neutral

loss of 109 amu, yielding the product ion *m/z* 366, $[M + H - 109]^+$. This corresponds to fragmentation of the *O*-fluorobenzyl bond of lapatinib. Figure 2.4A shows a representative LC-MS/MS chromatogram of *N*-dealkyl-LAP, monitoring the precursor to product transition m/*z* 475 → 366 (retention time 6.21 min).

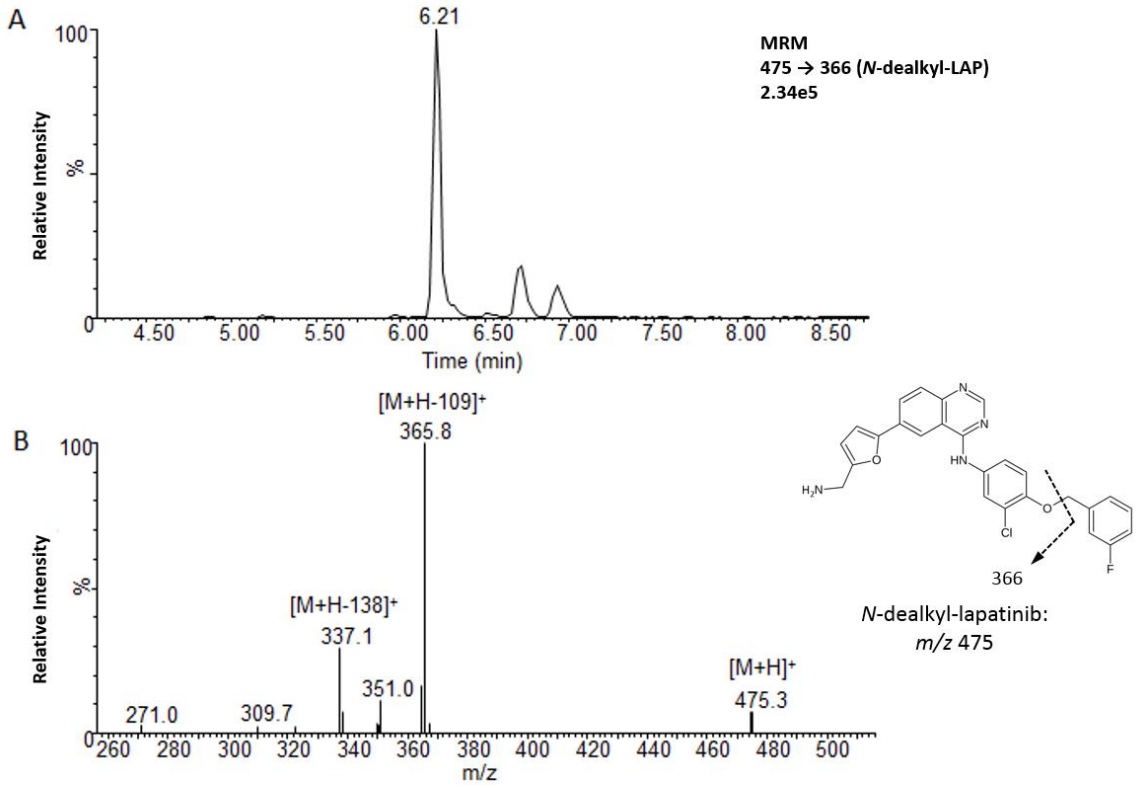

Figure 2.4 – ***LC-MS/MS analysis of the N-dealkylated metabolite of lapatinib (N-dealkyl-LAP).*** *HepaRG cells were treated with LAP (100 µM) for 24 hr. (A) Representative LC-MS/MS chromatogram of N-dealkyl-LAP, monitoring the precursor to product transition m/z 475 → 366. (B) Product ion scan of the MH^+ precursor ion m/z 475 obtained by collision induced dissociation in ESI+ mode.*

<u>*N*-Hydroxy Lapatinib (*N*-OH-LAP)</u>: *N*-OH-LAP was identified following treatment of HepaRG cells with LAP (100 µM) for 24 hr and analyzed using LC-MS/MS. The MH^+ ion of *N*-OH-LAP appears at *m/z* 597. Figure 2.5B shows the enhanced product ion spectrum of *N*-OH-LAP (*m/z* 597), which exhibited a

neutral loss of 138 amu, yielding the product ion *m/z* 459, $[M + H - 138]^+$. This corresponds to fragmentation adjacent to the *N*-OH group of lapatinib. Figure 2.5A shows a representative LC-MS/MS chromatogram of *N*-OH-LAP, monitoring the precursor to product transition *m/z* 597 → 459 (retention time 6.89 min).

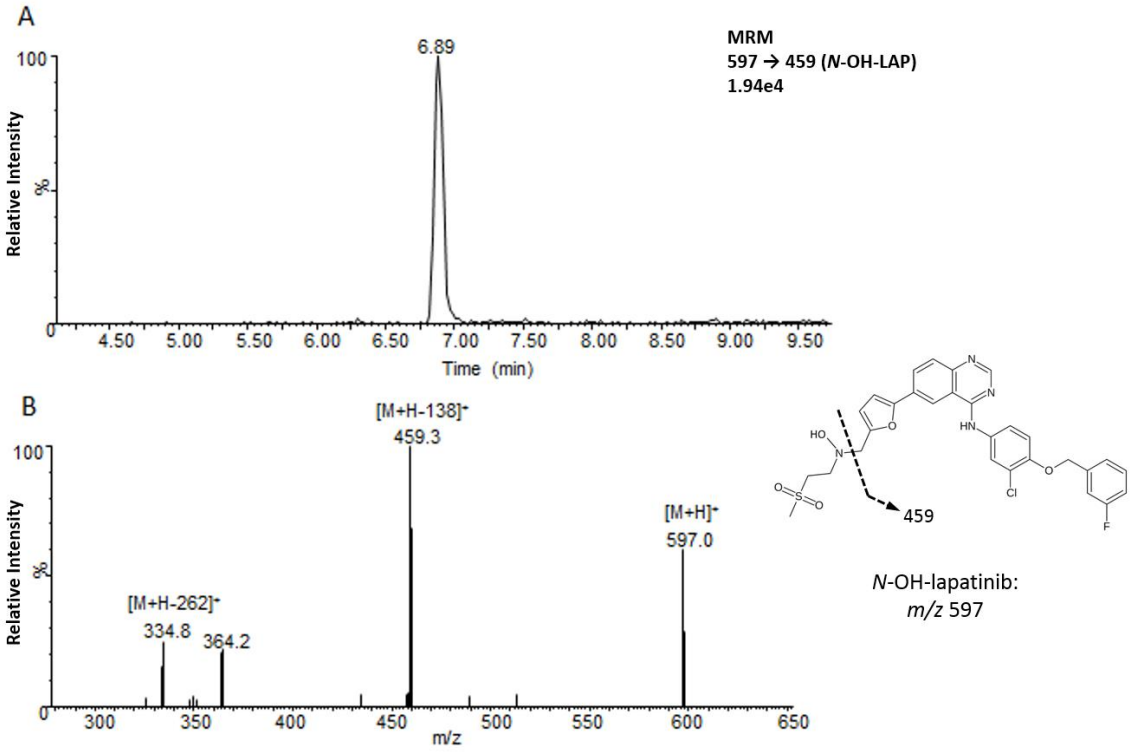

Figure 2.5 – ***LC-MS/MS analysis of the N-hydroxylated metabolite of lapatinib (N-OH-LAP).*** *HepaRG cells were treated with LAP (100 µM) for 24 hr. (A) Representative LC-MS/MS chromatogram of N-OH-LAP, monitoring the precursor to product transition m/z 597 → 459. (B) Product ion scan of the MH^+ precursor ion m/z 597 obtained by collision induced dissociation in ESI+ mode.*

Reactive Metabolite Glutathione Adduct (RM-SG): RM-SG adducts were identified following incubation of LAP-OH (100 µM) for 1 hr in pooled human liver microsomes (HLM) supplemented with NADPH and GSH (50 mM). Samples were analyzed using LC-MS/MS. The MH^+ ion of the RM-SG adduct

appears at *m/z* 778, collision-induced dissociation of which resulted in a neutral loss of 123 amu, which corresponds to fragmentation of the lapatinib portion of the molecule to yield the product ion *m/z* 655 $[M + H - 123]^+$. Subsequent neutral loss of 129 amu from the *m/z* 655 ion was also observed, resulting from loss of the elements of pyroglutamic acid from the GSH adduct, as previously described (Evans et al., 2004), to yield the product ion *m/z* 526 $[M + H - 252]^+$ (Figure 2.6A). This product ion spectrum is consistent with previous reports from LC-MS/MS analysis of the RM-SG adduct formed in human liver microsomes and recombinantly expressed CYP enzymes (Teng et al., 2010; Chan et al., 2012). Treatment of HepaRG cells with LAP (100 µM) resulted in levels of GSH adducts near the limit of detection; however, GSH adducts were readily detectable in cells treated with LAP-OH (100 µM). Figure 2.6B shows a representative LC-MS/MS chromatogram of the RM-SG adduct, monitoring the precursor to product transition *m/z* 778 → 655 (retention time 4.87 min).

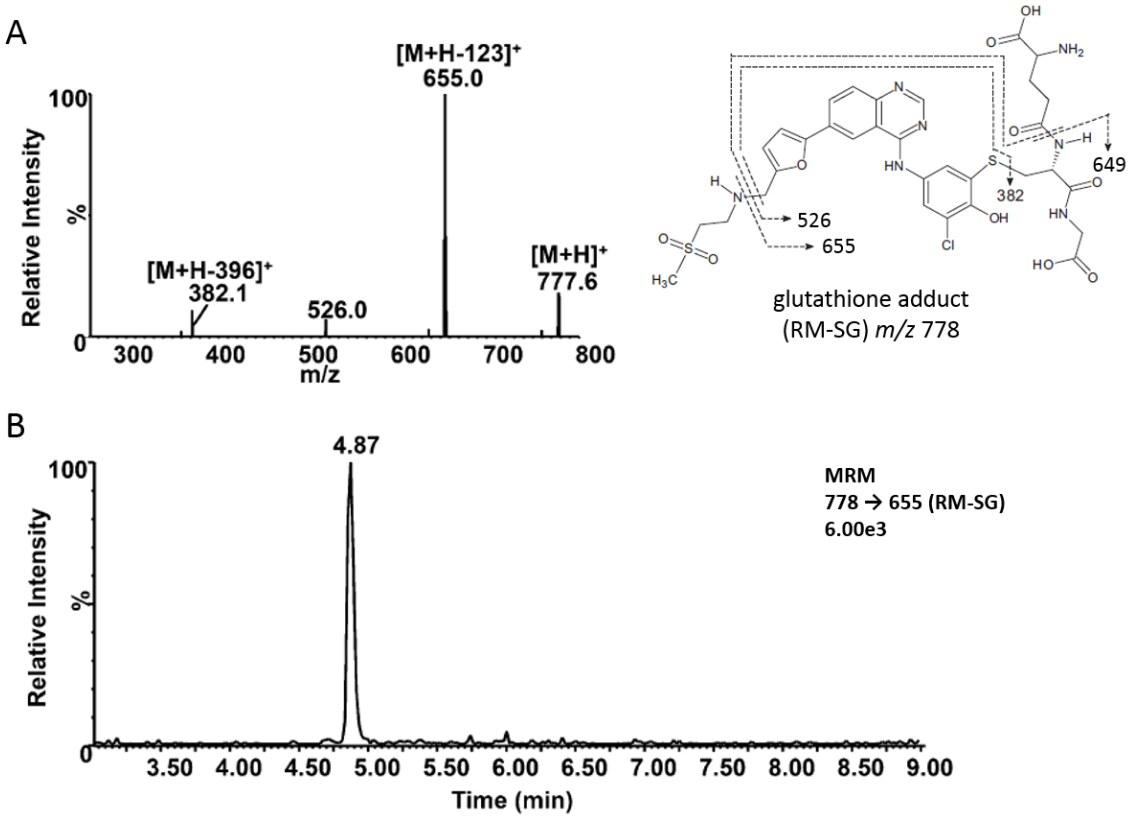

Figure 2.6 – ***LC-MS/MS analysis of the reactive metabolite glutathione lapatinib adduct (RM-SG).*** *(A) Enhanced product ion scan of the putative quinoneimine reactive metabolite-GSH adduct (RM-SG; m/z 778) formed in pooled human liver microsomes incubated with LAP-OH (100 µM) for 1 hr and supplemented with NADPH and GSH (50 mM). (B) MRM chromatogram of RM-SG from incubation of LAP-OH (100 µM) in HepaRG cells for 24 hr.*

Contributions of CYP3A4 and CYP3A5 Isoforms to Lapatinib Metabolism

The metabolism of lapatinib by CYP3A4 differs from its metabolism by CYP3A5. Previous studies from our laboratory demonstrated that formation of the *N*-OH-LAP metabolite was more than 10-fold lower in CYP3A5 incubations than in CYP3A4 incubations, and that MI complex formation did not occur with CYP3A5 as it did with CYP3A4 (Takakusa et al., 2011). In this experiment, metabolite formation was analyzed in incubations with recombinant CYP3A4 and CYP3A5 to specifically address whether there is an observable difference in the metabolic pathway between the two enzymes. Metabolite formation in a 30 min incubation with CYP3A5 Supersomes™ was compared with metabolite formation in a 30 min incubation with CYP3A4 Supersomes™ and the relative amounts of each metabolite formed are shown in Figure 2.7. LAP-OH was formed to a greater extent in CYP3A5 compared to CYP3A4, while *N*-OH-LAP remained the same and *N*-dealkyl-LAP was formed to a much lesser extent by CYP3A5.

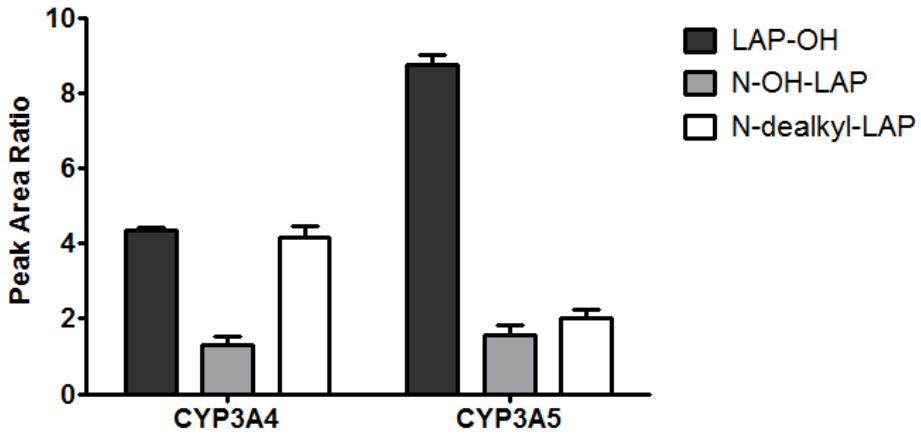

Figure 2.7 – ***Relative contributions of CYP3A4 and CYP3A5 isoforms to lapatinib metabolism.*** *LAP (50 µM) was incubated with CYP3A4 and CYP3A5 Supersomes™ for 30 min. The ratio of metabolite formation was determined by LC-MS analysis with MRM. Data represent the mean ± S.D. for triplicate samples.*

Along the *O*-debenzylation bioactivation pathway, lapatinib is metabolized to LAP-OH, which is further oxidized to an electrophilic quinoneimine capable of adducting to glutathione. To further probe the relative roles of CYP3A4 and CYP3A5 in the formation of LAP-OH and subsequent formation of RM-SG, CYP3A4 and CYP3A5 Supersomes™ (20 pmol/mL) were incubated with LAP (5 µM) for 1-30 min. Formation of LAP-OH and RM-SG adducts were quantified by LC-MS analysis with MRM. The formation of LAP-OH by CYP3A4 was linear until about 2 min, but autoinhibition was observed in longer incubations (Figure 2.8). LAP-OH formation by CYP3A5 was linear until about 10 min, at which point it started leveling off. The formation of RM-SG was relatively linear over the time period studied in both enzyme systems. From these observations, a 2 min incubation was chosen for future studies quantifying LAP-OH, as metabolite formation is linear for both CYP3A4 and CYP3A5 over that time period. A 20 min incubation was chosen for studies quantifying RM-SG.

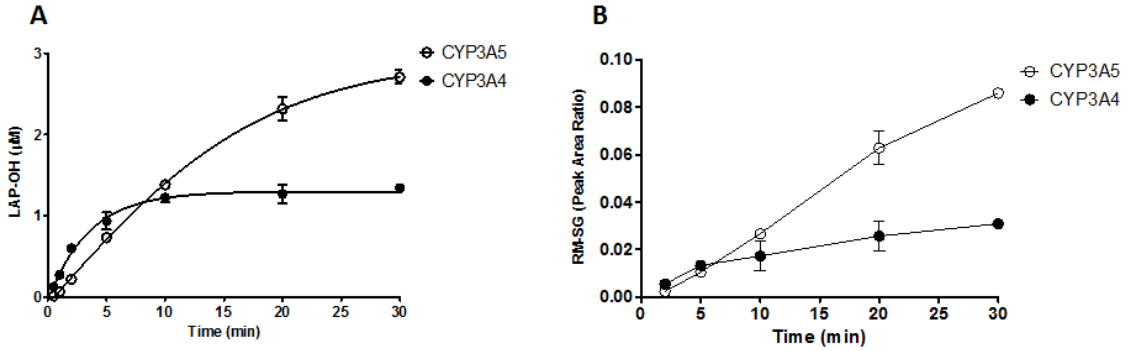

Figure 2.8 – ***Time course for formation of LAP-OH and RM-SG by recombinant CYP3A4 and CYP3A5.*** *LAP (5 µM) was incubated with CYP3A4 and CYP3A5 Supersomes™ (20 pmol/mL) for 1-30 min at 37°C. Formation of (A) LAP-OH and (B) RM-SG adduct were quantified by LC-MS analysis with MRM.*

Formation of LAP-OH and RM-SG Adducts by Individual CYP Isoforms

Although CYP3A4 and CYP3A5 are the major P450 isoforms responsible for the metabolism of lapatinib, CYP2C19 and CYP2C8 have also been identified as minor contributors (GlaxoSmithKline, 2007). Using the timecourse information from the previous study, incubations were carried out with Supersomes™ expressing nine different P450 isoforms. In the 2 min incubation, CYP3A4 and CYP3A5 were the only isoforms that metabolized LAP to LAP-OH (Figure 2.9A). In 20 min incubations, CYP3A4 was the most efficient at metabolizing LAP to RM-SG (Figure 2.9B), while CYP3A5 also resulted in detectable formation. The formation of RM-SG from LAP-OH was also catalyzed most effectively by CYP3A4, although CYP3A5 and CYP2D6 also formed RM-SG at approximately 1/3 the rate for CYP3A4. Based on these observations, CYP3A4 and CYP3A5 remain the most important isoforms to consider with respect to the *O*-debenzylation bioactivation pathway of lapatinib.

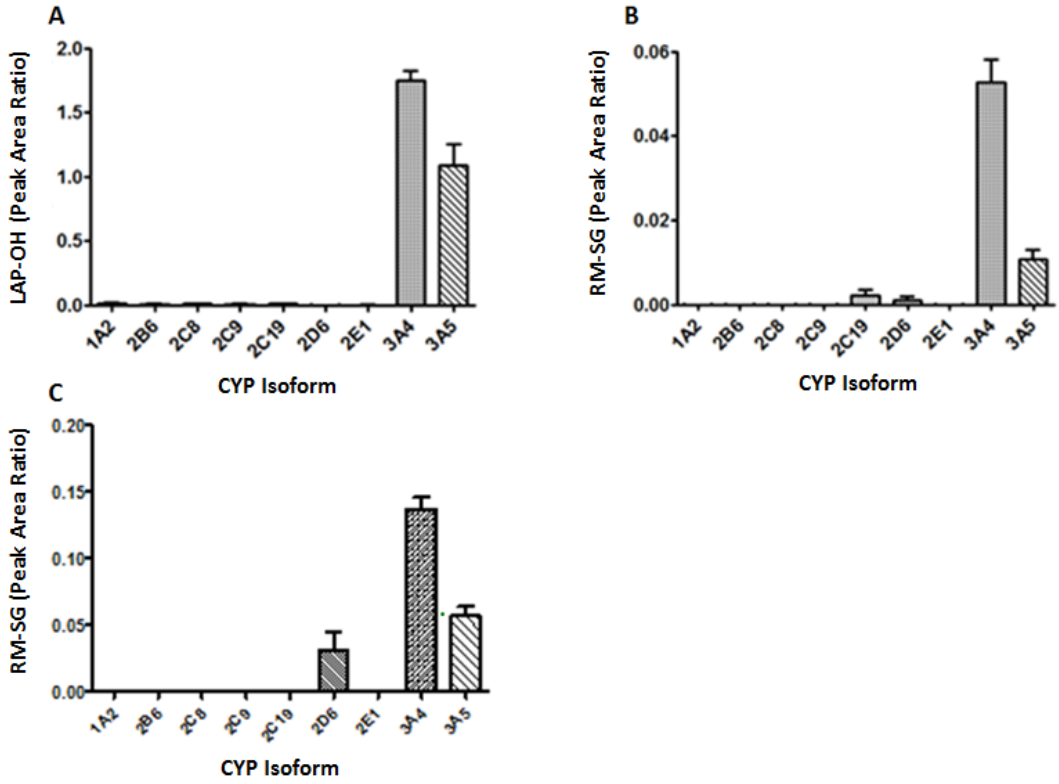

Figure 2.9 – ***Formation of LAP-OH and RM-SG by individual CYP isoforms.*** *To assess LAP-OH formation, CYP Supersomes™ (20 pmol CYP protein/mL) were incubated with (A) LAP (5 µM) for 2 min at 37°C. To assess the formation of reactive metabolite GSH adducts, CYP Supersomes™ (20 pmol CYP protein/mL) were incubated with (B) LAP (5 µM) or (C) LAP-OH (5 µM) plus GSH (50 mM) for 20 min. Formation of LAP-OH and LAP-SG was measured by LC-MS analysis with MRM. Data represent the mean ± S.D. of triplicate samples.*

Kinetic Experiments for the Formation of LAP-OH and RM-SG in HLM and Recombinant CYP3A4 and CYP3A5

Based on the observation that CYP3A4 and CYP3A5 are the P450 isoforms that are important in the metabolism of LAP to LAP-OH and RM-SG, the kinetic parameters of lapatinib *O*-debenzylation by CYP3A4 and CYP3A5 Supersomes™ were examined and compared to human liver microsomes (HLMs). CYP3A4 and CYP3A5 Supersomes™ (20 pmol/mL) and HLMs (0.1 mg protein/mL) were incubated with LAP (0.1-100 µM) for 2 min and formation of LAP-OH was quantified by LC-MS analysis with MRM. The velocity-substrate concentration plots for formation of LAP-OH by recombinant enzyme systems and HLMs are shown in Figure 2.10. The kinetic parameters were estimated by fitting data to a Michaelis-Menten kinetic model and are reported in Table 2.1. CYP3A4 and CYP3A5 Supersomes™ turned over lapatinib rapidly (V_{max} = 15-18 pmol min^{-1} $pmol^{-1}$ CYP3A) and with moderate affinity (K_m = 1.0-2.2 µM). CYP3A4 exhibited an overall 2.7-fold higher catalytic efficiency (CL_{int} = V_{max}/K_m) than CYP3A5 (Figure 2.10, Table 2.1).

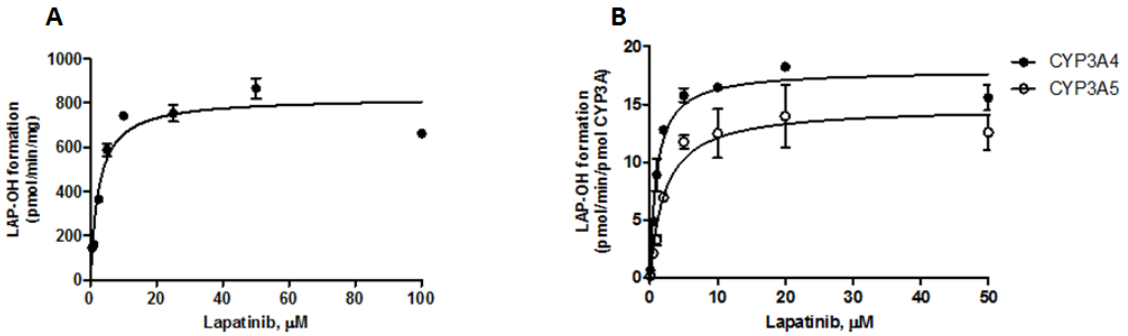

Figure 2.10 – ***Kinetics of the formation of LAP-OH in HLM and recombinant CYP3A4 and CYP3A5.*** *(A) LAP (0.1-100 µM) was incubated in pooled HLMs (0.1 mg protein/mL) for 2 min. (B) LAP (0.1-100 µM) was incubated in CYP3A4 or CYP3A5 Supersomes™ (20 pmol/mL) for 2 min. Formation of LAP-OH was quantified by LC-MS analysis with MRM. Data represent the mean ± S.D. of triplicate samples.*

	K_m (µM)	V_{max} (pmol min^{-1} mg protein)	CL_{int} (µL min^{-1} mg protein)
HLM	2.54 ± 0.52	10.2 ± 0.47	4.02
	K_m (µM)	V_{max} (pmol min^{-1} $pmol^{-1}$ CYP3A)	CL_{int} (µL min^{-1} $pmol^{-1}$ CYP3A)
CYP3A4	1.00 ± 0.16	18.0 ± 0.58	17.9
CYP3A5	2.21 ± 0.56	14.8 ± 0.88	6.68

Table 2.1 – ***Kinetic parameters for the formation of LAP-OH in pooled HLM and recombinant CYP3A4 and CYP3A5.*** *Data were fit to the Michaelis-Menten equation by non-linear regression analysis using GraphPad Prism 5 software to derive K_m and V_{max} values. Intrinsic clearance (CL_{int}) values were calculated as $CL_{int} = V_{max}/ K_m$. Data represent the mean ± S.D. of triplicate samples.*

CYP3A4 and CYP3A5 Supersomes™ (20 pmol/mL) were incubated with LAP (0.1-100 µM) for 20 min and HLMs (0.1 mg protein/mL) were incubated with LAP-OH (0.1-100 µM) for 20 min. The formation of RM-SG adducts were quantified by LC-MS analysis with MRM. CYP3A5 Supersomes™ were 7.2 times more efficient than CYP3A4 (Figure 2.11, Table 2.2).

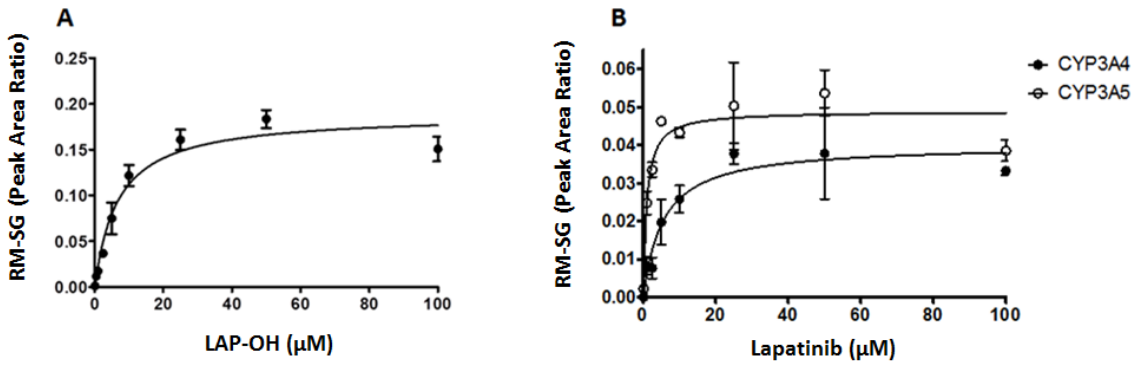

Figure 2.11 – ***Kinetics of the formation of RM-SG in HLM and recombinant CYP3A4 and CYP3A5.*** *(A) LAP-OH (0.1-100 mM) was incubated in pooled HLMs (0.1 mg protein/mL) for 20 min. (B) LAP (0.1-100 µM) was incubated in CYP3A4 or CYP3A5 Supersomes™ (20 pmol/mL) for 20 min. Formation of RM-SG was quantified by LC-MS analysis with MRM. Data represent the mean ± S.D. of triplicate samples.*

	K_m (µM)	V_{max} (pmol min^{-1} mg protein)	CL_{int} (µL min^{-1} mg protein)
HLM	6.83	0.19	0.028
	K_m (µM)	V_{max} (pmol min^{-1} $pmol^{-1}$ CYP3A)	CL_{int} (µL min^{-1} $pmol^{-1}$ CYP3A)
CYP3A4	5.51	0.040	0.0072
CYP3A5	0.944	0.049	0.0519

Table 2.2 – ***Kinetic parameters for the formation of RM-SG in pooled HLM and recombinant CYP3A4 and CYP3A5.*** *Data were fit to the Michaelis-Menten equation using non-linear regression analysis of GraphPad Prism 5 software to derive K_m and V_{max} values. Intrinsic clearance (CL_{int}) values were calculated as $CL_{int} = V_{max}/ K_m$. Data represent the mean ± S.D. of triplicate samples.*

Formation of RM-SG Adducts from LAP-OH in CYP3A5 Genotyped HLMs

To better understand the importance of CYP3A5 genetics *in vivo*, incubations were carried out in genotyped human liver microsomes (*CYP3A5*1/*1*, n = 1; *CYP3A5*1/*3*, n = 7; *CYP3A5*3/*3*, n = 9). Formation of RM-SG by each donor liver microsomal preparation (performed in duplicate) was measured. Analysis of the data by CYP3A5 genotype (Figure 2.13A) suggests a trend in RM-SG

formation according to the number of *CYP3A5*1* alleles. The levels of RM-SG were 1.85-fold higher (*P* = 0.03) in human liver microsomes from *CYP3A5*1* expressors compared to microsomes from *CYP3A5*3/*3* livers (Figure 2.13B).

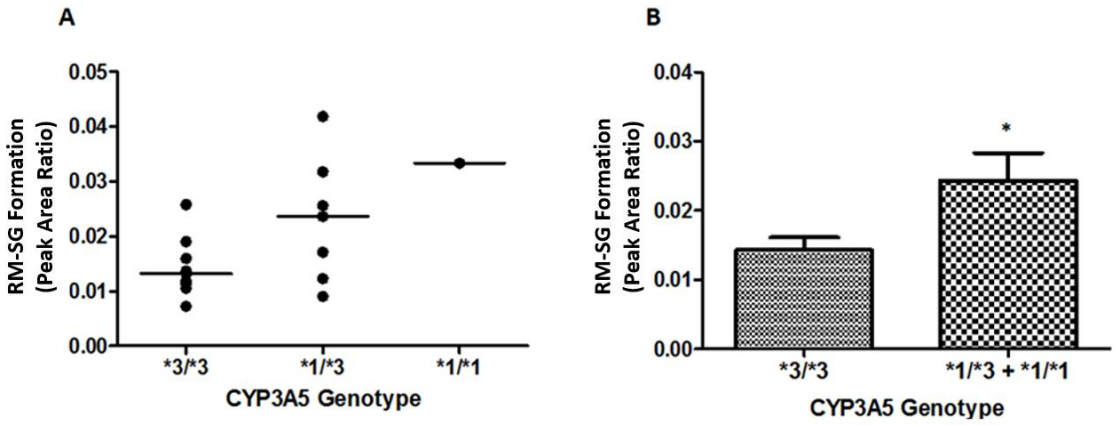

	CYP3A5*3/*3 (n = 9)	***CYP3A5*1/*3*** (n = 7)	***CYP3A5*1/*1*** (n = 1)
RM-SG formation *(peak area ratio)*	*0.013 (0.007 – 0.026)*	*0.024 (0.009 – 0.042)*	*0.033*

Figure 2.12 – ***Formation of RM-SG from LAP-OH in CYP3A5 genotyped HLMs.*** *Genotyped HLMs (0.1 mg protein/mL) were incubated for 20 min with LAP-OH (5 µM) and GSH (50 mM). Formation of RM-SG was measured by LC-MS analysis with MRM. (A) Data represent the mean of n=2 for each liver. (B) Data represent the mean ± S.E.M. for each group. *P < 0.05 compared with CYP3A5*3/*3 HLMs (unpaired t test, two-tailed P values).*

Discussion:

Synthesis, Detection, and Identification of Lapatinib Metabolites

Lapatinib has previously been shown to be metabolized by CYP3A4 via three primary metabolic pathways: *O*-dealkylation, *N*-dealkylation, and *N*-hydroxylation (Figure 1.8; Takakusa et al., 2011; Castellino et al., 2012). *N*-dealkylation and/or *N*-hydroxylation pathways lead to the formation of a

nitroso intermediate, which forms a coordination complex with the heme iron of CYP3A4 (Takakusa et al., 2011). This MI complex is potentially clinically important because of the DDIs that may occur upon coadministration with other drugs that are CYP3A4 substrates (GlaxoSmithKline, 2007). Metabolism via the *O*-dealkylation pathway leads to formation of an *O*-dealkylated phenolic metabolite, which can be further oxidized to a reactive quinoneimine intermediate (Teng et al., 2010). It is this pathway that may lead to the observed hepatotoxicity of lapatinib and that was the focus of these investigations.

The major metabolites in all main pathways were detected and identified in incubations with human liver microsomes and HepaRG cells. These included LAP, LAP-OH, *N*-dealkyl-LAP, *N*-OH-LAP, and RM-SG. The mass spectrometry product ion scanning and MRM methods were developed and used in subsequent metabolism studies to identify lapatinib metabolites and provide semi-quantitative data on their rates of formation.

Contributions of CYP3A4 and CYP3A5 Isoforms to Lapatinib Metabolism

The contributions of CYP3A4 and CYP3A5 to the metabolism of lapatinib differ, which may lead to the observed differences in MI complex formation between the two isoforms (Takakusa et al., 2011). Initial experiments suggested that the *O*-debenzylation metabolic pathway dominates in incubations with CYP3A5 (30 min incubation, 50 µM LAP), while the *N*-dealkylation and *O*-debenzylation pathways are equally important in incubations with CYP3A4 (Figure 2.7). Because CYP3A5 polymorphisms lead to differences in relative expression levels of these two enzymes, and thus may affect DDIs and liver injury in an individual, further studies on the contribution of individual isoforms to the *O*-debenzylation metabolic pathway were warranted.

Lapatinib is a pseudo-irreversible mechanism-based inhibitor of CYP3A4 (Takakusa et al., 2011), and thus the role of CYP3A4 in lapatinib metabolism may be most important at the beginning of therapy and diminish thereafter. A similar phenomenon is observed for the metabolism of imatinib, another tyrosine kinase inhibitor, by CYP3A4 and CYP2C8 (Filppula et al., 2013). In this case, the importance of CYP2C8 increases with time as CYP3A4 is inhibited. A timecourse analysis of the formation of LAP-OH and RM-SG by recombinant CYP3A4 and CYP3A5 demonstrated increased activity by CYP3A5 at the 30 min time point, as seen in the previous experiment, but revealed that CYP3A4 had already started to exhibit autoinhibition by lapatinib at this time point (Figure 2.8). The formation of LAP-OH was linear for only about 2 min in CYP3A4, and about 10 min in CYP3A5 incubations. The formation of RM-SG was relatively linear over the 30 min incubation in both enzyme systems. From these observations, a 2 min incubation was chosen for studies quantifying LAP-OH since metabolite formation is linear for both isoforms over that time period. A 20 min incubation was chosen for studies quantifying RM-SG.

Formation of LAP-OH and RM-SG Adducts by Individual CYP Isoforms

Lapatinib biotransformation via the *O*-debenzylation pathway was investigated in nine different CYP isoforms including CYP3A4 and CYP3A5, the major isoforms responsible for its metabolism, and CYP2C19 and CYP2C8, which have been identified as minor contributors (GlaxoSmithKline, 2007). Based on these results, CYP3A4 and CYP3A5 remain the important isoforms to consider with respect to the *O*-debenzylation bioactivation pathway of lapatinib, although minor contributions were observed from CYP2D6 and CYP2C19. CYP3A4 was more active than CYP3A5 in metabolizing LAP to LAP-OH, which is consistent with the timecourse data (Figure 2.8A). Interestingly, however, these results show that RM-SG levels are higher for CYP3A4 compared to CYP3A5 after a 20 min incubation with lapatinib. This is in contrast to the timecourse experiment with LAP-OH where CYP3A5 generated more RM-SG at 20 min than CYP3A4 (Figure 2.8B). Based on this discrepancy, further studies were

deemed necessary to assess the relative importance of CYP3A4 and CYP3A5, the major contributors to lapatinib *O*-debenzylation.

Kinetic Experiments for the Formation of LAP-OH and RM-SG in HLM and Recombinant CYP3A4 and CYP3A5

Based on the results from the previous experiment, which suggested that CYP3A4 and CYP3A5 were the two primary enzymes important in the biotransformation of lapatinib via *O*-debenzylation, further kinetic studies were performed on metabolite formation by these isoforms. Incubations carried out with recombinant CYP3A4 and CYP3A5 Supersomes™ demonstrated rapid turnover and high affinity for lapatinib. The catalytic efficiency (CL_{int} = k_{cat}/K_m) for the conversion of LAP to LAP-OH was the highest for CYP3A4, followed by CYP3A5, and then HLMs (Table 2.1). The relative efficiencies of CYP3A4 and CYP3A5 for this step in the metabolic pathway following a 2 min incubation are in line with previous experiments (Figure 2.8A). Following a 20 min incubation with LAP, CYP3A5 Supersomes™ were 7.2 times more efficient than CYP3A4 in generating RM-SG. These observations are consistent with the timecourse data (Figure 2.8B), but not with the results obtained from the CYP isoform screen (Figure 2.9).

Formation of RM-SG Adducts from LAP-OH in CYP3A5 Genotyped HLMs

The *in vitro* results described herein suggest that CYP3A5 may be an important contributor to lapatinib bioactivation in recombinant enzyme systems and pooled HLMs. *In vivo*, CYP3A5 is polymorphically expressed because of mutations in the *CYP3A5* gene, specifically a point mutation in exon 11 (Jounaidi et al., 1996). The alleles that an individual carries determine their expression of CYP3A5 protein. Individuals that carry a *CYP3A5*1* allele express high levels of the functional protein, whereas

individuals homozygous for *CYP3A5*3* alleles have low to undetectable levels of CYP3A5. As discussed earlier, 10-30% of Caucasians, 30-40% of Asians of different ethnic groups, and 50-70% of African Americans express at least one *CYP3A5*1* allele (Kuehl et al., 2001; Lamba et al., 2002). To better understand the role of CYP3A5 expression *in vivo*, genotyped HLMs were incubated with LAP-OH, and formation of RM-SG was analyzed. A positive correlation between RM-SG formation and the number of *CYP3A5*1* alleles was observed (Figure 2.13A), and there was a statistically significant difference between the formation of RM-SG in human liver microsomes from *CYP3A5*1* expressors compared to microsomes from *CYP3A5*3/*3* livers (Figure 2.13B). Because metabolism via the *O*-debenzylation pathway may be implicated in the observed hepatotoxicity of lapatinib, polymorphic expression of CYP3A5 may be an important factor in this toxicity.

In conclusion, assessment of the kinetics of lapatinib metabolism by expressed P450 enzymes suggests that lapatinib *O*-debenzylation is efficiently catalyzed by CYP3A4 and CYP3A5. The findings described herein also suggest that pharmacogenetic polymorphisms of CYP3A5 in HLMs can affect lapatinib metabolism *in vitro*. The contributions of CYP3A5 to lapatinib metabolism may be especially important clinically during long-term medication because of time-dependent inhibition of CYP3A4. A high activity CYP3A5 genotype results in increased formation of the reactive metabolite glutathione conjugate (RM-SG) *in vitro*, suggesting that genetic polymorphisms of CYP3A5 contribute to the overall bioactivation of lapatinib and may result in variations in the incidence of hepatotoxicity *in vivo*. The link between the metabolism and lapatinib and its toxicity will be explored further in the following chapter.

Chapter 3: Metabolism and Cytotoxicity of Lapatinib and its Debenzylated Metabolite in a Hepatocyte Cell Line

Objective: The objective of this investigation was to characterize the role of CYP3A4-mediated metabolic activation in lapatinib-induced hepatotoxicity utilizing HepaRG cells as a model. An important sub aim was to establish the link between CYP3A4 induction by dexamethasone and reactive metabolite formation to provide mechanistic insight into the effect of dexamethasone on lapatinib hepatotoxicity.

Introduction:

Clinical interactions between lapatinib and dexamethasone

Dexamethasone is a corticosteroid commonly used to manage the symptoms of peritumoral edema (such as headache, nausea, vomiting, and mental state alterations) and associated increased intracranial pressure caused by brain metastasis of cancers (Ryken et al., 2010). Dexamethasone is effective, with 75% of patients reporting neurological improvement within 1-3 days after initiation of the drug (Soffietti et al., 2006). Because 37% of patients with HER2 positive tumors have central nervous system (CNS) metastases (Brufsky et al., 2011; Leyland-Jones, 2009) and lapatinib demonstrates modest CNS antitumor activity (Lin et al., 2008; Lin et al., 2009), it is not surprising that concomitant usage of lapatinib and dexamethasone does occur. Dexamethasone has been shown to induce CYP3A4 at clinically relevant concentrations via PXR gene activation (McCune et al., 2000; Pascussi et al., 2000). Since lapatinib is predominantly metabolized by CYP3A4, simultaneous use of the two drugs is expected to lead to a decrease in the effective concentration of lapatinib. Because of this potential DDI, lapatinib's product monograph warns against taking any CYP3A4 inducers while on lapatinib, and dexamethasone is explicitly mentioned. The monograph states that if the two drugs

must be taken simultaneously, the lapatinib dose should be titrated up to 4.5 or 5.5 grams per day, depending on the indication. Indeed, a recent retrospective clinical study demonstrated that concomitant use of dexamethasone and lapatinib by patients with metastatic breast cancer increased the likelihood of the development of hepatotoxicity by 4.57 times (Teo et al., 2012). This same group also demonstrated that treatment of TAMH (transforming growth factor α mouse hepatocyte) cells with lapatinib and dexamethasone resulted in an increase in cytotoxicity compared to treatment with lapatinib alone (Teo et al., 2012). These findings suggest that an increase in lapatinib metabolism following CYP3A4 induction, combined with the necessary increase in dose to keep the effective concentration of lapatinib the same, may lead to a dramatic increase in the formation of lapatinib metabolites, including the reactive debenzylated metabolite discussed herein.

HepaRG cell line: a model for hepatotoxicity

A responsive, human-relevant hepatocyte model is essential to characterize the relationship between reactive metabolite formation and lapatinib-induced hepatotoxicity. While primary human hepatocytes have long served as the gold standard, there are several limitations to their use that made them inadequate for these studies including limited availability, variations between donors, and a loss of drug metabolizing enzyme (CYP3A4) function over time in culture. HepaRG cells are an immortalized liver progenitor cell line that has recently emerged as a useful model for evaluating metabolism-mediated drug toxicity (Andersson et al., 2012). These cells are derived from human hepatocellular carcinoma and can be differentiated into hepatocyte-like and biliary epithelial-like cells (Aninat et al., 2006; Guillouzo et al., 2007) with a stable phenotype. Several different groups have demonstrated that differentiated HepaRG cells express most relevant drug-metabolizing enzymes, including CYP3A4, and many important drug transporters and transcription factors at levels comparable to freshly isolated hepatocytes (Aninat et al., 2006; Rogue et al., 2012; Kanebratt and

Andersson, 2008b; Antherieu et al., 2010; Guillouzo et al., 2007). While most drug metabolizing enzymes appear to be present and active at levels similar to those of primary human hepatocytes, there are a few notable variations. HepaRG cells are derived from a specific genotype, which expresses genotypically variant alleles for CYP2D6 and CYP2C9 (Andersson et al., 2012). The intermediate genotype of these two enzymes expressed by the HepaRG cell line has a slower metabolic capacity than the wild-type enzyme, which results in low CYP2D6 metabolic activity as measured using dextromethorphan as the substrate (Kanebratt and Andersson, 2008b) and low CYP2C9-dependent hydroxylation of diclofenac and tolbutamide (Aninat et al., 2006; Kanebratt and Andersson, 2008b). In comparison with freshly isolated primary human hepatocytes, the activities of CYP2E1 and CYP1A2 were also relatively low in differentiated HepaRG cells (Turpeinen et al., 2009; Aninat et al., 2006; Kanebratt and Andersson, 2008b). Despite these notable differences between HepaRG cells and primary human hepatocytes in enzyme function, Zanelli et al. found that the *in vitro* clearance of 26 P450 substrates in HepaRG cultures was in quantitative agreement with the clearance of these same drugs in primary human hepatocytes (Zanelli et al., 2012).

Another important component of the hepatocyte model used in these studies was the ability for drug metabolizing enzyme levels to be induced and inhibited. HepaRG cells have been shown to respond to prototypical P450 inducers such as omeprazole, phenobarbital and rifampicin at both mRNA and enzyme activity levels (Aninat et al., 2006; Antherieu et al., 2010; Kanebratt and Andersson, 2008a; McGinnity et al., 2009; Kaneko et al., 2010). PXR, PPARα, and CAR have all been detected in HepaRG cells (Aninat et al., 2006; Kanebratt and Andersson, 2008a).

Some investigations into toxicity of xenobiotics using HepaRG cells have been completed. McGill et al. demonstrated that many features of reactive metabolite-mediated cell injury by acetaminophen

were the same as seen in mouse hepatocytes *in vitro* and rodent livers *in vivo*, including the time course of injury, depletion of cellular glutathione, covalent modification of liver proteins by reactive metabolites, and formation of reactive oxygen and nitrogen species (McGill et al., 2011).

The objective of the current investigation was to utilize HepaRG cells as a model to characterize the role of CYP3A4-mediated metabolic activation in lapatinib-induced hepatotoxicity. An important aim was to establish the link between CYP3A4 induction and reactive metabolite formation by directly testing whether increased CYP3A4 activity resulted in elevated reactive metabolite formation and enhanced cytotoxicity.

Materials and Methods:

Materials

All reagents used in previous studies described in this thesis were obtained from the same sources and prepared in the same manner. LAP-OH was chemically synthesized from lapatinib, as described in Chapter 2. Midazolam and D_4-1'-hydroxymidazolam (Figure 3.1) were purchased from Cerilliant (Rock Round, TX). Cryopreserved differentiated and undifferentiated HepaRG cells were supplied by BioPredic International (Rennes, France). Cryopreserved platable human hepatocytes from two adult donors, one male (lot no. Hu4246) and one female (lot no. Hu1389), were generously provided by Life Technologies (Carlsbad, CA). HepaRG supplements 650 and 670 were purchased from Life Technologies.

L-buthionine sulfoximine (BSO) was purchased from Sigma Aldrich (St Louis, MO). The WST-1 cell viability assay was purchased from Clontech Laboratories, Inc. (Mountain View, CA). All other chemicals and reagents were of analytical grade and were purchased from commercial sources.

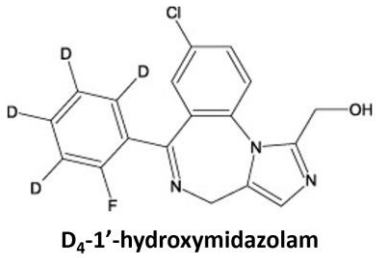

D_4-1'-hydroxymidazolam

Figure 3.1 ***Chemical structure of D_4-1'-hydroxymidazolam.***

HepaRG Cell Culture

Undifferentiated HepaRG cells were terminally differentiated in-house according to the supplier's protocols, as described previously (Gripon et al., 2002). Briefly, cells were first grown for 2 weeks to confluence in culture medium provided by supplier followed by culturing for two weeks in culture media supplemented with 2% DMSO. All cell incubation studies were carried out at 37°C in a humidified atmosphere with 21% O_2 and 5% CO_2. Differentiated cells were plated at a density of approximately 7 x 10^4 cells/well in collagen-coated 96-well microtiter plates according to the manufacturer's instructions and maintained in general purpose medium composed of Williams E medium with GlutaMAX-I supplemented with HepaRG™ Thaw, Seed, and General Purpose supplement 670.

To induce CYP3A4, HepaRG cells were incubated with serum-free induction media composed of Williams E with GlutaMAX-I supplemented with HepaRG™ Serum-free Induction Medium Supplement 650 and containing dexamethasone (100 µM) or rifampicin (4 µM). Test compounds were dissolved in DMSO and added into HepaRG cell media (final concentration 0.1% DMSO). Cells were incubated for a total of 72 hr in induction media, with media changed every 24 hr. Control incubations were conducted with DMSO (0.1%). Initial experiments were carried out to determine maximal induction of CYP3A4 using a range of concentrations of dexamethasone (0.1 – 500 µM). Dexamethasone

treatment alone was not cytotoxic to HepaRG cells over a range of concentrations tested. Following the induction period, CYP3A4 activity in HepaRG cells was measured using midazolam as a probe substrate. Cells were incubated with serum-free incubation media containing midazolam (3 µM) for 1 hr. The reaction was quenched by addition of an equal volume of ice-cold methanol containing D_4-1'-hydroxymidazolam (100 ng/mL), and the supernatant was collected for analysis of 1'-hydroxymidazolam by LC-MS/MS, as described previously (Kirby et al., 2006). Treatment with 100 µM dexamethasone was found to yield maximal induction (approximately 7-fold) of midazolam 1'-hydroxylation activity, compared to treatment with vehicle; thus, 100 µM dexamethasone was used for all subsequent induction studies. Following the 72-h induction period, cell media was replaced with cytotoxicity medium composed of Williams E media with GlutaMAX-I supplemented with HepaRG™ Tox media supplement 630 (HRPG630). Cells were incubated with LAP (10 – 100 µM) or LAP-OH (10 – 100 µM) for 24 hr. Test compounds were dissolved in DMSO:acetonitrile (4:1), and added into HepaRG cell media to a final concentration of 0.4% DMSO, 0.1% acetonitrile. For CYP3A4 inhibition, cells were co-incubated with ketoconazole (4 µM) for 24 hr. In a preliminary range-finding study, incubation of HepaRG cells with 4 µM ketoconazole was found to inhibit CYP3A4 activity by >90%, as measured by midazolam 1'-hydroxylation.

Primary Human Hepatocytes

Hepatocyte donors were fully characterized by the supplier and selected based on the relative extent of CYP3A4 induction, as characterized by the supplier. Cryopreserved hepatocytes were thawed and plated according to the supplier's protocol. Briefly, cells were thawed at 37°C for 60-90 seconds followed by dilution into 50 mL of warmed CHRM® Medium (Cryopreserved Hepatocyte Recovery Medium; Life Technologies). The cell suspension was centrifuged at 100 x g for 10 min. Cells were plated in Williams E medium (without phenol red) containing the Hepatocyte Plating Supplement

Pack (Life Technologies) on 96-well collagen-coated Geltrex™ plates (Life Technologies) at a seeding density of 0.5-0.7 x 10^5 cells/well. After 6 hr, the medium was replaced with incubation medium containing Williams E Medium and Hepatocyte Maintenance Supplement Pack (serum-free). Primary hepatocyte cultures were maintained in incubation medium for 48 hr, followed by incubation with LAP (100 μM) for 24 hr.

Cell Viability and Metabolite Formation

Cell viability in differentiated HepaRG cells and primary human hepatocytes was assessed using WST-1 cell viability assays according to the manufacturer's instructions. Control incubations were conducted by incubation of cells with vehicle control (0.4% DMSO, 0.1% acetonitrile). Briefly, 10 μl of the premixed WST-1 cell proliferation reagent was added to each well of the 96-well plate (1:10 final dilution), and the plate was incubated for 30 min at 37°C, followed by shaking at room temperature for 1 min. Absorbance was measured at 440 nm using a Tecan Infinite M200 microplate reader (Tecan Systems, Inc., San Jose, CA). The reference wavelength was 690 nm. Cell viability following treatment with test compounds was quantified by calculating the % viability compared to cell incubations with vehicle control (untreated).

To determine the extent of lapatinib metabolite formation following incubations in HepaRG cells, 100 μL of ice-cold acetonitrile containing 100 ng/mL of D_4-LAP-OH (*internal standard*) was added to each well in a 96-well microtiter plate. Cells were scraped, and the supernatant was transferred to a 1.7-mL centrifuge tube, vortexed and sonicated for 1 min, followed by centrifugation at 14,000 g for 10 min at 4°C. The supernatant was transferred to a separate vial and dried under N_2 gas at 37°C using a Biotage TurboVap (Biotage, Charlotte, NC). Samples were reconstituted in 100 μL of an acetonitrile:water (1:1) mixture and transferred to LC-MS vials for analysis. For detection and analysis

of reactive metabolite glutathione (RM-SG) and cysteine (RM-Cys) adducts, the supernatant from cell extracts was dried under N_2 gas as described above, and samples were reconstituted in 50 µL of an acetonitrile:water (3:7) mixture for LC-MS/MS analysis.

Analysis and Quantitation of Metabolites by LC-MS/MS

Drug metabolites from cell incubations were analyzed using mass spectrometry, as described in Chapter 2. The gradient program for analysis of lapatinib metabolites was as follows: isocratic at 15% B (0–1.5 min), linear gradient from 15 to 95% B (1.5-5 min), isocratic at 95% B (5-7 min), returned to 15% B (7-7.1 min), and isocratic at 15% B (7.1-9.1 min). The operational conditions of the mass spectrometer were as described in Chapter 2. The MS data were acquired in MS-MRM mode with a collision energy of 30 V. The following LC-MS/MS method was developed to permit the detection and quantitation of lapatinib and lapatinib metabolites based on structurally specific fragmentation obtained from collision-induced dissociation: LAP *m/z* 581 → 365, retention time 6.8 min (Figure 2.1); LAP-OH *m/z* 473 → 350, retention time 5.2 min (Figure 2.2); *N*-OH-LAP *m/z* 597 → 459, retention time 6.9 min (Figure 2.4); RM-SG adduct *m/z* 778 → 655 (Figure 2.5), retention time 4.9 min; internal standard, D_4-LAP-OH *m/z* 477 → 352, retention time 5.2 min. The MS spectral data were analyzed and deconvoluted using MassLynx version 4.1.

Glutathione Depletion

HepaRG cells were pretreated with BSO (25 µM) for 24 hr, followed by incubation with LAP (10, 50, and 100 µM) or vehicle control for 24 hr. BSO treatment alone was not cytotoxic to HepaRG cells over the range of concentrations tested (25-200 µM). Cell viability was monitored using WST-1 assays as described above.

Statistical Analysis

All cell incubations were performed in triplicate in one to three independent experiments (as indicated). The mean and standard deviation (S.D.) or standard error of the mean (S.E.M.) for each experiment were determined using GraphPad Prism 5.0 software (GraphPad Software, San Diego, CA). Treatment groups were compared to their respective controls using Student's *t*-test for unpaired data. P values were calculated by two-tailed analysis, and differences at $P < 0.05$ were considered significant.

Results:

Comparison of the Cytotoxicity of Lapatinib in HepaRG cells and Primary Human Hepatocytes

The cytotoxic effects of lapatinib were examined in HepaRG cells and compared to primary human hepatocytes to evaluate HepaRG cells as a model to study lapatinib-induced hepatotoxicity. Figure 3.2 shows the percent viability of primary human hepatocytes from two donors (Hu4246 and Hu1389) treated with LAP (100 µM) for 24 hr in triplicate for each donor and percent viability of HepaRG cells treated with LAP (100 µM) for 24 hr in three independent experiments performed in triplicate. Treatment of primary human hepatocytes Hu4286 and Hu1389 with LAP for 24 hr resulted in 66.4% ± 18.5% ($P = 0.0151$) and 53.4% ± 28.6% viability ($P = 0.0095$), respectively, compared with the control. Similarly, incubation of HepaRG cells with LAP resulted in 50.9% ± 11.7% viability (mean ± S.D., $P < 0.0001$), compared with the control (Figure 3.2). There was no statistically significant difference between the viability of primary human hepatocytes versus HepaRG cells treated with LAP. These data demonstrate that lapatinib induces cytotoxicity to a similar extent in primary human hepatocytes and HepaRG cells.

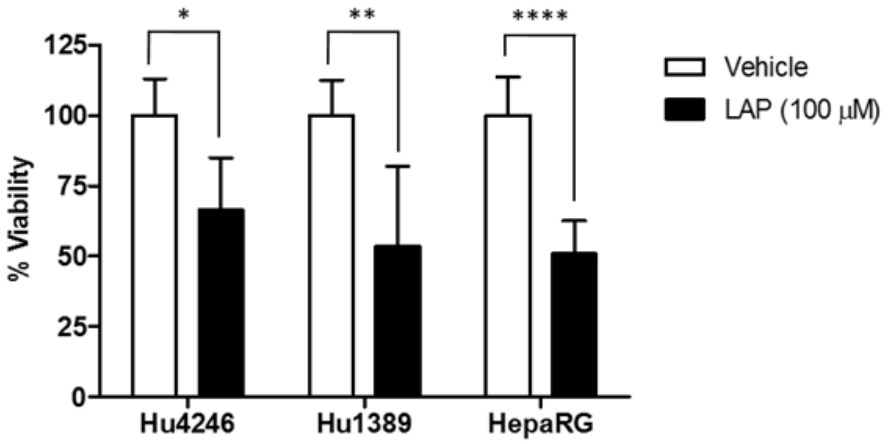

Figure 3.2 – ***Cytotoxicity of LAP in primary human hepatocytes and HepaRG cells.*** *Cryopreserved plated human hepatocytes from two donors (Hu4246 and Hu1389) and HepaRG cells were treated with LAP (100μM) for 24 hr. Cell viability was monitored using WST-1 cell proliferation assays, and viability is expressed as the percent viability compared with vehicle treatment. Data represent the mean ± S.D. of triplicate values of Hu4246 and Hu1389, and the mean ± S.D. of triplicate values from three independent experiments for HepaRG cells. *P < 0.05; **P < 0.01; ****P < 0.0001 compared with vehicle (unpaired t test, two-tailed P values).*

Induction and Inhibition of CYP3A4 in HepaRG Cells

To determine whether our *in vitro* model system, HepaRG cells, could be used to probe the role of metabolism by CYP3A in lapatinib hepatotoxicity, we used dexamethasone, rifampicin, and ketoconazole to induce and inhibit CYP3A4 activity. First, the extent to which dexamethasone induces CYP3A4 activity in HepaRG cells was monitored using midazolam as a CYP3A4 probe substrate. Maximal induction of CYP3A4-dependent midazolam hydroxylation (approximately 7-fold) was achieved with 100 μM dexamethasone (Figure 3.3A), compared with the vehicle control. CYP3A4 activity was also monitored in cells treated with the prototypical CYP3A4 inducer rifampicin. Treatment of cells with 2-4 μM rifampicin resulted in an 18.5-fold increase in midazolam 1'-hydroxylase activity, and midazolam 1'-hydroxylation remained significantly elevated up to 20 μM rifampicin (Figure 3.3B), compared with the vehicle control. In addition, HepaRG cells were treated

with ketoconazole, a prototypical CYP3A4 inhibitor. All concentrations of ketoconazole used (1-20 μM) resulted in a decrease of 96% or greater, as measured by midazolam 1'-hydroxylation (Figure 3.3C). These data confirm that CYP3A4 can be inhibited and induced in HepaRG cells using prototypical inhibitors and inducers, as well as dexamethasone.

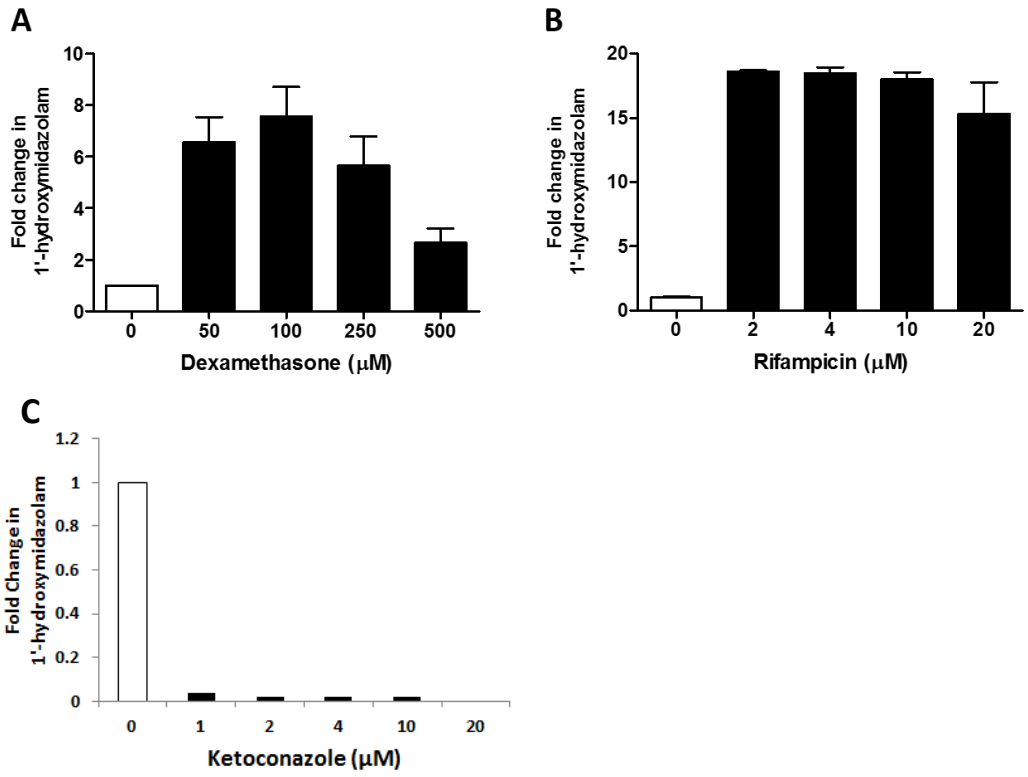

Figure 3.3 – ***Induction and inhibition of CYP3A4 activity by (A) dexamethasone, (B) rifampicin, and (C) ketoconazole.*** *HepaRG cells were pre-treated with varying concentrations of a test compound or vehicle for 72 hr, followed by incubation with midazolam (3 μM) for 1 hr. CYP3A4 activity was assessed by measurement of 1'-hydroxymidazolam using LC-MS/MS. Fold change in 1'-hydroxymidazolam was calculated by comparison to vehicle control (DMSO) pre-treatment. Data represent mean ± S.E.M. of three or four values.*

Effect of CYP3A4 Induction on the Cytotoxicity of Lapatinib in HepaRG Cells

To further probe the role of CYP3A4-mediated metabolism in lapatinib hepatotoxicity, the effect of dexamethasone induction of CYP3A4 in HepaRG cells on lapatinib-induced cytotoxicity was evaluated.

Cell viability was assessed using a WST-1 cell viability assay. Pre-treatment with 100 µM dexamethasone resulted in increased cytotoxicity of LAP at each concentration tested (10 µM, *P* = 0.0006; 50 µM, *P* = 0.0114; and 100 µM, *P* = 0.0093), compared to cells treated with LAP alone (Figure 3.4A). Because dexamethasone is not considered a prototypical inducer, rifampicin was used as a positive control inducer to verify the effect of CYP3A4 induction on lapatinib's cytotoxicity. Similarly to dexamethasone, pre-treatment of HepaRG cells with rifampicin (4 µM) resulted in a significant decrease in cell viability, compared to treatment with LAP alone (Figure 3.4B).

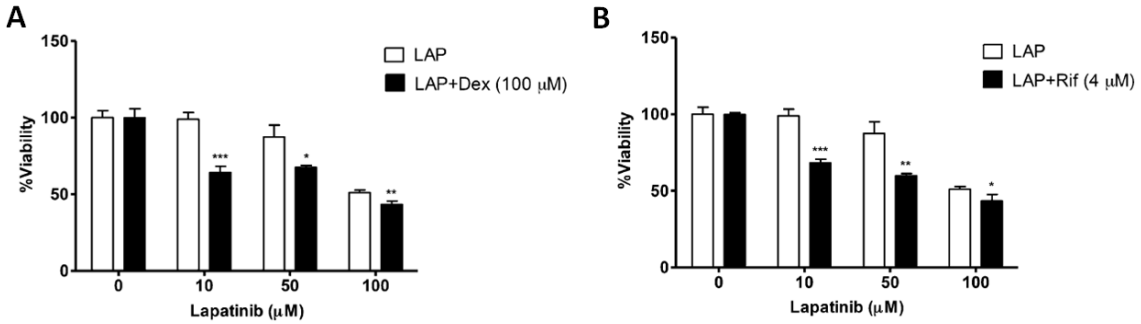

Figure 3.4 – ***Effect of CYP3A4 induction by dexamethasone and rifampicin on the cytotoxicity of lapatinib in HepaRG cells.*** *HepaRG cells were pre-treated with (A) 100 µM dexamethasone or (B) 4 µM rifampicin or vehicle for 72 hr, followed by incubation with LAP (10, 50, 100 µM) or vehicle control for 24 hr. Cell viability was monitored using WST-1 assays and compared with incubation with LAP alone at each concentration. Data represent the mean ± S.D. of triplicate values (n=3). *P < 0.05; **P < 0.01; ***P < 0.001 (unpaired t test, two-tailed P values).*

Additionally, HepaRG cells that had been pre-incubated with dexamethasone (100 µM) were co-incubated with LAP (100 µM) and ketoconazole (1 µM) to determine the effect of CYP3A4 induction on cytotoxicity. Pre-treatment with dexamethasone resulted in a 43% decrease in cell viability (*P* = 0.0034), whereas cell viability was not different from the lapatinib-only control upon treatment with both dexamethasone and ketoconazole (Figure 3.5).

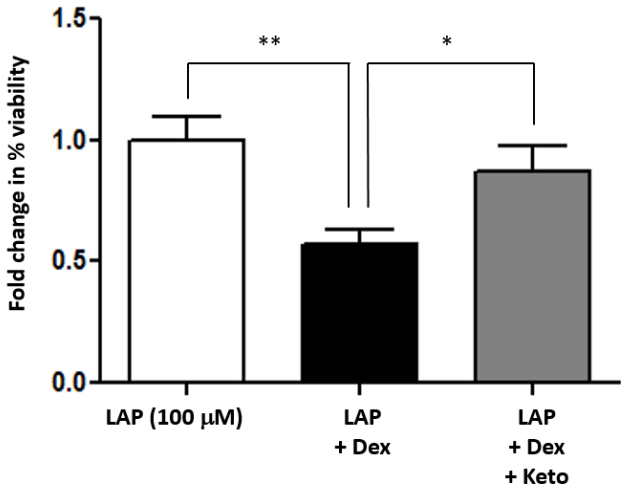

Figure 3.5 – ***Effect of CYP3A4 induction and inhibition by dexamethasone and ketoconazole on lapatinib cytotoxicity in HepaRG cells.*** *For CYP3A4 induction, HepaRG cells were incubated with dexamethasone (100 µM) for 72 hr, followed by incubation with LAP (100 µM) for 24 hr. For CYP3A4 inhibition, HepaRG cells were co-incubated with ketoconazole (1 µM) and LAP (100 µM) for 24 hr. (Mean ± S.E.M., n = 6 for LAP and LAP+Dex; n = 3 for LAP+Dex+Keto, ** P < 0.01 for LAP+Dex compared to treatment with LAP alone; * P < 0.05 for LAP+Dex+Keto compared to LAP+Dex.) Dex = dexamethasone; Keto = ketoconazole*

Cytotoxicity of Lapatinib vs. Lapatinib Metabolites

The increase in the cytotoxicity of lapatinib observed with CYP3A4 induction is consistent with the toxicity arising from a metabolite rather than the parent drug alone. To better address this possibility, a direct comparison was made between the cytotoxicity of LAP versus its debenzylated metabolite (LAP-OH). HepaRG cells were treated with LAP or LAP-Oh for 24 hr and cell viability was measured using a WST-1 cell viability assay. The viability of cells treated with 50 µM LAP was 97.5% ± 8.70% compared to 51.90% ± 4.17% for cells treated with 50 µM LAP-OH (P = 0.0002). Cell viability was 50.0% ± 3.36% for cells treated with 100 µM LAP compared to 34.9% ± 3.49% for cells treated with 100 µM LAP-OH (P = 0.0067) (Figure 3.6). This demonstrates that LAP-OH is significantly more cytotoxic to

HepaRG cells than lapatinib itself, especially for concentrations under 200 µM. The cytotoxicity of lapatinib was compared with that of *N*-OH-LAP; *N*-OH-LAP was not cytotoxic over the range of concentrations tested (Figure 3.7).

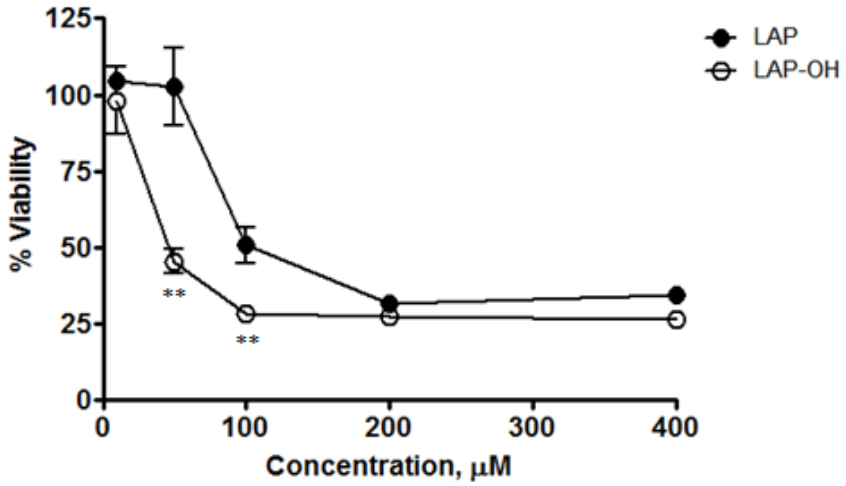

Figure 3.6 – ***Comparison of HepaRG cell viability between treatment with LAP and LAP-OH.*** *HepaRG cells were incubated with varying equimolar concentrations of LAP and LAP-OH for 24 hr. Cell viability was monitored using WST-1 cell proliferation assays. (Mean ± S.E.M., n = 6, ** P < 0.01.)*

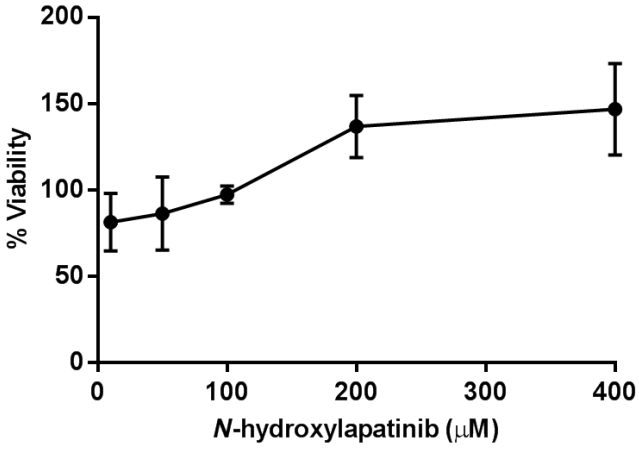

Figure 3.7 – ***Cytotoxicity of N-OH-LAP in HepaRG cells.*** *HepaRG cells were incubated with varying concentrations of N-OH-LAP 24 hr. Cell viability was monitored using WST-1 cell proliferation assays. (Mean ± S.E.M., n = 6.)*

Effect of Glutathione Depletion of the Cytotoxicity of Lapatinib

Previous studies have shown that LAP-OH can undergo further metabolism to an electrophilic quinoneimine intermediate (Teng et al., 2010; Chapter 2). Quinoneimines can readily react with cellular nucleophiles, such as GSH or cysteine residues of proteins, potentially leading to toxicities (Park et al., 2005; Park et al., 2011; Stachulski et al., 2013). On the basis of this observation, an experiment was carried out to determine whether depletion of intracellular GSH could modulate lapatinib cytotoxicity. BSO is an inhibitor of γ-glutamylcysteine synthetase, which catalyzes the rate-limiting step in glutathione biosynthesis, and thus BSO was used experimentally to deplete intracellular GSH stores. In control incubations, treatment with BSO (25 μM) alone was not cytotoxic to the cells. However, pretreatment with BSO sensitized the cells to cytotoxicity by lapatinib at subtoxic doses (10 μM) and augmented the toxicity of lapatinib and debenzylated lapatinib at higher doses (50 μM and 100 μM) compared with cells treated with lapatinib or debenzylated lapatinib alone (Figure 3.8B).

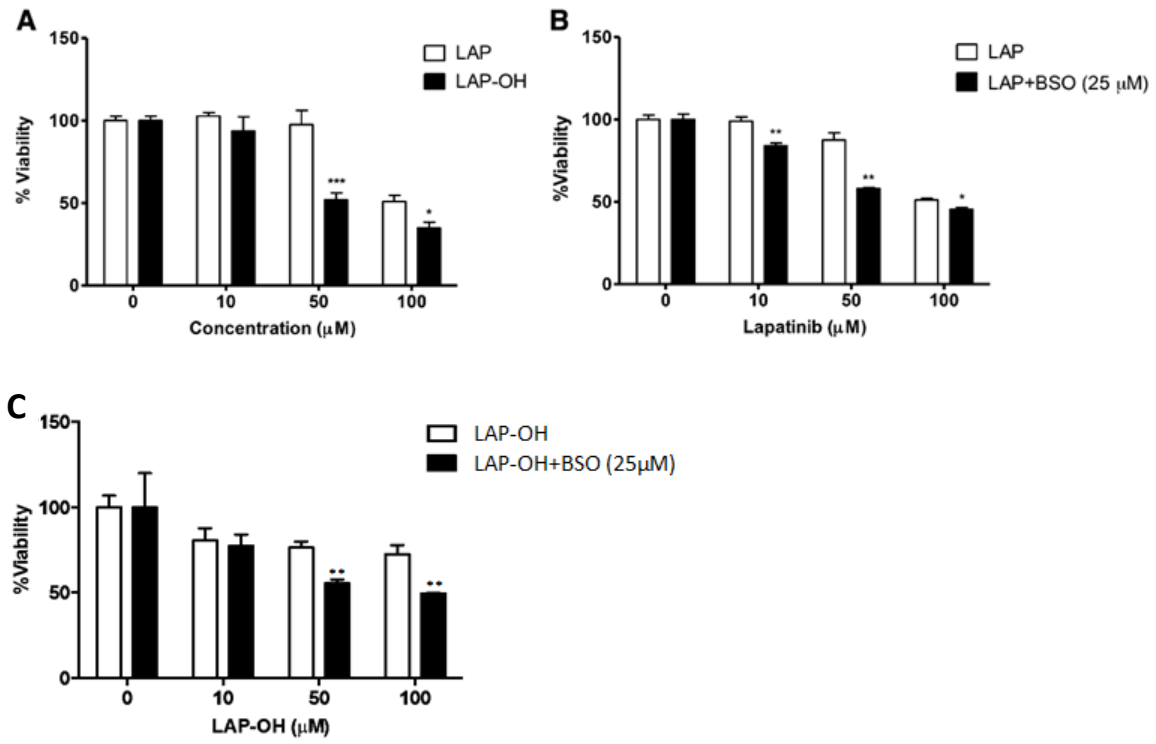

Figure 3.8 – ***Cytotoxicity of lapatinib versus debenzylated lapatinib in HepaRG cells and the effect of glutathione depletion by BSO on LAP-induced and LAP-OH-induced cytotoxicity.*** *(A) HepaRG cells were incubated with LAP or LAP-OH (10, 50, 100 μM) or vehicle control for 24 hr. (B) HepaRG cells were pretreated with 25 μM BSO for 24 hr, prior to incubation with LAP (10, 50, 100 μM) or vehicle control for 24 hr. (C) HepaRG cells were pre-treated with 25 μM BSO for 24 hr, prior to incubation with LAP-OH (10, 50, 100 μM) or vehicle control for 24 hr. For (A), LAP-OH was compared with incubation with LAP at each concentration. Data represent means ± S.E.M. of triplicate values from three independent experiments. For (B), incubation with LAP + BSO was compared with LAP alone at each concentration. Data represent the mean ± S.D. of triplicate values. *P < 0.05 (n=3); **P < 0.01; ***P < 0.001 (unpaired t test, two-tailed P values). For (C), incubation with LAP-OH + BSO was compared with LAP-OH alone at each concentration. Data represent the mean ± S.D. of triplicate values. **P < 0.01 (unpaired t test, two-tailed P values).*

Effect of CYP3A4 Induction on the Metabolism of Lapatinib in HepaRG Cells

After establishing that CYP3A4 induction and GSH depletion both potentiate the cytotoxicity of lapatinib, the effect of CYP3A4 induction on the formation of lapatinib metabolites was monitored to evaluate the correlation between cytotoxicity and metabolism. The LAP-OH metabolite and glutathione adducts were measured following pre-incubation with dexamethasone and incubation with lapatinib. Dexamethasone increased LAP-OH levels by 2.4-fold (P = 0.0002) compared to treatment with lapatinib alone (Figure 3.9A) and rifampicin increased LAP-OH formation 4-fold ($P < 0.0001$) compared to treatment with lapatinib alone Figure 3.9C). Co-incubation with the CYP3A4 inhibitor ketoconazole (4 μM) attenuated the effect of dexamethasone (P = 0.0001) and rifampicin ($P < 0.0001$) on formation of LAP-OH (Figure 3.9).

The generation of reactive metabolite thiol adducts were also investigated as a surrogate for conversion of LAP-OH to the electrophilic quinoneimine intermediate. In HepaRG cell incubations carried out with GSH, the formation of reactive metabolite glutathione (RM-SG) adducts was increased 5.3-fold in the presence of dexamethasone (P = 0.0023), compared to treatment with lapatinib alone (Figure 3.9B). Co-incubation with ketoconazole (4 μM) again attenuated the effect of dexamethasone.

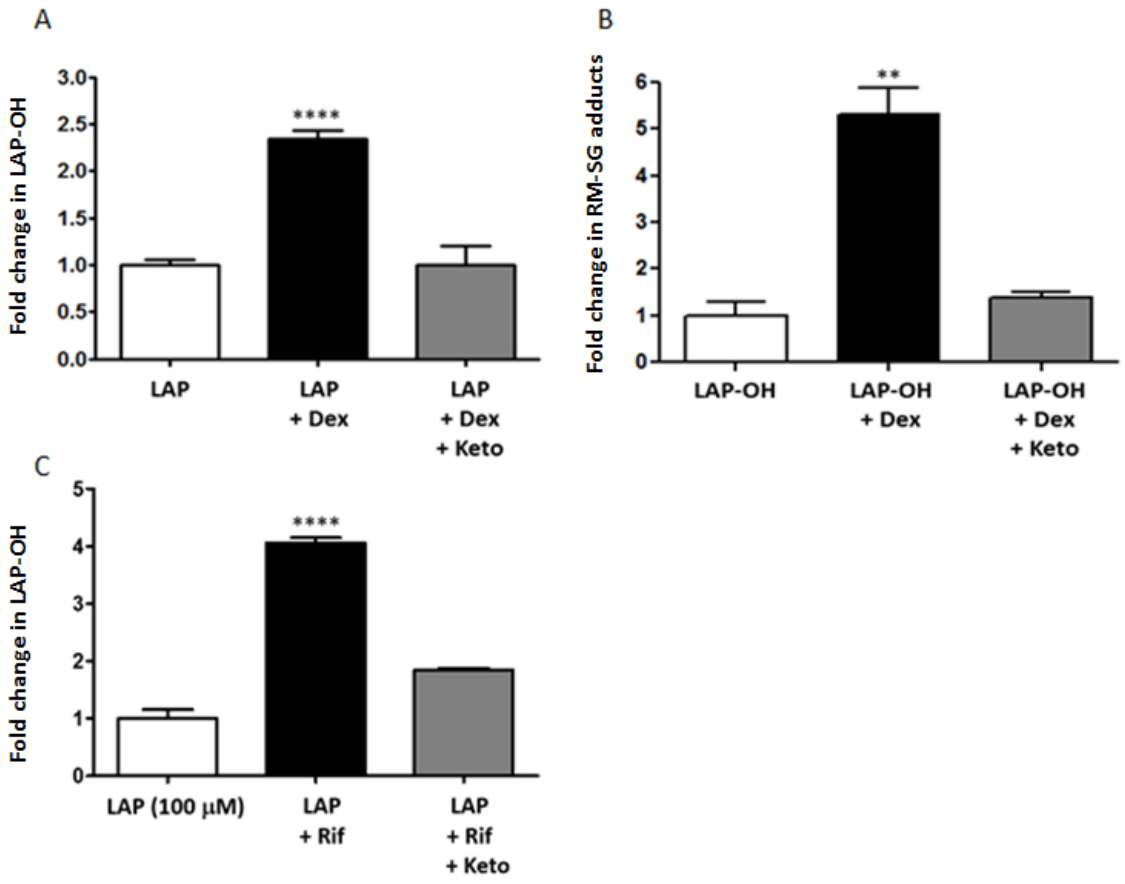

Figure 3.9 – ***Effect of CYP3A4 induction and inhibition on formation of (A, C) LAP-OH and (B) RM-SG in HepaRG cells.*** *HepaRG cells were incubated with dexamethasone (100 µM) or rifampicin (4 µM) for 72 hr, followed by incubation with LAP (100 µM) or LAP-OH (50 µM), with or without co-incubation with ketoconazole (4 µM) for 24 hr. Formation of LAP-OH and RM-SG adducts were quantified by LC-MS analysis with MRM. (Mean ± S.E.M., n = 6, **P < 0.01, ****P < 0.0001, unpaired t test, two-tailed P values).*

The tripeptide portion of GSH S-conjugates can undergo subsequent metabolism to yield cysteinyl-glycine and cysteine S-conjugates via the sequential actions of γ-glutamyl transferase and dipeptidases (Hinchman and Ballatori, 1994). The cysteinyl-glycine conjugate of the quinoneimine intermediate of lapatinib has previously been identified in human liver microsomal incubations with LAP or LAP-OH that were supplemented with GSH (Teng et al., 2010). The formation of cysteine *S*-

conjugates of the quinoneimine (RM-Cys), generated as downstream detoxication products in HepaRG cells treated with LAP or LAP-OH, were evaluated.

The predicted precursor ion of the RM-Cys adduct is at *m/z* 592 when analyzed by LC-MS in positive ion mode. Cysteine adducts were readily detectable in HepaRG cells following a 24 hr incubation with LAP or LAP-OH (100 µM). The enhanced product ion spectrum of the RM-Cys adduct in culture media from HepaRG cells treated with LAP-OH for 24 hr is shown in Figure 3.10A. The product ion spectrum reveals the expected fragmentation pattern of RM-Cys adducts resulting from neutral loss of 123 amu to yield the product ion *m/z* 469 $[M + H - 123]^+$. This corresponds to fragmentation of the lapatinib portion of the molecule and secondary loss of 87 amu corresponding to fragmentation of the cysteine moiety to yield the major product ion, *m/z* 382 $[M + H - 210]^+$ (Figure 3.10A). Based on these findings, an LC-MS/MS method was developed for RM-Cys with the major precursor to product ion transition *m/z* 592 → *m/z* 382. Figure 2.6B shows a representative LC-MS/MS chromatogram from analysis of RM-Cys adducts in the cell supernatant following incubation of HepaRG cells with LAP-OH (100 µM) for 24 hr. A chromatographic peak at 4.83 min was detected from MRM analysis of RM-Cys (Figure 3.10B).

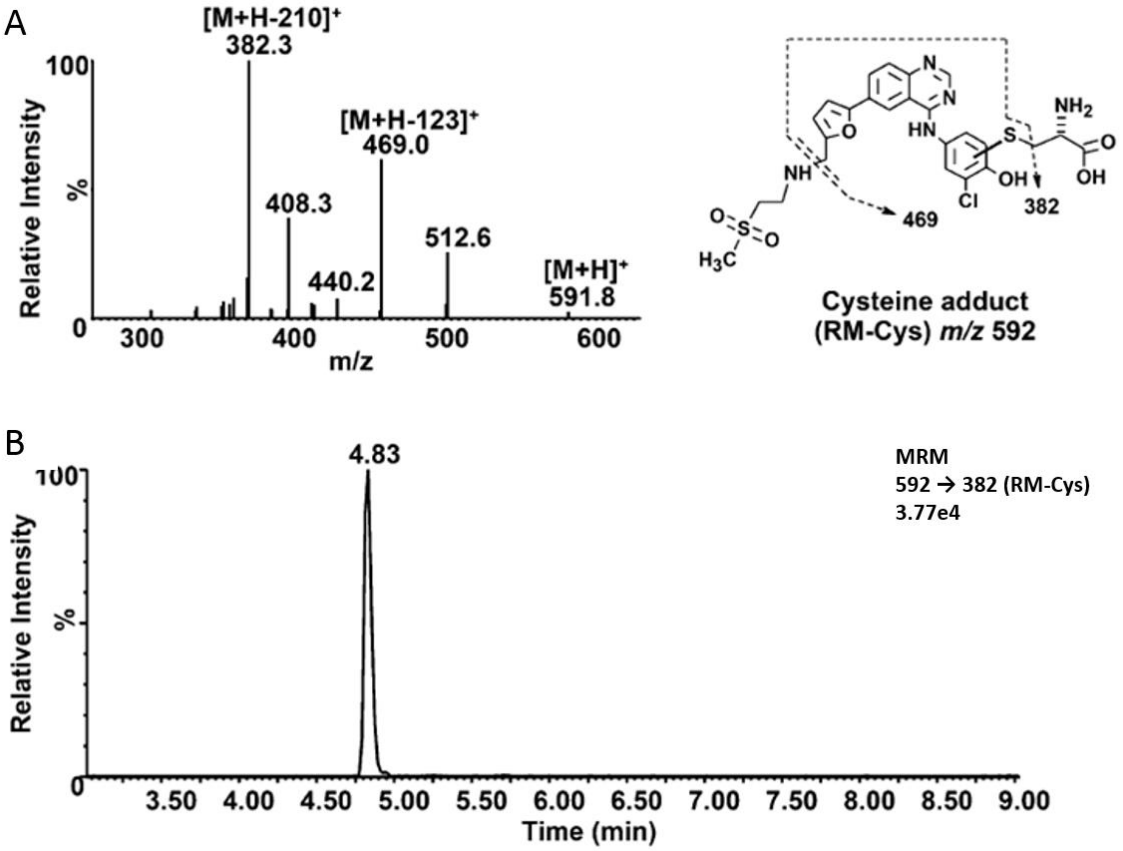

Figure 3.10 ***LC-MS/MS analysis of reactive metabolite cysteine adduct (RM-Cys).*** *HepaRG cells were treated with LAP-OH (100 µM) for 24 hr and supplemented with GSH (50 mM). (A) Representative LC-MS/MS chromatogram of the putative quinoneimine reactive metabolite-cysteine adduct (RM-Cys), monitoring the precursor to product transition m/z 592 → 382. (B) Enhanced product ion scans of RM-GSH. Precursor ion m/z 592 obtained by collision induced dissociation in ESI+ mode.*

The effect of CYP3A4 induction on the formation of RM-Cys was evaluated to further elucidate the role of CYP3A4 in the bioactivation of lapatinib. Relative quantitation of RM-Cys adducts in the cell supernatant was achieved by LC-MS analysis with MRM utilizing the method described above. Pretreatment with dexamethasone increased the levels of RM-Cys adducts approximately 3-fold (P = 0.0068) in HepaRG cells compared with cells treated with LAP alone (Figure 3.11A), and induction by rifampicin (4 µM) increased the levels of RM-Cys adducts approximately 6-fold (P = 0.0030) (Figure

3.11B). Coincubation with ketoconazole attenuated the effect of dexamethasone (P = 0.0053) and rifampicin (P = 0.0031) on RM-Cys adduct formation.

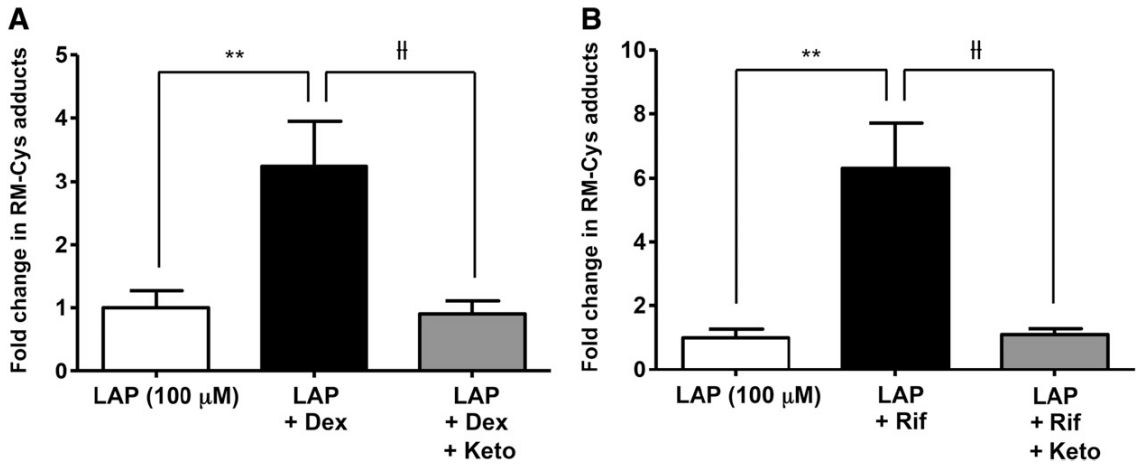

Figure 3.11 – ***Effect of CYP3A4 induction and inhibition on formation of RM-Cys in HepaRG cells.*** *HepaRG cells were incubated with (A) dexamethasone (100 μM) or (B) rifampicin (4 μM) for 72 hr, followed by incubation with LAP (100 μM), with or without co-incubation with ketoconazole (4 μM) for 24 hr. Formation of RM-Cys adducts were quantified by LC-MS analysis with MRM. Data represent the mean ± S.D. of triplicate samples. **P < 0.01, ****P < 0.0001, unpaired t test, two-tailed P values.*

Discussion:

Comparison of the Cytotoxicity of Lapatinib in HepaRG cells and Primary Human Hepatocytes

In this study, HepaRG cells were used to investigate the role of metabolic activation in the cytotoxicity of lapatinib. Unlike primary human hepatocytes, which are the gold standard model for human drug metabolism and toxicity studies, HepaRG cells maintain high levels of CYP3A4 expression and activity even over long periods in culture. In fact, the 3A4 expression is shown to be markedly higher than primary hepatocytes and may potentially overemphasize the impact of 3A4 (Lübberstedt et al., 2011). Figure 3.2 shows that the cytotoxic effect of lapatinib appears comparable in HepaRG cells and

primary human hepatocytes and validates the choice of HepaRG cells as a surrogate model to further study lapatinib toxicity.

Induction and Inhibition of CYP3A4 in HepaRG Cells

A feature that sets HepaRG apart from other hepatic cell lines is the inducibility of CYP3A4 expression using prototypical CYP3A4 inducers (Kanebratt and Andersson, 2008a; Anthérieu et al., 2010). In the present investigation, dexamethasone (100 μM) significantly induced CYP3A4 activity in HepaRG cells. Treatment of HepaRG cells with dexamethasone for 72 hours induced CYP3A4 activity by 7-fold compared to control, as measured by midazolam 1'-hydroxylation (Figure 3.3A). It should be noted that the concentrations of dexamethasone to elicit this effect are well above the therapeutic levels, which are in the low nanomolar to sub-micromolar range (McCune et al., 2000). Low concentrations, such as these, are proposed to activate the glucocorticoid receptor, increase PXR expression, and lead to an increased rate of CYP3A4 gene expression (Pascussi et al., 2001). The clinical dexamethasone-lapatinib interaction noted by Teo et al., (2012) may reflect CYP3A4 mRNA induction through this secondary glucocorticoid receptor-mediated response. On the other hand, concentrations of dexamethasone greater than 10 μM cause direct activation of PXR (Pascussi et al., 2001). The concentration of dexamethasone (100 μM) used in HepaRG cells here is consistent with the direct activation of PXR to produce maximal CYP3A4 induction. These concentrations are above the therapeutic levels of dexamethasone. However, in the clinical setting, co-administration of lapatinib and dexamethasone in the presence of other PXR inducers may result in CYP3A4 induction at therapeutically relevant concentrations. Thus, these studies have potential implications for the *in vivo* situation.

Effect of CYP3A4 Induction on the Cytotoxicity of Lapatinib in HepaRG Cells

To expand upon work carried out in microsomal preparations and recombinant systems, an intact and inducible cell system, HepaRG, was used to directly test the impact of CYP3A4 induction on lapatinib metabolism and toxicity. Pretreatment of HepaRG cells with dexamethasone or rifampicin, followed by incubation with LAP (100 μM), significantly elevated lapatinib-induced cytotoxicity, as assessed by overall cell viability (Figure 3.4). Previous studies have shown that drug-mediated nuclear receptor activation and CYP induction leading to increased metabolic activation can increase drug-induced toxicity. Gonzalez and colleagues demonstrated that treatment of mice humanized for PXR and CYP3A4 with acetaminophen and rifampicin enhanced acetaminophen-induced liver injury compared to mice treated with acetaminophen alone (Cheng et al., 2009). In addition, Zhang et al. showed that phenobarbital, a well-known activator of the constitutive androstane receptor (CAR), induced expression of CYP1A2 and CYP3A11 mRNAs in wild-type CAR mice and markedly enhanced acetaminophen toxicity, whereas CAR-knockout mice were resistant to acetaminophen toxicity (Zhang et al., 2002). The results described herein are consistent with increased CYP3A4 activity with dexamethasone treatment and permit some correlation with increased reactive metabolite formation from lapatinib.

Cytotoxicity of Lapatinib vs. Lapatinib Metabolites

A direct comparison of the cytotoxicity of LAP vs. LAP-OH also was performed, and LAP-OH was found to be significantly more cytotoxic to HepaRG cells than lapatinib itself (Figure 3.6). This finding strongly suggests that the toxicity is due, at least in part, to conversion of the parent drug to metabolite(s) and that LAP-OH is likely a precursor metabolite to the putative cytotoxic species. LAP-OH is a significant metabolite in humans following oral administration of lapatinib (Castellino et al., 2012). In a recent study on the human metabolism of lapatinib, LAP-OH was found to be primarily excreted in feces and

was not detected in plasma (Castellino et al., 2012). The median value reported for this metabolite was 4% of the dose, but it may represent up to 19.2% of the excreted dose in humans (Castellino et al., 2012).

Effect of Glutathione Depletion of the Cytotoxicity of Lapatinib

The formation of reactive drug metabolites has been proposed as an initial step in the development of drug-induced liver injury (Park et al., 2005). *In vitro* investigations have shown that LAP-OH can be further oxidized to a reactive quinoneimine intermediate, which can covalently adduct GSH and potentially other cellular nucleophiles (Teng et al., 2010; Park et al., 2011; Stachulski et al., 2013). If this is the case, one might expect that depletion of GSH could increase the cellular accumulation of reactive metabolites of lapatinib, resulting in increased susceptibility of HepaRG cells to injury. Treatment of cells with BSO to deplete GSH resulted in potentiation of lapatinib-induced cytotoxicity (Figure 3.8B). This synergistic effect suggests that detoxification of reactive metabolites by GSH conjugation may play an important role in preventing cellular injury from electrophilic intermediates derived from lapatinib. It has been proposed that reactive metabolites of lapatinib may cause cellular damage by direct adduction to cellular proteins (Teng et al., 2010; Castellino et al., 2012) and/or redox cycling and oxidative stress (Castellino et al., 2012; Baillie and Rettie, 2011). Thus, environmental or genetic factors that compromise the detoxication and antioxidant defense pathways involved in the inactivation of toxic metabolites could be expected to contribute to individual susceptibility to idiosyncratic lapatinib-induced hepatotoxicity.

Effect of CYP3A4 Induction on the Metabolism of Lapatinib in HepaRG Cells

The increase in lapatinib cytotoxicity from induction of CYP3A4 occurred in parallel with increased formation of lapatinib metabolites on the proposed bioactivation pathway (Figure 1.8). Induction of

CYP3A4 by dexamethasone and rifampicin resulted in an increase in cytotoxicity of lapatinib (Figures 3.4 and 3.5) in conjunction with increased formation of LAP-OH (Figure 3.9). GSH conjugates of the putative quinoneimine intermediate of lapatinib were reported previously from incubation of LAP or LAP-OH in human liver microsomes and recombinantly expressed P450 enzymes (Teng et al., 2010; Chan et al., 2012; Chapter 2). In the present study, RM-SG adducts were detected in HepaRG cells incubated with LAP-OH utilizing LC-MS/MS analysis (Figure 3.9B). Induction of CYP3A4 markedly increased the formation of the LAP-OH metabolite, RM-SG adducts, and RM-Cys adducts in HepaRG cells treated with lapatinib plus dexamethasone or rifampicin compared to treatment with lapatinib alone. Co-incubation with the CYP3A4 inhibitor ketoconazole significantly reduced the levels of LAP-OH, RM-SG adducts, and RM-Cys adducts. These findings are consistent with the view that metabolic activation by CYP3A4 plays a causative role in lapatinib-induced cytotoxicity.

It should be noted that the peak plasma concentrations of lapatinib following an oral dose of 1,250 mg are between 1.57 and 3.77 µg/mL, which is equivalent to 2.70 to 6.49 µM (GlaxoSmithKline, 2007). This is lower than the concentrations of lapatinib used in the present study, which were 50 - 100 µM. However, neither the intracellular concentrations of lapatinib reached in HepaRG cells, nor the concentration of lapatinib in human liver after chronic dosing are known, so direct comparisons cannot be made. A recent preclinical investigation showed that oral administration of [^{14}C]lapatinib to a male rat resulted in the highest levels of radioactivity in the liver when analyzed by whole-body autoradiography, suggesting significant accumulation of lapatinib in liver (Polli et al., 2008). Regardless, the potential discrepancy in lapatinib concentrations that elicit cytotoxicity *in vitro* and hepatotoxicity *in vivo* is an important caveat to the conclusions drawn here and a more comprehensive experimental model would be needed to fully understand the contribution of P450-mediated bioactivation to *in vivo* mechanisms of lapatinib-induced idiosyncratic hepatotoxicity.

In conclusion, the liver cell experiments described herein provide further evidence that lapatinib bioactivation by CYP3A4 may play an important role in initiating hepatocellular injury. Induction of CYP3A4 by dexamethasone and rifampicin markedly enhanced the cytotoxicity of lapatinib, which was correlated with increased formation of LAP-OH, RM-SG adducts, and RM-Cys adducts in HepaRG cells. Additional studies are required to provide further insight into the genetic and environmental factors that contribute to patient susceptibility to lapatinib idiosyncratic hepatotoxicity.

Chapter 4: Understanding Molecular Interactions through Use of a Lapatinib Analog and a CYP3A4 Mutant

Objective: The objective of this investigation was to probe the molecular interactions between lapatinib and human CYP3A4 through reactions with deuterium-substituted lapatinib analogs and comparisons of metabolism by wild-type and mutant CYP3A4. The most informative lapatinib analog was substituted at the putative site of *O*-debenzylation and CYP3A4 was mutated at a single position in the active site, Phe 108, thought to be important in the orientation and metabolism of lapatinib.

Introduction:

Structure-Activity Relationships for Lapatinib

The core of lapatinib's chemical structure is an anilinoquinazoline moiety that serves to mimic the adenine element of ATP. Adenine is important in the binding of ATP to the intracellular kinase domain (Traxler PM, 1997; Traxler PM, 1998). The positioning of the anilino substructure in the small, lipophilic binding pocket of EGFR has been described for erlotinib, another tyrosine kinase inhibitor (Stamos et al., 2002). Lapatinib binding is similar, but the bulky anilinoquinazoline substituent of lapatinib reaches deep into an opened back pocket, causing its COOH terminal portion to shift and partially block the opening of the inhibitor binding site (European Medicines Agency, 2008). For this reason, dissociation of lapatinib may require a conformational change in EGFR, reflected in the observed slow dissociation rate constant value of 0.0023 ± 0.0002 min^{-1}, which translates to a half-life of 300 minutes for the lapatinib-EGFR complex (Wood et al., 2004).

Deuterium Isotope Effect

Deuterium can serve as a powerful tool for investigating the mechanism of specific chemical reactions that involve carbon-hydrogen bond cleavage. Deuterium is a naturally occurring, stable, nonradioactive isotope of hydrogen with a mass of 2.014 amu, 1.006 amu greater than that of hydrogen. The carbon-deuterium bond has a lower zero point energy due to its lower vibrational frequency (Shao and Hewitt, 2010), which results in a lower C-D bond energy compared to that of C-H. Thus, the activation energy for C-D bond cleavage is higher than for C-H bond cleavage, resulting in a slower reaction rate. This effect on rate is known as the deuterium isotope effect (DIE) and is expressed as k_H/k_D, which is defined as the ratio of a kinetic parameter such as V_{max} or CL_{int} (V_{max}/K_m) obtained for a nondeuterated chemical entity relative to a deuterated chemical entity (Nelson and Trager, 2003). The theoretical limit for an intrinsic primary DIE is about 9 at 37°C in the absence of tunneling effects (Nelson and Trager, 2003; Fisher et al., 2006). Depending on the location of the deuterium atoms and the compound's route of metabolism, deuteration can alter a compound's metabolism and thus can be useful as a mechanistic probe (Harbeson and Tung, 2011). Specifically, the magnitude of the deuterium isotope effect is a measure of the degree of symmetry of the transition state (Nelson and Trager, 2003). While there are no deuterated drugs on the market, the incorporation of deuterium into pharmacologically active agents can result in reduced rates of metabolism and/or metabolic switching (Mutlib et al., 2000), leading to improved disposition and decreased production of toxic metabolites (Kushner et al., 1999). The effects of deuterium on the pharmacokinetics and pharmacodynamics of a drug fall into three different categories (Figure 4.1).

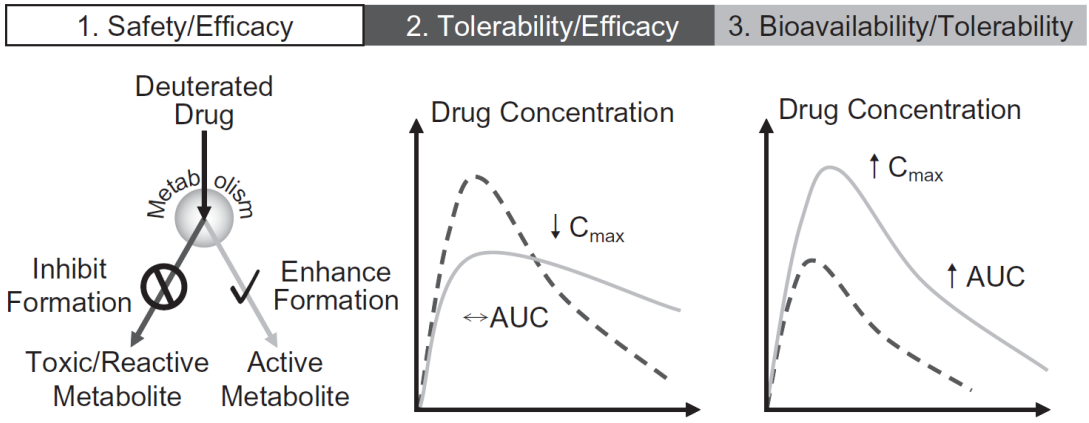

Figure 4.1 – ***Pharmacological expressions of drug deuteration effects.*** *Panel 1: Metabolic shunting resulting in reduced exposure to undesirable metabolites or increased exposure to desired active metabolites. Panel 2: Reduced systemic clearance resulting in increased half-life. Panel 3: Decreased pre-systemic metabolism resulting in higher bioavailability of unmetabolized drug. AUC is area under the curve and represents drug exposure over time.* C_{max} *is the maximum or peak concentration of a drug. (Figure from Harbeson and Tung, 2014).*

An example of a change in toxicity as a result of deuteration has been reported for nevirapine (Viramune®), which is a non-nucleoside reverse transcriptase inhibitor used in the treatment of HIV infection. Covalent binding to hepatic proteins in mouse and rat hepatic microsomes was reduced approximately 5-fold in an analog deuterated at the methyl position, compared with nevirapine itself, suggesting that the reactive species was a quinone methide (Sharma et al., 2012; Sharma et al., 2013).

In vitro experiments have also been carried out to determine the effect of deuterium substitution at the site of *O*-deethylation of phenacetin to form acetaminophen. In hamster liver microsomes, a deuterium isotope effect of approximately 2 was observed (Nelson et al., 1978). Similar studies with human CYP1A2 revealed deuterium isotope effects of 2-3 (Yun et al., 2000). In hamsters, the incidence and extent of hepatic necrosis is decreased approximately 3-fold, but blood methemoglobin

concentrations were increased by about 50% (Nelson et al., 1978). This suggests a shift in metabolism from oxidative *O*-deethylation to hydrolysis to form the aniline metabolite, *p*-phenetidine, which is known to be oxidized to metabolites that cause methemoglobinemia and hemolysis (Heymann et al., 1969).

CoNCERT Pharmaceuticals, Inc® has reported Phase I clinical results for CTP-347, a deuterated analog of paroxetine (Gallegos et al., 2009). Paroxetine is a centrally active selective serotonin reuptake inhibitor (SSRI) for the treatment of major depressive disorder, panic disorder, social anxiety disorder, and premenstrual dysphoric disorder. The deuterated analog is in development for the treatment of hot flashes. Paroxetine is metabolized by CYP2D6 and also irreversibly inactivates the same enzyme via a reactive carbene metabolite (Murray, 2000), potentially inhibiting its own metabolism as well as the metabolism of other CYP2D6 substrates. Coadministration of paroxetine and thioridazine, an antipsychotic drug metabolized by CYP2D6, is contraindicated (Paxil, 2012). *In vitro* experiments with the deuterated analog (di-deuterated on the dioxolone ring) demonstrated little or no CYP2D6 inactivation, presumably due to metabolic switching to a pathway that favored ring opening to yield innocuous metabolites (Gallegos et al., 2009). This preliminary clinical study with CTP-347 was claimed as the first demonstration of deuteration resulting in avoidance of the formation of undesired metabolites in humans.

Structural Differences Between CYP3A4 and CYP3A5

As mentioned earlier, CYP3A4 and CYP3A5 share 85% sequence homology and display overlap in substrate specificity (Thummel and Wilkinson, 1998). Limitations in the availability of chemical tools with the ability to differentiate between the activities of the two enzymes has led to possibly erroneous conclusions about their relative importance. Historically, the two enzymes have sometimes

been treated as one (CYP3A), while in other instances all of the observed activity is attributed to CYP3A4 (Li et al., 2014). CYP3A4 is more abundant in pooled human liver microsomes because a large portion of the population does not express CYP3A5. In individuals that do express CYP3A5, however, levels of these two enzymes can be similar (Lin et al., 2002).

CYP3A4 and CYP3A5 differ in product regioselectivity (Huang et al., 2004), and many examples exist. OSI-930, a thiophene-containing anticancer drug, has been shown to be a mechanism-based inactivator of CYP3A4, but no inactivation was observed in studies with CYP3A5 (Lin et al., 2011). Modeling of the OSI-930 molecule to the active sites of CYP3A4 (Protein Data Bank ITQN) and the homology model of CYP3A5 reveals a different binding conformation to each enzyme. The absence of specific hydrogen bonds, a reduction of the binding energy (ΔG), and an increased distance from the heme iron to the thiophene sulfur all may contribute to the observed decrease in the oxidation of the thiophene sulfur by CYP3A5 (Lin et al., 2011). These workers suggest further that Arg212 plays an important role in the thiophene sulfur oxidation because it forms hydrogen bonds with OSI-903 and because the extended side chain allows the trifluoromethoxy group to form hydrogen bonds with three other residues and stabilize the conformation.

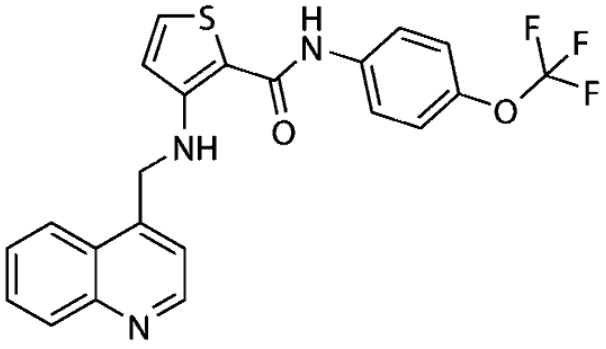

Figure 4.2 – ***The chemical structure of OSI-930.***

In silico docking studies to CYP3A4 and CYP3A5 have also been carried out for lapatinib. An analysis of binding energies revealed that *N*-hydroxylation is the preferred route of metabolism by CYP3A4 whereas *O*-dealkylation is preferred by CYP3A5. Modeling further identified Phe108 as a particularly important residue contributing to this difference (Chan et al., 2012). Phe108 is substituted with a leucine in CYP3A5 (Figure 4.3). A π-stacking interaction between Phe108 and the 3-chloro-4-methoxy phenyl ring of lapatinib has been proposed to orient the compound such that the alkyl-amino group is near the heme center in CYP3A4 (Figure 4.4A). In contrast, the leucine in CYP3A5 results in reorientation of lapatinib so the heme group can interact with the fluorobenzyl methylene carbon (Figure 4.4B). These hypotheses (Chan et al., 2012) are investigated further here using site-directed mutagenesis.

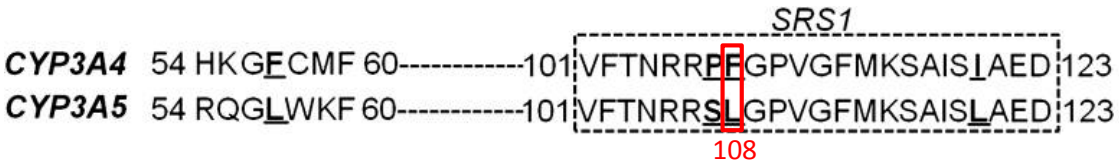

Figure 4.3 – ***Residues that differ between CYP3A4 and CYP3A5 in the Substrate Recognition Site 1 (SRS1).*** *(Figure modified from Lu et al., 2012.)*

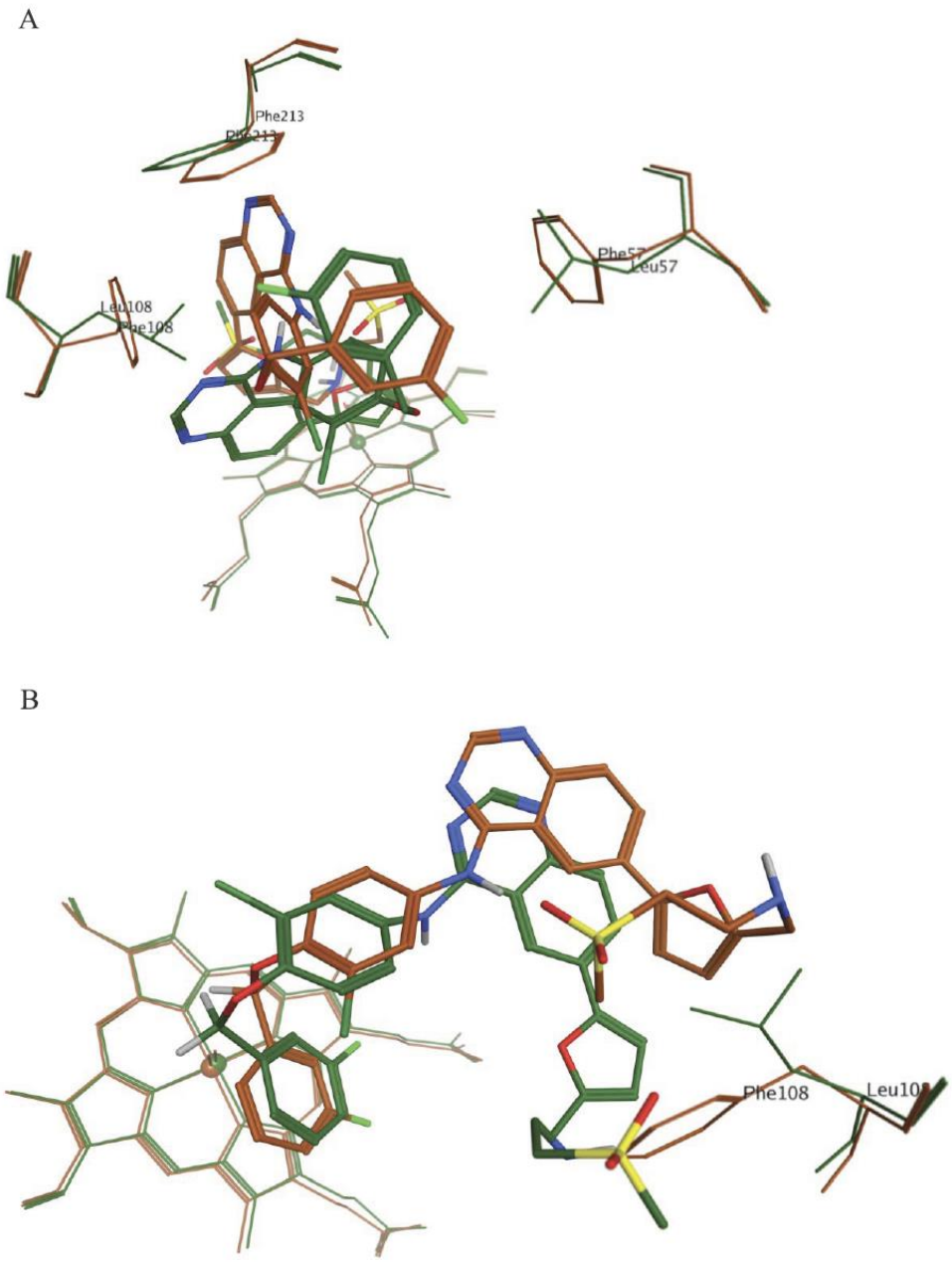

Figure 4.4 – ***Metabolic conformations of lapatinib in CYP3A4 and CYP3A5.*** *(A) Conformation for N-hydroxylation, showing the involvement of Phe57, Phe108, and Phe213 in CYP3A4 and the lack of involvement of these residues in CYP3A5. (B) Conformation for O-dealkylation, showing the involvement of unfavorable steric interaction between lapatinib and Phe108 in CYP3A4 if it adopts that conformation. Conformations in CYP3A4 are drawn in brown and conformations in CYP3A5 are drawn in dark green. (Figure from Chan et al., 2012.)*

Site Directed Mutagenesis of P450s to Elucidate Key Amino Acid Determinants of Ligand Interactions

Site-directed mutagenesis has been used to identify CYP active site residues in a number of CYP enzyme systems. In CYP2D6, Asp301 was determined to play an important role in substrate specificity and activity because of an electrostatic interaction between the carboxylate group of the amino acid residue and the basic nitrogen atom in CYP2D6 substrates (Paine et al., 2003). Mutation of the Ile114 residue in CYP2B1 to a valine did not alter susceptibility to inactivation of the enzyme by chloramphenicol, whereas mutation to an alanine at this position suppressed inactivation (Halpert and He, 1993). In an effort to make dog CYP2B11 more like rat CYP2B1 or rabbit CYP2B5, residues thought to be important in substrate recognition were mutated to those found in the rat or rabbit isoforms. Three mutations resulted in altered metabolic profiles, and these same three residues (Val114, Asp290, and Leu363) were identified as substrate contact residues in modeling studies (Hasler et al., 1994). In a study of sulfoxidation of RPR 106541, a steroid developed for the treatment of asthma, CYP3A4 mutants L210A, F304A, A305V, and A370V, all resulted in altered ratios of *R*-sulfoxide to *S*-sulfoxide (Stevens et al., 1999). Finally, mutation of the Val113 and Phe114 residues in CYP2C9 were found to change the enzyme's substrate specificity (Haining et al., 1999). The importance of these amino acid sites for ligand binding to CYP2C9 was subsequently confirmed from the crystal structure of flurbiprofen bound to the enzyme (Wester et al., 2004).

The objective of the current investigation was to utilize deuterium substitution and site directed mutagenesis to probe the molecular interactions in the lapatinib/CYP3A system. Deuterium analogs, including one substituted at the putative site of debenzylation, were used to investigate metabolism and cytotoxicity. Information about an important residue in CYP3A metabolism inferred from *in silico* modeling was used to create a CYP3A4 mutant that may shed light on differences in lapatinib metabolism between CYP3A4 and CYP3A5.

Materials and Methods:

Materials

All reagents used in previous studies described in this thesis were obtained from the same sources and prepared in the same manner. Deuterated analogs of lapatinib and lapatinib metabolites (Figure 4.5) were provided by CoNCERT Pharmaceuticals, Inc® (Lexington, MA). Pooled human liver microsomes (BD UltraPool™ HLM 150-donor; mixed gender) and human CYP3A4 Supersomes™ coexpressed with cytochrome P450 reductase and cytochrome b_5 were purchased from BD Biosciences (San Jose, CA). $MgCl_2$ was purchased from BD Biosciences. Undifferentiated HepaRG cells were supplied by BioPredic International (Rennes, France). HepaRG™ Tox media supplement 630 was purchased from Life Technologies (Carlsbad, CA). Salts for the potassium phosphate buffer were purchased from Mallinckrodt Baker, Inc. (Phillipsburg, NJ). SK-BR-3 cells were obtained from the Max Planck Institute (Martinsried, Germany). McCoy's 5A medium was purchased from Sigma Aldrich (St Louis, MO). Anti-phospho-EGFR (Tyr1068) and anti-human HER2 primary antibodies were purchased from Cell Signaling Technology (Beverly, MA). The anti-HSP60 primary antibody was purchased from Sigma Aldrich, and anti-phosphotyrosine 4G10 was obtained from Max Planck Institute. Secondary anti-mouse and anti-rabbit HRP-conjugated antibodies were purchased from Pierce (Rockford, IL). Oligonucleotide primers were obtained from Eurofins Genomics (Huntsville, AL). The expression vector pCW 3A4-His6 was provided by Dr. Ron Estabrook (University of Texas Southwestern Medical Center, Dallas, TX). The QuikChange site-directed mutagenesis kit was purchased from Stratagene (La Jolla, CA). His-Tagged wild type CYP3A4 expressed and purified from E. Coli CD41(DE3) cells was generously provided by Dr. Bill Atkins (University of Washington Department of Medicinal Chemistry, Seattle, WA). All other chemicals and reagents were of analytical grade and were purchased from commercial sources.

Quantification of Metabolite Formation from Multiple Deuterated Lapatinib Analogs

To compare amounts of the corresponding debenzylated metabolite formed from each deuterated analog, HLM (0.5 mg/mL final concentration) were incubated with 25 µM of the test compound, 2 mM NADPH, and 3 mM $MgCl_2$ in 0.1 M potassium phosphate buffer (pH = 7.4). Reaction mixtures were incubated for 10 min at 37°C and were stopped by the addition of acetonitrile. The amount of metabolite formed was quantitated by LC-MS/MS.

Kinetic Experiments on the Formation of LAP-OH in HLM and Recombinant CYP3A4

In order to determine the rates of hepatic oxidative *O*-debenzylation of lapatinib (LAP) or [D_2-benzyl]-lapatinib (D_2-LAP), pooled human liver microsomes (BD UltraPool™ HLM 150-donor) and human CYP3A4 Supersomes™ co-expressed with P450 reductase and cytochrome b_5 were incubated with varying concentrations of LAP and D_2-LAP (0.1-100 µM). The formation of the debenzylated metabolite (LAP-OH) was monitored. Preliminary incubations were performed with 5 µM LAP to determine microsomal metabolite formation under linear conditions with respect to protein concentration and time of incubation. HLM incubations contained 0.1 mg of protein/mL and Supersome™ incubations contained 20 pmol of protein/mL. All incubations were carried out in 100 mM potassium phosphate buffer (pH = 7.4). The reaction mixture was pre-incubated for 5 min at 37°C and initiated by the addition of 10 µL a 20 mM solution of NADPH (final concentration, 1 mM) or potassium phosphate buffer as a control. Reactions were incubated at 37°C for a period of 5 min (HLM incubations) or 2 min (Supersome™ incubations) at a final volume of 200 µL in a 96-well plate. The final concentration of organic solvent in the incubation was 1% (0.1% DMSO and 0.9% acetonitrile). Following the incubation, reactions were quenched with 200 µL of ice-cold acetonitrile containing 0.1 ng/µL of D_4-debenzylated lapatinib (D_4-LAP-OH) as the internal standard and cooled on ice. HLM

reactions were centrifuged at 1300 g for 20 min at 4°C and Supersome™ reactions were centrifuged at 14,000 g for 20 min at 4°C. The supernatant was transferred to LC-MS vials for analysis. Assays were conducted in duplicate.

Incubations with pooled liver microsomes for reactive metabolite-GSH adduct quantification

LAP and D_2-LAP (50 µM) were incubated in pooled HLMs (0.5 mg of protein/mL) fortified with NADPH and GSH to assess the formation of reactive metabolite-GSH adducts. Incubations were carried out in 100 mM potassium phosphate buffer (pH = 7.4), containing 50 mM GSH with an NADPH regenerating system consisting of 1.3 mM $NADP^+$, 3.3 mM glucose-6-phosphate, 0.4 U/mL glucose-6-phosphate dehydrogenase, and 3.3 mM $MgCl_2$. The samples were pre-warmed for 5 min at 37°C. Reactions were initiated by addition of NADPH regenerating system solution B (40 U/mL glucose-6-phosphate dehydrogenase) and incubated at 37°C for 1 hr at a final volume of 500 µL. The final concentration of organic solvent in the incubation was 0.4% (0.1% DMSO and 0.3% acetonitrile). Reactions were quenched with two volumes of ice-cold acetonitrile containing 0.1 ng/µL of D_4-LAP-OH as the internal standard and cooled on ice. The samples were centrifuged at 14,000 g for 10 min at 4°C and the supernatant was transferred to a separate vial and dried under N_2 gas. Samples were reconstituted in 100 µL of 3:7 acetonitrile:water mobile phase and transferred to LC-MS vials for analysis. Assays were conducted in triplicate.

HepaRG cells

Undifferentiated HepaRG cells were terminally differentiated in-house according to the supplier's protocols as described previously (Gripon et al., 2002). Differentiated cells were plated in collagen-

coated 96-well plates according to the manufacturer's instructions and maintained in general purpose media composed of Williams E media with GlutaMAX-I supplemented with HepaRG Thaw, Seed, and General Purpose supplement 670 for 72 hr at 37°C in a humidified atmosphere, 5% CO_2. At the end of this period, media was aspirated and replaced with cytotoxicity media composed of Williams E media with GlutaMAX-I supplemented with HepaRG™ Tox medium supplement 630 containing varying concentrations of LAP or D_2-LAP. Cells were incubated for 24 hr (37°C, 5% CO_2) with LAP or D_2-LAP. Cell viability was assessed using WST-1 cell viability assays according to the manufacturer's instructions. Briefly, 10 µL of the premixed WST-1 cell proliferation reagent was added to each well of the 96-well plate (1:10 final dilution), and the plate was incubated for 30 min (37°C, 5% CO_2) followed by shaking for 1 min. Absorbance was measured at 440 nm using an Infinite® M200 microplate reader (Tecan, San Jose, CA). The reference wavelength was 690 nm. Relative cell viability was quantified by calculating the % viability of cells treated with LAP or D_2-LAP compared to cells treated with vehicle control (0.4% DMSO, 0.1% acetonitrile). All incubations were performed in triplicate in two separate experiments, for a total of n=6.

To determine the extent of lapatinib metabolite formation following the 24 hr incubation, 200 µL of ice-cold acetonitrile containing 0.1 ng/µL of D_4-LAP-OH (internal standard) was added to each well. Cells were scraped, the supernatant and cell lysate were combined in a 1.7 mL centrifuge tube, vortexed and sonicated for 1 min, and centrifuged at 14,000 g for 10 min at 4°C. The supernatant was transferred to a separate vial and dried under N_2 gas. Samples were reconstituted in 100 µL 1:1 acetonitrile/water and transferred to LC-MS vials for analysis.

Analysis and Quantitation of Metabolites by LC-MS/MS

An LC-MS/MS system was used to quantify LAP metabolites, as described in Chapter 2. The gradient program for analysis of LAP-OH was as described previously (Chapter 2), and the following gradient

program was used for analysis of GSH adducts: isocratic at 15% B (0-1.5 min), linear gradient from 15 to 95% B (1.5-5 min), isocratic at 95% B (5-7 min), returned to 15% B (7-7.1 min), and isocratic at 15% B (7.1-9.1 min). The operational conditions of the mass spectrometer were as described in Chapter 2. The MS data were acquired in MS-MRM mode with a collision energy of 30 V. Production of LAP-OH was measured by MRM for the precursor to product transitions *m/z* 473 → 350, corresponding to LAP-OH, and *m/z* 477 → 352, corresponding to D_4-LAP-OH (internal standard). Samples were run with a standard curve for LAP-OH over a range of concentrations (0.005 – 1.0 ng/µL) under the same experimental conditions using heat-inactivated enzyme without NADPH to calculate the concentration of metabolite formation. Relative quantitation of reactive metabolite GSH adducts was carried out by LC-MS analysis with MRM monitoring the transitions *m/z* 778 → 655. The MS spectral data were analyzed and deconvoluted using MassLynx version 4.1.

Effect of Lapatinib and D_2-lapatinib on HER2 Activity in a HER2-overexpressing Breast Cancer Cell Line – Cell Treatment and Immunoblotting

SK-BR-3 cells were maintained in McCoy's 5A medium supplemented with 10% FBS. The cells were treated with 1 µM LAP, LAP-OH, D_2-LAP, or DMSO vehicle control for 24 hr. Cells were lysed in buffer (50 mM HEPES, 150 mM NaCl, 1 mM EDTA, 10% glycerol, 1% TritonX-100, 10 mM sodium phosphate) containing protease and phosphatase inhibitor (10 mM sodium fluoride, 2 mM sodium orthovanadate, 1 mM phenylmethylsulfonyl, 0.1 µg/mL aprotinin). Protein concentrations were determined by the BCA method (Pierce) and the level of phosphorylated EGFR (Tyr1068) was measured by western blot using 30 µg total protein resolved on a 6% SDS gel. Phospho-HER2 detection involved additional immunoprecipitation before western blotting with a phosphotyrosine antibody, 4G10. To accomplish this, cell lysate (300 µg) was incubated with anti-HER2 antibodies on ice followed by protein A + G beads (Amersham). The mixture was incubated at 4°C overnight on a rotating

platform. The beads were washed with lysis buffer three times followed by the addition of SDS-PAGE sample buffer. The immunoprecipitated complexes were resolved by SDS-PAGE and transferred to a PVDF membrane. For both EGFR and HER2 detection, the respective membranes were first blocked for 1 hr at room temperature with 5% BSA and 1x gelatin-NET (0.25% gelatin, 0.14 M NaCl, 5 mM EDTA, 0.05 M Tris-HCL, pH 7.5, 0.05% TritonX-100), and then incubated in the respective primary antibodies diluted in TBS with 0.05% (v/v) Tween 20 and 5% (w/v) non-fat milk or bovine serum albumin (BSA) or 1x gelatin-NET. Primary antibodies used were anti-phospho-EGFR (Tyr1068) and anti-human HER2, anti-HSP60, and anti-phosphotyrosine 4G10. Bound antibodies were visualized after incubation with secondary anti-mouse and anti-rabbit HRP-conjugated antibodies by enhanced chemiluminescence (Pierce).

Mutagenesis and Expression of CYP3A4

Recombinant CYP3A4 protein was produced in *Escherichia coli* XL1-Blue cells using the expression vector pCW 3A4-His6. To make the mutation F108L, the same plasmid pCW 3A4-His6 was used as the template for amplification reactions with the QuikChange site-directed mutagenesis kit, following the manufacturer's instructions. Oligonucleotide primers used in the mutagenesis procedure were as follows:

F108L forward, 5' CTTCACAAACCGGAGGCCTTT**A**GGTCCAGTGGGATTTATG 3'

F108L reverse, 5' CATAAATCCCACTGGACC**T**AAAGGCCTCCGGTTTGTGAAG 3'

The bold and underlined nucleotides were altered to introduce the desired mutation. Standard PCR conditions were used to generate the mutated P450 CYP3A4 cDNA, followed by *DpnI* digestion. The mutated P450 3A4 cDNA was subsequently inserted into the pCW expression vector using standard cloning techniques. The vector containing the mutated cDNA was then transformed into XL1-Blue cells, and plasmids from the resulting single colonies were isolated. The mutated cDNA sequence was

verified by full-length sequencing (University of Washington Sequencing Center). Growth and induction of *E. coli* were performed as described by Gillam et al. (Gillam et al., 1993). Imidazole was added to a final concentration of 25 mM and the wild-type and mutant P450s were purified on ProBond nickel resin columns (Invitrogen). The column was washed with 20 column volumes of wash buffer (50 mM KPi, pH 7.4, 20% glycerol, 40 mM imidazole, 0.2% cholate, 2 mM BME, and 50 μM testosterone). Subsequently, the column was eluted with a minimal volume of elution buffer (50 mM KPi, pH 7.4, 20% glycerol, 500 mM imidazole and 0.2% cholate). The eluted protein was then dialyzed using Slide-A-Lyzer dialysis cassettes (Pierce) against storage buffer (100 mM potassium phosphate, 20% glycerol, pH 7.4), and stored at -80°C. The specific content for the mutant CYP3A4 enzyme was 8.0 nmol/mg protein, and for the wild type CYP3A4 enzyme was 17.4 nmol/mg protein.

Cytochrome P450 content was determined by reduced carbon monoxide (CO) difference spectra. Proteins were reduced with 1 mg/mL sodium dithionite. Absorption spectra of enzyme solutions were recorded using an Olis-modernized Aminco™ DW-2 spectrophotometer (Olis, Bogart, GA). The amount of cytochrome P450 was calculated from the absorbance at 450 nm using the cytochrome P450 extinction coefficient, 91 $mM^{-1} \cdot cm^{-1}$ (Omura and Sato, 1964).

Recombinant CYP3A4 and the CYP3A4 F108L mutant (500 pmol) were reconstituted in a mixture of three phospholipids (1:1:1 DLPC/DOPC/PS) with P450 reductase (1.0 nmol) and cytochrome b_5 (500 pmol). The formation of LAP-OH, *N*-dealkyl-LAP, and *N*-OH-LAP metabolites was examined by incubation of LAP (50 μM) with the reconstituted enzyme for 30 min. To evaluate the formation of reactive metabolite GSH (RM-SG) adducts, LAP (50 μM) was incubated with the enzyme system supplemented with GSH (5 mM) and an NADPH regenerating system for 20 min at 37°C. Relative levels of LAP-OH, *N*-dealkyl-LAP, *N*-OH-LAP, and GSH adducts were measured by LC-MS analysis with MRM.

Results:

Quantification of Metabolism of Deuterated Lapatinib Analogs

To probe the mechanism of lapatinib debenzylation and associated toxicity, studies were carried out using deuterated analogs of lapatinib. Four deuterated analogs of lapatinib, as well as their corresponding debenzylated metabolites, were used in subsequent studies. Structures are shown in Figure 4.5.

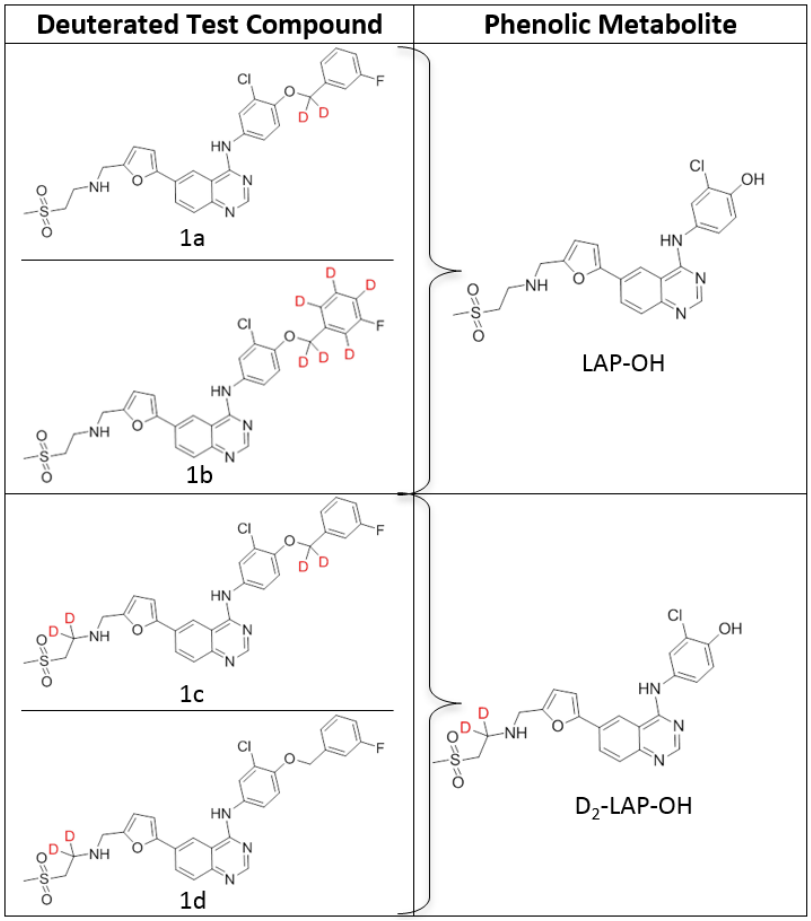

Figure 4.5 – ***Deuterated lapatinib isotopologues and their phenolic metabolites.*** *(Compounds were provided by CoNCERT Pharmaceuticals, Inc®.)*

The formation of the phenolic metabolite from each deuterated lapatinib analog was measured in HLM incubations. Analogs 1a, 1b, and 1c, which were all deuterated at the benzylic position, exhibited a large reduction (61 to 72%) in the amount of debenzylated metabolite formed in incubations (Figure 4.6 and Table 4.1). Analog 1d was deuterated at the site of *N*-dealkylation and not at the site of *O*-debenzylation. It exhibited no change from lapatinib itself in the amount of debenzylated lapatinib formed. Analog 1a, which contained only two deuterium atoms (both at the benzylic position), had the largest reduction in the amount of debenzylated metabolite formed in the HLM incubation (Figure 4.6 and Table 4.1). Deuterium substitution at additional sites (analogs 1b and 1c) had no additional effect on decreasing debenzylation.

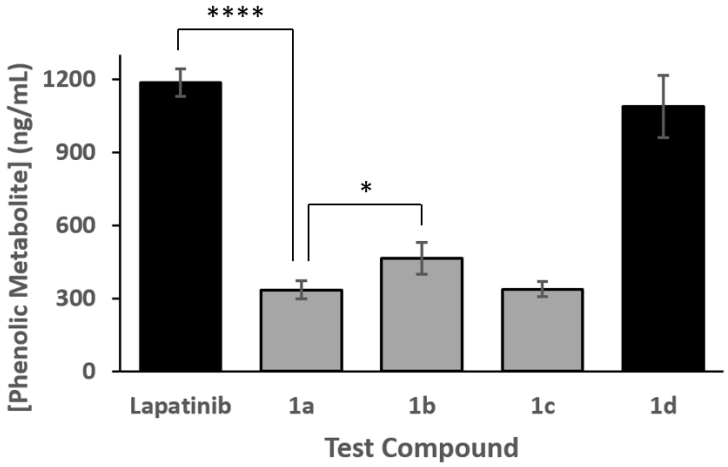

Test Compound	[Phenolic Metabolite] (ng/mL)
LAP	1187 ± 57
1a	335 ± 38
1b	464 ± 65
1c	338 ± 32
1d	1090 ± 128

Figure 4.6 and Table 4.1 – ***Phenolic metabolite formation from deuterated lapatinib analogs.*** *Test compounds (25 μM) were incubated with HLM (0.5 mg/mL) for 10 min at 37°C. The amount of metabolite formed was quantitated by LC-MS/MS. Data represent mean ± S.E.M. of three values. Grey bars represent analogs with deuterium substituted at the benzylic position, and black bars represent analogs with no deuterium substitution at the benzylic position. Data represent the mean ± S.D. of triplicate values (n=3). *P < 0.05; ****P < 0.0001 (unpaired t test, two-tailed P values).*

Based on these results, analog 1a was chosen for further studies to investigate the role of debenzylation in lapatinib metabolism and toxicity in HLM and HepaRG cells.

Metabolism of LAP and D_2-LAP in HLM and Recombinant CYP3A4

The kinetic parameters of LAP and D_2-LAP *O*-debenzylation by HLMs and CYP3A4 Supersomes™ were examined. CYP3A4 Supersomes™ (20 pmol/mL) and HLMs (0.1 mg protein/mL) were incubated with LAP and D_2-LAP (0.1-100 µM) for 2 min and the formation of LAP-OH was quantified by LC-MS analysis with MRM. The velocity-substrate concentration plots for formation of LAP-OH by recombinant enzyme systems and HLMs are shown in Figure 4.7. The kinetic parameters were estimated by fitting data to a Michaelis-Menten kinetic model and are reported in Table 4.2. The substitution of deuterium for hydrogen at the benzylic position resulted in a decrease in catalytic efficiency in HLM and CYP3A4 Supersomes™. This ratio is reported as a kinetic deuterium isotope effect (KDIE), which is the ratio of intrinsic clearance (CL_{int} values) of the nondeuterated compound (LAP) to the deuterated compound (D_2-LAP). In this non-competitive intermolecular isotope experiment, the KDIE in HLM was 3.78, while the KDIE in CYP3A4 Supersomes™ was 4.33 (Table 4.2).

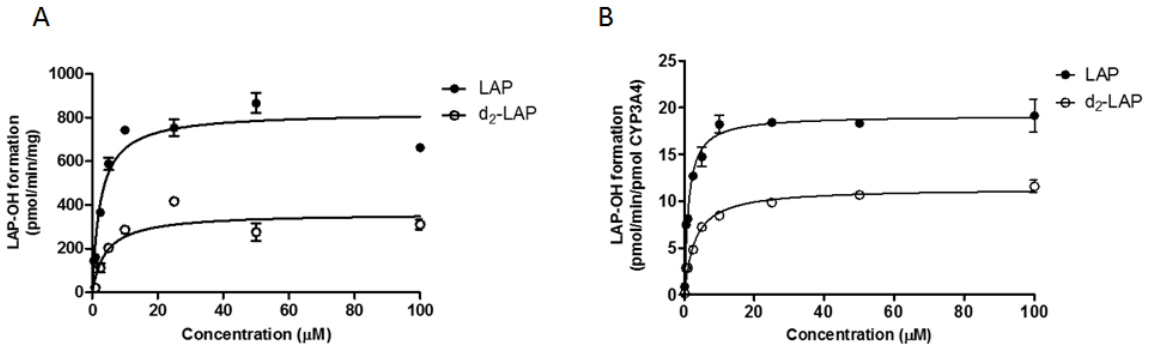

Figure 4.7 – ***Kinetics of the formation of LAP-OH from LAP or D_2-LAP in HLMs and CYP3A4 Supersomes™.*** *LAP or D_2-LAP (0.1-100 µM) were incubated in (A) pooled HLMs (0.1 mg of protein/mL) or (B) CYP3A4 Supersomes™*

(20 pmol/mL) for 2 min. Formation of LAP-OH was quantified by LC-MS analysis with MRM. Data represent the mean ± S.D. of triplicate samples.

A

	K_m (μM)	V_{max} (pmol min^{-1} mg^{-1})	CL_{int} (μL min^{-1} mg^{-1})	KDIE ($CL_{int(H)}/CL_{int(D)}$)
LAP	2.54 ± 0.52	825 ± 38.2	325	3.78
D_2-LAP	4.21 ± 1.64	362 ± 33.8	86.0	

B

	K_m (μM)	V_{max} (pmol min^{-1} $pmol^{-1}$ CYP3A4)	CL_{int} (μL min^{-1} $pmol^{-1}$ CYP3A4)	KDIE ($CL_{int(H)}/CL_{int(D)}$)
LAP	1.15 ± 0.13	19.2 ± 0.41	16.7	4.33
D_2-LAP	2.95 ± 0.30	11.4 ± 0.27	3.86	

Table 4.2 – ***Kinetic parameters for the formation of LAP-OH from LAP or D_2-LAP in (A) pooled HLMs and (B) CYP3A4 Supersomes™.*** *Data were fit to the Michaelis-Menten equation by non-linear regression analysis using GraphPad Prism 5 software to derive K_m and V_{max} values. Intrinsic clearance (CL_{int}) values were calculated as $CL_{int} = V_{max}/ K_m$. The kinetic deuterium isotope effect (KDIE) is the ratio of CL_{int} for LAP to D_2-LAP. Data represent the mean ± S.D. of triplicate samples.*

Because LAP-OH can undergo further metabolism to an electrophilic quinoneimine intermediate that can readily react with cellular nucleophile such as GSH, glutathione conjugates were also measured in HLM incubations. LAP and D_2-LAP (50 μM) were incubated in HLMs for 1 hr in the presence of GSH and formation of LAP-OH and the GSH adducts (RM-SG) were quantified by LC-MS/MS. Deuterated lapatinib formed 63% less LAP-OH ($P < 0.0001$) and 42% less RM-SG ($P < 0.01$) than lapatinib itself (Figure 4.8).

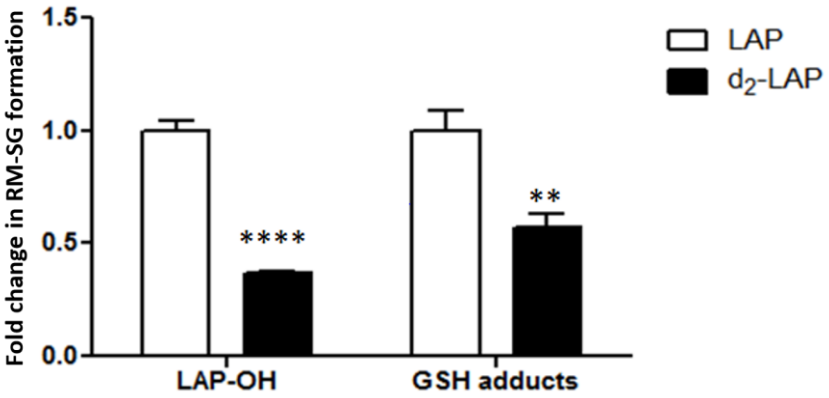

Figure 4.8 ***– Fold change in LAP-OH and RM-SG formation from LAP and D_2-LAP in HLMs.*** *LAP (50 µM) and D_2-LAP (50 µM) were each incubated in HLMs for 1 hr in the presence of GSH (50 mM). Formation of LAP-OH and the GSH adducts (RM-SG) were quantified by LC-MS analysis with MRM. Data represent the mean ± S.D. of triplicate samples. ** P < 0.01, **** P < 0.0001.*

Metabolism and Cytotoxicity of LAP and D_2-LAP in HepaRG Cells

HepaRG cells were established as a model to study LAP-induced hepatotoxicity as described in the previous chapter. The formation of LAP-OH from LAP (100 µM) and D_2-LAP (100 µM) was assessed in differentiated HepaRG cells following a 24 hr incubation. LAP-OH formation in cells treated with D_2-LAP was decreased by 72% ($P < 0.0001$) compared to cells treated with lapatinib (Figure 4.9).

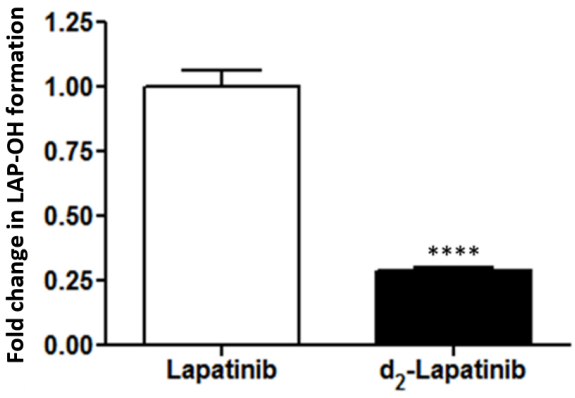

Figure 4.9 ***– Formation of LAP-OH in HepaRG cells treated with LAP and D_2-LAP.*** *Differentiated HepaRG cells were treated with LAP (100 µM) and D_2-LAP (100 µM) for 24 hr. Metabolites were quantified by LC-MS analysis with MRM. (Mean ± SEM, n = 6, **** p < 0.0001.)*

Results outlined in the previous chapter suggested that metabolism plays a role in lapatinib cytotoxicity and that LAP-OH is likely a precursor to the putative cytotoxic species. Experiments with D_2-LAP demonstrated that its ability to form LAP-OH is reduced. It would thus be expected that the toxicity of D_2-LAP to HepaRG cells would be lower than that of LAP itself. To establish a link between the metabolism of D_2-lapatinib and toxicity, HepaRG cells were treated with varying concentrations of LAP and D_2-LAP for 24 hr. Cell viability was monitored using a WST-1 cell viability assay. The viability of cells treated with 100 µM D_2-lapatinib was 76% compared to 52% for cells treated with 100 µM lapatinib ($P < 0.01$). Cell viability was 59% for cells treated with 200 µM D_2-lapatinib compared to 31% for cells treated with 200 µM lapatinib ($P < 0.0001$) (Figure 4.10). This demonstrates that LAP is significantly more toxic to HepaRG cells than D_2-LAP.

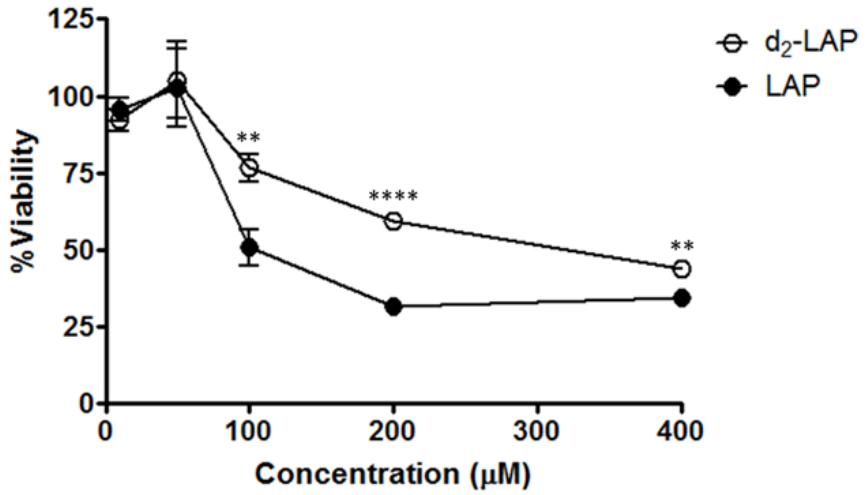

Figure 4.10 – ***Cytotoxicity of LAP and D_2-LAP in differentiated HepaRG cells.*** *HepaRG cells were incubated with varying concentrations of LAP and D_2-LAP for 24 hr. Cell viability was monitored using WST-1 cell proliferation assays. (Mean ± SEM, n = 6, ** P < 0.01, **** P < 0.0001.)*

Inhibition of Phosphorylation by LAP and D_2-LAP in SK-BR-3 Cells

The studies discussed thus far in this thesis have focused on the metabolism and toxicity of LAP and its analogs. Deuterated lapatinib appears to have decreased metabolism to the potential toxic metabolite (LAP-OH) and exhibits decreased cytotoxicity in HepaRG cells. While the safety profile of D_2-lapatinib may be improved over lapatinib itself, D_2-lapatinib must also maintain the therapeutic properties of lapatinib. Any changes to the structure of a drug can result in altered efficacy. In the case of lapatinib, deuterium substitution could disrupt its binding to tyrosine kinases HER2 and EGFR, which would limit its ability to inhibit phosphorylation of the kinase domains. Experiments were thus carried out by our collaborators at the National University of Singapore in the lab of Han Kiat to determine the effect of LAP, LAP-OH, and D_2-LAP on HER2 levels, phosphorylated-HER2 levels, and phosphorylated-EGFR levels in a HER2-overexpressing breast cancer cell line, SK-BR-3.

The total amount of HER2 remained constant with all treatments, but the amount of phospho-tyrosine decreased substantially in cells treated with D_2-LAP and LAP compared to cells treated with LAP-OH and the control cells (Figure 4.11). The amount of phosphor-EGFR also decreased with D_2-LAP and LAP treatments. There was no observable difference between the effect of D_2-LAP and LAP on phosphorylation in this cell line.

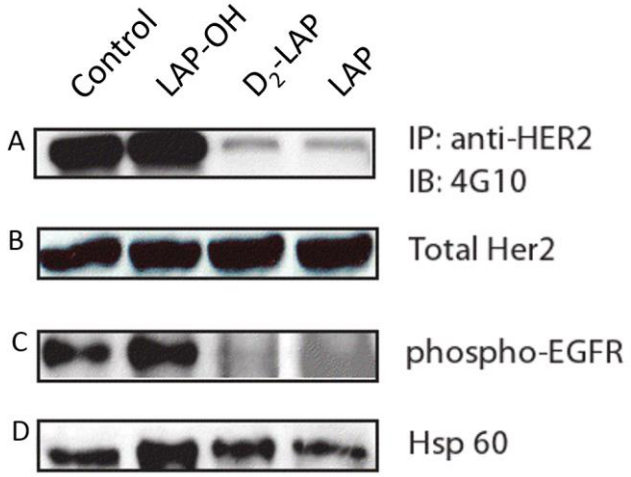

Figure 4.11 – ***LAP and D_2-LAP inhibition of HER2 and EGFR activity in a HER2-overexpressing breast cancer cell line.*** *IP = immunoprecipitate; IB = immunoblot (Data courtesy of Han Kiat, National University of Singapore.)*

Metabolism of Lapatinib by CYP3A4 and the Phe108Leu Mutant

The Phe108 residue of wild-type CYP3A4 (CYP3A4 WT) has been identified through *in silico* docking studies as an important contributor to the difference in preferred routes of metabolism of lapatinib by CYP3A4 and CYP3A5 (Chan et al., 2012). This residue was mutated to the corresponding amino acid of CYP3A5 (leucine) to evaluate its contribution to the differential metabolism of lapatinib by these enzymes *in vitro*. The CO difference spectrum showed minimal P420 absorbance, indicating that the enzyme had not been denatured (Figure 4.12). The P450 concentration calculated from the CO

difference spectrum was 66.5 µM. The specific content for the CYP3A4 F108L mutant was 8.0 nmol/mg protein, and for the wild type CYP3A4 enzyme was 17.4 nmol/mg protein.

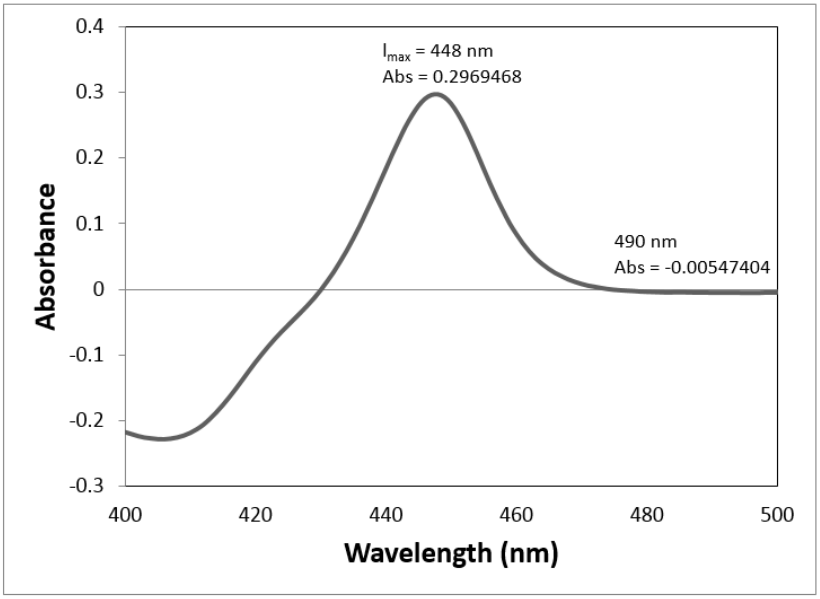

Figure 4.12 – ***CO-difference spectrum of CYP3A4 F108L mutant enzyme.*** *The enzyme was reduced with sodium dithionite. The sample was diluted 20-fold to make these measurements.*

To gain an understanding of the effect of the CYP3A4 F108L mutation on catalytic activity and likely substrate orientation in the active site, the formation of the *N*-dealkyl-LAP, *N*-OH-LAP, and LAP-OH metabolites were measured. Formation of *N*-dealkyl-LAP and *N*-OH-LAP decreased by about 20-fold in the F108L mutant compared to CYP3A4 WT (Figure 4.13). In contrast, the formation of LAP-OH only decreased by about 30% compared to the wild type. The relative metabolite formation profile for the F108 mutant to CYP3A4 WT is very similar to the relative profile for CYP3A5 to CYP3A4 (Figure 2.7).

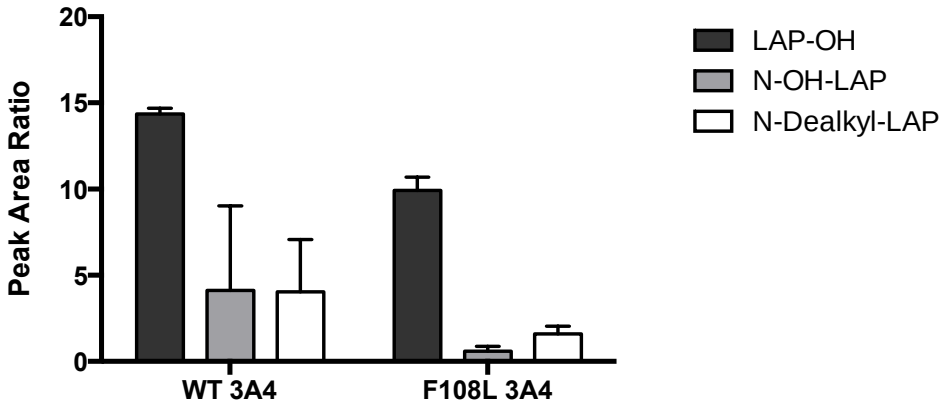

Figure 4.13 – ***Relative contributions of CYP3A4 WT and CYP3A4 F108L mutant isoforms to lapatinib metabolism.*** *LAP (50 µM) was incubated with recombinant CYP3A4 WT and CYP3A4 F108L mutant for 30 min. The ratio of metabolite formation was determined by LC-MS analysis. Data represent the mean and standard deviation of triplicate samples. Data represent the mean ± S.D. for triplicate samples.*

Discussion:

Quantification of Metabolism of Deuterated Lapatinib Analogs

Deuteration of drugs at sites of metabolism, as a means of enhancing pharmacokinetic and toxicological properties, has gained momentum in the past several years (Sharma et al., 2012). In addition, deuterated compounds can be helpful in defining the mechanisms of specific chemical reactions (Nelson and Trager, 2003). Four deuterated analogs of lapatinib were synthesized (Figure 4.4) and formation of the corresponding phenolic metabolite from each was measured in HLM. Deuteration at the benzylic position, as seen in analogs 1a, 1b, and 1c, resulted in a significant reduction in the amount of debenzylated metabolite that was formed compared with lapatinib (Figure 4.5 and Table 4.1). Deuteration at the site of *N*-dealkylation (analog 1d) did not result in a significant reduction in debenzylation, and deuteration on the benzene ring did not further reduce formation of the phenolic metabolite. These results suggest that cleavage of the benzylic C-H bond in lapatinib is

important for formation of the corresponding phenolic metabolite. Secondary kinetic isotope effects, in which a deuterium substitution at a position remote to the bond being broken affects the rate of the chemical reaction (Hennig et al., 2006), were not observed. These results established that further experiments should be carried out with lapatinib and compound 1a (Figure 4.6), which is deuterated only at the site of debenzylation.

Metabolism of LAP and D_2-LAP in HLM and Recombinant CYP3A4

Kinetic parameters for the debenzylation of LAP and D_2-LAP were determined in HLMs and CYP3A4 Supersomes™. The kinetic deuterium isotope effect for the intrinsic clearance (CL_{int}) of lapatinib was 3.78 in HLMs (Table 4.2A) and 4.33 in CYP3A4 Supersomes™ (Table 4.2B). The theoretical limit for the KDIE is about 9 at 37°C in the absence of tunneling effects (Nelson and Trager, 2003; Fisher et al., 2006), and a KDIE of 5-6 is considered to be large (Melander and Saunders, 1980). The KDIE for the 3A4-catalyzed *O*-debenzylation of 7-benzyloxyquinoline, measured using a similar non-competitive intermolecular isotope experiment, was 3.0 ± 0.3 (Krauser and Guengerich, 2005). Although the KDIE values determined here do not reflect the intrinsic isotope effect, the observed CL_{int} isotope effect suggests that a carbon-hydrogen bond cleavage step is at least partially rate-limiting. Many factors can lead to observed isotope effects that are lower than the intrinsic isotope effects, especially for P450 enzymes. In P450 enzymatic reactions, the first irreversible step in the scheme is the conversion of the enzyme-substrate complex to the substrate-bound active oxygenating perferryl oxene enzymatic species (EOS) (Nelson and Trager, 2003). Because this step is not isotopically sensitive, deuterium isotope effects on CL_{int} are often completely or partially masked (Korzekwa et al., 1989). There are several mechanisms and experimental conditions that can lead to unmasking of the isotope effects (Atkins and Sligar, 1987; Atkins and Sligar, 1988; Korzekwa et al., 1989), but the observed effects are still typically lower than the intrinsic effects.

The formation of glutathione adducts (RM-SG) from LAP and D_2-LAP in HLMs was also measured as an indication of the electrophilic quinoneimine intermediate formation. The formation of RM-SG was significantly less (42% decrease) from D_2-LAP than from LAP (Figure 4.8), although the difference was slightly less than the difference in LAP-OH formation (63% decrease).

It is clear from these results that the metabolism of lapatinib is altered in HLMs and CYP3A4 Supersomes™ by deuterium substitution at the benzylic position. Based on the results of previous experiments described herein, this decrease in metabolism may correlate to a decrease in toxicity in HepaRG cells. This relationship was examined further.

Metabolism and Cytotoxicity in HepaRG Cells

Experiments described in Chapter 2 provided evidence that HepaRG cells are a good model to study lapatinib metabolism and toxicity. As in HLMs and CYP3A4 Supersomes™, the formation of LAP-OH in HepaRG cells was decreased by 72% from D_2-LAP compared to LAP (Figure 4.9). This effect is very similar to the 63% decrease observed in HLMs, again confirming the value of HepaRG cells as a model. The decrease in formation of the debenzylated metabolite from D_2-LAP in every model system analyzed, combined with the correlation that was found between debenzylation and cytotoxicity in Chapter 2, gives reason to believe that D_2-LAP is less cytotoxic than LAP itself. Indeed, treatment of HepaRG cells with D_2-LAP resulted in less cytotoxicity than LAP at concentrations of 100 µM to 400 µM (Figure 4.10). Taken together, these experiments in HepaRG cells confirm the earlier results suggesting that metabolism by the debenzylation pathway plays a role in lapatinib cytotoxicity.

Inhibition of Phosphorylation by LAP and D_2-LAP in SK-BR-3 Cells

To assess whether there was any decrease in the likely therapeutic efficacy of D_2-lapatinib compared to lapatinib itself, the inhibition of tyrosine kinase phosphorylation by LAP, LAP-OH, and D_2-LAP was measured in a HER2-overexpressing breast cancer cell line, SK-BR-3. There was no change in overall HER2 levels for any of the test compounds compared to the control (Figure 4.11B). LAP-OH was significantly less active than lapatinib as an inhibitor of HER2 and EGFR phosphorylation in SK-BR-3 cells (Figures 4.11A and 4.11C). This is in agreement with published data that LAP-OH is approximately 100-fold less potent in inhibition of HER2-dependent tumor cell growth *in vitro* (European Medicines Agency, 2008). It is in contrast, however, to the finding that LAP-OH produced approximately equipotent inhibition of EGFR-dependent tumor cell growth (European Medicines Agency, 2008). This could be a result of differing study design. The study described here looked at EGFR phosphorylation in a HER2-overexpressing cell line, while the study in the Assessment Report looked at inhibition of EGFR-dependent tumor cell growth. Treatment of the cells with D_2-LAP and LAP resulted in much lower levels of phosphorylated HER2 and EGFR than treatment with the control or LAP-OH (Figures 4.11A and 4.11C). There was no detectable difference between the effect of D_2-LAP and LAP on phosphorylation in this cell line.

Metabolism of Lapatinib by CYP3A4 Mutant

CYP3A4 and CYP3A5 differ in 78 of 503 amino acids, 17 of which fall within the six putative substrate recognition site (SRS) domains shown to be responsible for the substrate specificity of CYP3A4 with a wide range of compounds (Emoto and Iwasaki, 2006). Several studies have implicated Phe108, a residue in SRS 1, in the enzyme's catalytic activity and product specificity. This residue is in the Phe cluster (Phe108, Phe213, Phe215, Phe219, Phe220, Phe241, and Phe304), which forms a hydrophobic roof to the CYP3A4 active site (Williams et al., 2004; Yano et al., 2004). The residues in the cluster are highly ordered and have an average B factor of 41 $Å^2$, compared with the average of 66 $Å^2$ over the

entire structure (Williams et al., 2004). The CYP3A4 F108L mutant demonstrates decreased metabolism of testosterone and aflatoxin B1 (Wang et al., 1998) and the CYP3A5 L108F mutant has altered maraviroc metabolic ratios that resemble those of CYP3A4 (Lu et al., 2012). A CYP3A5 homology model constructed on the basis of the CYP3A4 crystal structure shows overlapping overall folding between CYP3A5 and CYP3A4 (Pearson et al., 2007). This suggests that the leucine residue in CYP3A5 is located in the roof of the active site, as it is in CYP3A4.

When Phe108 in CYP3A4 was mutated to Leu108, the metabolic profile was shifted slightly to more closely resemble that of CYP3A5. Formation of the *N*-dealkyl-LAP and *N*-OH-LAP decreased significantly and the metabolism observed was primarily through the *O*-debenzylation pathway. This provides further evidence for the claim that substitution of leucine for phenylalanine at this location may result in reorientation of the lapatinib structure to favor interaction of the distal fluorobenzyl methylene carbon with the heme group (Chan et al., 2012). This study provides *in vitro* evidence for the importance of Phe108 for CYP3A activity in lapatinib metabolism as well as its role in contributing to the differing metabolic activity between CYP3A4 and CYP3A5. Additional active site residue differences between CYP3A4 and CYP3A5 likely also play a role in the differences observed, including C239 in CYP3A4, which is substituted for a serine in CYP3A5 (Pearson et al., 2007) and R212, which is substituted for a leucine in CYP3A5 (Lin et al., 2011).

In conclusion, deuteration at the site of oxidative debenzylation of lapatinib significantly decreased its metabolism to the debenzylated metabolite and subsequent oxidation to the putative reactive metabolite. This decrease in metabolism also corresponds to a decrease in lapatinib cytotoxicity in HepaRG cells, further confirming that metabolism and toxicity of lapatinib are linked. A CYP3A4 mutant with a single site mutation that changed an important active site residue (Phe108) to the

corresponding residue (Leu) in CYP3A5 shifted the metabolic profile of lapatinib to one more similar to that of CYP3A5. This residue contributes to the differential metabolism of lapatinib by CYP3A4 and CYP3A5, possibly by playing a role in the orientation of lapatinib in the active site of each enzyme.

When compared to lapatinib itself, D_2-LAP produced less LAP-OH in all *in vitro* systems studied, exhibited decreased cytotoxicity in the HepaRG cell line, and inhibited phosphorylation of HER2 and EGFR to a comparable degree as lapatinib. These findings demonstrate that D_2-LAP represents a powerful tool for studying the mechanisms of lapatinib metabolism and toxicity. The potential benefit to the toxicological profile of lapatinib, combined with the maintenance of pharmacological activity, also makes D_2-LAP a compound that merits consideration as a candidate for drug development.

References:

Andersson TB, Kanebratt KP, and Kenna JG (2012) The HepaRG cell line: a unique in vitro tool for understanding drug metabolism and toxicology in human. *Expert Opin Drug Metab Toxicol* **8**:909-920.

Aninat C, Piton A, Glaise D, Le Charpentier T, Langouet S, Morel F, Guguen-Guillouzo C, and Cuillouzo A (2006) Expression of cytochromes P450, conjugating enzymes and nuclear receptors in human hepatoma HepaRG cells. *Drug Metab Dispos* **34**:75-83.

Antherieu S, Chesne C, Li R, Camus S, Lahoz A, Picazo L, Turpeinen M, Tolonen A, Uusitalo J, Guguen-Guillouzo C, and Guillouzo A (2010) Stable expression, activity, and inducibility of cytochromes P450 in differentiated HepaRG cells. *Drug Metab Dispos* **38**:516-525.

Antoine DJ, Williams DP, and Park BK (2008) Understanding the role of reactive metabolites in drug-induced hepatotoxicity: state of the science. *Expert Opin Drug Metab Toxicol* **4**:1415-1427.

Atkins WM and Sligar SG (1987) Metabolic switching in cytochrome P-450_{cam}: deuterium isotope effects on regiospecificity and the monooxygenase/oxidase ratio. *J Am Chem Soc* **109**L3754-3760.

Atkins WM and Sligar SG (1988) Deuterium isotope effects in norcamphor metabolism by cytochrome P-450_{cam}: kinetic evidence for the two-electron reduction of a high-valent iro-oxo intermediate. *Biochemistry* **27**:1610-1616.

Azim HA Jr, Agbor-Tarh D, Bradbury I, Dinh P, Baselga J, Di Cosimo S, Greger JG Jr, Smith I, Jackisch C, Kim SB, et al. (2013) Pattern of rash, diarrhea, and hepatic toxicities secondary to lapatinib and their association with age and response to neoadjuvant therapy: analysis from the NeoALTTO trial. *J Clin Oncol* **31**:4504-4511.

Baillie TA and Rettie AR (2011) Role of biotransformation in drug-induced toxicity: influence of intra- and inter-species differences in drug metabolism. *Drug Metab Pharmacokinet* **26**:15-29.

Ballet F (1997) Hepatotoxicity in drug development: detection, significance and solutions. *J Hepatol* **26**:26-36.

Baselga J, Bradbur I, Eidtmann H, Di Cosimo S, de Azambuja E, Aura C, Gomez H, Dinh P, Fauria K, Van Dooren V, et al. (2012) Lapatinib with trastuzumab for HER2-positive early breast cancer (NeoALTTO): a randomised, open-label, multicentre, phase 3 trial. *Lancet* **379**:633-640.

Bence AK, Anderson EB, Halepota MA, Doukas MA, DeSimone PA, Davis GA, Smith DA, Koch KM, Stead AG, Mangum S, et al. (2005) Phase I pharmacokinetic studies evaluating single and multiple doses of oral GW572016, a dual EGFR-ErbB2 inhibitor, in healthy subjects. *Invest New Drugs* **23**:39-49.

Bernal W, Cross TJ, Auzinger G, Sizer E, Heneghan MA, Bowels M, Muiesan P, Rela M, Heaton N, Wendon J, and O'Grady JG (2009) Outcome after wait-listing for emergency liver transplantation in acute liver failure: a single centre experience. *J Hepatol* **50**:306-313.

Beutler B (2000) Tlr4: central component of the sole mammalian LPS sensor. *Curr Opin Immunol* **12**:20-26.

Boelsterli UA (2003a) Diclofenac-induced liver injury: a paradigm of idiosyncratic drug toxicity. *Toxicol Appl Pharmacol* **192**:307-322.

Boelsterli UA (2003b) Disease-related determinants of susceptibility to drug-induced idiosyncratic hepatotoxicity. *Curr Opin Drug Discov Devel* **6**:81-91.

Boelsterli UA and Lim PL (2007) Mitochondrial abnormalities--a link to idiosyncratic drug hepatotoxicity? *Toxicol Appl Pharmacol* **220**:92-107.

Brennan PJ, Kumagai T, Berezov A, Murali R, and Greene MI (2000) HER2/neu: mechanisms of dimerization/oligomerization. *Oncogene* **19**:6093-6101.

Brufsky AM, Mayer M, Rugo HS, Kaufman P, Tan Chiu E, Tripathy D, Tudor IC, Wang LI, Brammer MG, Sing M, et al. (2011) Central nervous system metastases in patients with HER2-positive metastatic breast cancer: incidence, treatment, and survival in patients from registHER. *Clin Cancer Res* **17**:4834-4843.

Buchweitz JP, Ganey PE, Bursian SJ, and Roth RA (2002) Underlying endotoxemia augments toxic responses to chlorpromazine: is there a relationship to drug idiosyncrasy? *J Pharmacol Exp Ther* **300**:460-467.

Cameron D, Casey M, Press M, Lindquist D, Pienkowski T, Romieu CG, Chan S, Jagiello-Gruszfeld A, Kaufman B, Crown J, et al. (2008) A phase III randomized comparison of lapatinib plus capecitabine versus capecitabine alone in women with advanced breast cancer that has progressed on trastuzumab: updated efficacy and biomarker analyses. *Breast Cancer Res Treat* **112**:533-543.

Castellino S, O'Mara M, Koch K, Borts DJ, Bowers GD, and MacLauchlin C (2012) Human metabolism of lapatinib, a dual kinase inhibitor: implications for hepatotoxicity. *Drug Metab Dispos* **40**:139-150.

Chan EC, New LS, Chua TB, Yap CQ, Ho HK, and Nelson SD (2012) Interaction of lapatinib with cytochrome P450 3A5. *Drug Metab Dispos* **40**:1414-1422.

Chen W, Koenigs LL, Thompson SJ, Raimund MP, Rettie AE, Trager WF, and Nelson SD (1998) Oxidation of acetaminophen to its toxic quinone imine and nontoxic catechol metabolites by baculovirus-expressed and purified human cytochromes P450 2E1 and 2A6. *Chem Res Toxicol* **11**:295-301.

Chen WG, Zhang C, Avery MJ, and Fouda HG (2001) Reactive metabolite screen for reducing candidate attrition in drug discovery. In Dansette PM, Snyder R, Delaforge M, Gibson GG, Greim H, Jollow DJ, Monks TJ, Siepes IG (Eds). *Biological Reactive Intermediates VI: Chemical and Biological Mechanisms in Susceptibility to and Prevention of Environmental Diseases*. Kluwer Academic/Plenum Press, New York, NY, USA: 521-524.

Cheng J, Ma X, Krausz KW, Idle JR, and Gonzalez FJ (2009) Rifampicin-activated human pregnane X receptor and CYP3A4 induction enhance acetaminophen-induced toxicity. *Drug Metab Dispos* **37**:1611-1621.

Cho HS, Mason K, Ramyar KX, Stanley AM, Gabelli SB, Denney DW Jr, and Leahy DJ (2003) Structure of the extracellular region of HER2 alone and in complex with the Herceptin Fab. *Nature* **421**:756-760.

Chung WH, Hung SI, Hong HS, Hsih MS, Yang LC, Ho HC, Wu JY, and Chen YT (2004) Medical genetics: a marker for Stevens-Johnson syndrome. *Nature* **428**:486.

Corsini A and Bortolini M (2013) Drug-induced liver injury: the role of drug metabolism and transport. *J Clin Pharmacol* **53**:463-474.

Cristofanilli M, Johnston SR, Manikhas A, Gomez HL, Gladkov O, Shao Z, Safina S, Blackwell KL, Alvarez RH, Rubin SD, et al. (2013) A randomized phase II study of lapatinib + pazopanib versus lapatinib in patients with HER2+ inflammatory breast cancer. *Breast Cancer Res Treat* **137**:471-482.

Dahlin DC, Miwa GT, Lu AY, and Nelson SD (1984) N-acetyl-p-benzoquinone imine: a cytochrome P-450-mediated oxidation product of acetaminophen. *Proc Natl Acad Sci USA* **81**:1327-1331.

Deng X, Stachlewitz RF, Liquori MJ, Blomme EA, Waring JF, Luyendyk JP, Maddox JF, Ganey PE, and Roth RA (2006) Modest inflammation enhances diclofenac hepatotoxicity in rats: role of neutrophils and bacterial translocation. *J Pharmacol Exp Ther* **319**:1191-1199.

Dennison JB, Jones DR, Renbarger JL, and Hall SD (2007) Effect of CYP3A5 expression on vincristine metabolism with human liver microsomes. *J Pharmacol Exp Ther* **321**:553-63.

Dennison JB, Kulanthaivel P, Barbuch RJ, Renbarger JL, Ehlhardt WJ, and Hall SD (2006) Selective metabolism of vincristine in vitro by CYP3A5. *Drug Metab Dispos* **34**:1317-1327.

Duckett DR and Cameron MD (2010) Metabolism considerations for kinase inhibitors in cancer treatment. *Expert Opin Drug Metab Toxicol* **6**:1175-1193.

Elkins S, Stresser DM, and Williams JA (2003) *In vitro* and pharmacophore insights into CYP3A enzymes. *Trends Pharmacol Sci* **24**:161-166.

Emoto C and Iwasaki K (2006) Enzymatic characteristics of CYP3A5 and CYP3A4: a comparison of the in vitro kinetic and drug-drug interaction patterns. *Xenobiotica* **36**:219-233.

European Medicines Agency (2008) Assessment report for Tyverb. Available at: http://www.ema.europa.eu/docs/en_GB/document_library/EPAR_-_Public_assessment_report/human/000795/WC500044960.pdf.

Evans DC, Watt AP, Nicoll-Griffith DA, and Baillie TA (2004) Drug-protein adducts: an industry perspective on minimizing the potential for drug bioactivation in drug discovery and development. *Chem Res Toxicol* **17**:3-16.

Feng JY, Johnson AA, Johnson KA, and Anderson KS (2001) Insights into the molecular mechanism of mitochondrial toxicity by AIDS drugs. *J Biol Chem* **276**:23832-23837.

Filppula AM, Neuvonen M, Laitila J, Pertti JN, and Backman JT (2013) Autoinhibition of CYP3A4 leads to important role of CYP3C8 in imatinib metabolism: variability in CYP2C8 activity may alter plasma concentrations and response. *DMD* **41**:50-59.

Fisher MB, Henne KR, and Boer J (2006) The complexities inherent in attempts to decrease drug clearance by blocking sites of CYP-mediated metabolism. *Curr Opin Drug Discov Devel* **9**:101-109.

Franklin MR (1974) The formation of a 455 nm complex during cytochrome P-450-dependent *N*-hydroxyamphetamine metabolism. *Mol Pharmacol* **10**:975-985.

Gallegos R, Uttamsingh V, Morales A, Cheng C, Bridson G, Liu F, Tung R, Zelle R, Harbeson S, and Wells DS (2009) Abstract 88, *The 16th North American Meeting of the International Society of Xenobiotics*, Baltimore MD.

Ganey PE and Roth RA (2001) Concurrent inflammation as a determinant of susceptibility to toxicity from xenobiotic agents. *Toxicology* **169**:195-208.

Geyer CE, Forster J, Lindquist D, Chan S, romieu CG, Pienkowski T, Jagiello-Gruszfeld A, Crown J, Chan A, Kaufman B, et al. (2006) Lapatinib plus capecitabine for HER2-positive advanced breast cancer. *N Engl J Med* **355**:2733-43.

Gillam EMJ, Baba T, Kim B-R, Ohmori S, Guengerich FP (1993) Expression of modified human cytochrome P450 3A4 in *Escherichia coli* and purification and reconstitution of the enzyme. *Arch Biochem Biophys* **305**:123-131.

GlaxoSmithKline (2007) Tykerb (lapatinib) product information. Available at: http://us.gsk.com/products/assets/us_tykerb.pdf. Accessed on October 8, 2013.

Gomez HL, Doval DC, Chavez MA, Ang PC, Aziz Z, Nag S, Ng C, Franco SX, Chow LW, Arbushites MC, et al. (2008) Efficacy and safety of lapatinib as first-line therapy for ErbB2-amplified locally advanced or metastatic breast cancer. *J Clin Oncol* **26**:2999-3005.

Goss PE, Smith IE, O'Shaughnessy J, Ejlertsen B, Kauffman M, Boyle F, Buzdar AU, Fumoleau P, Gradishar W, Martin M, et al. (2013) Adjuvant lapatinib for women with early-stage HER2-positive breast cancer: a randomised, controlled, phase 3 trial. *Lancet Oncol* **14**:88-96.

Gripon P, Rumin S, Urban S, Le Seyec J, Glaise D, Cannie I, Guomard C, Lucas J, Trepo C, and Guguen-Guillouzo C (2002) Infection of a human hepatoma cell line by hepatitis B virus. *Proc Natl Acad Sci USA* **99**:15655-15660.

Guengerich FP (1999) Cytochrome P-450 3A4: regulation and role in drug metabolism. *Annu Rev Pharmacol Toxicol* **39**:1-17.

Guillouzo A, Corlu A, Aninat C, Glaise D, Morel F, and Guguen-Guillouzo C (2007) The human hepatoma HepaRG cells: a highly differentiated model for studies of liver metabolism and toxicity of xenobiotics. *Chem Biol Interact* **168**:66-73.

Haining RL, Jones JP, Henne KR, Fisher MB, Koop DR, Trager WF, and Rettie AE (1999) Enzymatic determinants of the substrate specificity of CYP2C9: role of B'-C loop residues in providing the pi-stacking anchor site for warfarin binding. *Biochemistry* **38**:3285-3292.

Halpert JR and He YA (1993) Engineering of cytochrome P450 2B1 specificity. Conversion of an androgen 16 beta-hydroxylase to a 15 alpha-hydroxylase. *J Biol Chem* **268**:4453-4457.

Harbeson SL and Tung RD (2011) Deuterium in Drug Discovery and Development. *Annu Rep Med Chem* **46**:403-417.

Harbeson SL and Tung RD (2014) Deuterium Medicinal Chemistry: A New Approach to Drug Discovery and Development. *Medchem News* **24**:8-22.

Hasler JA, Harlow GR, Szklarz GD, John GH, Kedzie KM, Burnett VL, He YA, Kaminsky LS, and Halpert JR (1994) Site-directed mutagenesis of putative substrate recognition sites in cytochrome P450 2B11: importance of amino acid residues 114, 290, and 363 for substrate specificity. *Mol Pharmacol* **46**:338-345.

Hennig C, Oswal RB, and Schmatz S (2006) Secondary kinetic isotope effect in nucleophilic substitution: A quantum-mechanical approach. *Journal of Phys Chem A* **110**:3071-3079.

Heymann E, Krisch K, Buch H, Buzello W (1969) Inhibition of phenacetin and acetanilide induced methemoglobinemia in the rat by the carboxylesterase inhibitor bis (*p*-nitrophenyl)phosphate. *Biochem Pharmacol* **18**:801-811.

Hinchman CA and Ballatori N (1994) Glutathione conjugation and conversion to mercapturic acids can occur as an intrahepatic process. *J Toxicol Environ Health* **41**:387-409.

Hu YF, Qiu W, Liu ZQ, Zhu LJ, Liu ZQ, Tu JH, Wang D, Li Z, He J, Zhong GP, Zhou G, and Zhou HH (2006) Effects of genetic polymorphisms of CYP3A4, CYP3A5 and MDR1 on cyclosporine pharmacokinetics after renal transplantation. *Clin Exp Pharmacol Physiol* **33**:1093-1098.

Huang W, Lin YS, McConn DJ 2nd, Calamia JC, Totah RA, Isoherranen N, Glodowski M, and Thummel KE (2004) Evidence of significant contribution from CYP3A5 to hepatic drug metabolism. *Drug Metab Dispos* **32**:1434-1445.

Huang YS, Chern HD, Su WJ, Wu JC, Lai SL, Yang SY, Chang FY, and Lee SD (2002) Polymorphism of the N-acetyltransferase 2 gene as a susceptibility risk factor for antituberculosis drug-induced hepatitis. *Hepatology* **35**:883-889.

Hung SI, Chung WH, Liou LB, Chu CC, Lin M, Huang HP, Lin YL, Lan JL, Yang LC, Hong HS, et al. (2005) HLA-B*5801 allele as a genetic marker for severe cutaneous adverse reactions caused by allopurinol. *Proc Natl Acad Sci USA* **102**:4134-4139.

Jelovac D and Wolff AC (2012) The adjuvant treatment of HER2-positive breast cancer. *Curr Treat Options Oncol* **13**:230-239.

Jounaidi Y, Hyrailles V, Gervot L, and Maurel P (1996) Detection of CYP3A5 allelic variant: A candidate for the polymorphic expression of the protein. *Biochem Biophys Res Commun* **221**:466-470.

Ju C and Uetrecht JP (2002) Mechanism of idiosyncratic drug reactions: reactive metabolite formation, protein binding and the regulation of the immune system. *Curr Drug Metab* **3**:367-377.

Kalgutka AS and Soglia JR (2005) Minimising the potential for metabolic activation in drug discovery. *Expert Opin Drug Metab Toxicol* **1**:91-142.

Kanebratt KP and Andersson TB (2008a) HepaRG cells as an in vitro model for evaluation of cytochrome P450 induction in humans. *Drug Metab Dispos* **36**:137-145.

Kanebratt KP and Andersson TB (2008b) Evaluation of HepaRG cells as an in vitro model for human drug metabolism studies. *Drug Metab Dispos* **36**:1444-1452.

Kaneko A, Kato M, Endo C, Nakano K, Ishigai M, and Takeda K (2010) Prediction of clinical CYP3A4 induction using cryopreserved human hepatocytes. *Xenobiotica* **40**:791-799.

Kaplowitz N (2001) Drug-induced liver disorders: implications for drug development and regulation. *Drug Saf* **24**:483-490.

Kaplowitz N (2005) Idiosyncratic drug hepatotoxicity. *Nat Rev Drug Discov* **4**:489-499.

Kashuba ADM and Bertino JS (2005) Mechanisms of Drug Interactions in Piscitella and Rodvold (Eds.), *Infectious Disease: Drug Interactions in Infectious Diseases, 2nd Edn.* Humana Press Inc., Totowa, NJ, USA: 13-39.

Khazaie K, Schirmacher V, and Lichtner RB (1993) EGFR receptor in neoplasia and metastasis. C*ancer Metastasis Rev* **12**:255-274.

Kirby B, Kharasch ED, Thummel KT, Narang VS, Hoffer CJ, Unadkat JD (2006) Simultaneous measurement of in vivo P-glycoprotein and cytochrome P450 3A activities. *J Clin Pharmacol* **46**:1313-1319.

Kolios G, Valatas V, and Kouromalis E (2006) Role of Kupffer cells in the pathogenesis of liver disease. *World J Gastroenterol* **12**:7413-7420.

Korzekwa KR, Trager WF, and Gillette R (1989) Theory for the observed isotope effects from enzymatic systems that form multiple products via branched reaction pathways: cytochrome P-450. *Biochemistry* **28**:9012-9018.

Krauser JA and Guengerich FP (2005) Cytochrome P450 3A4-catalyzed Testosterone 6β-Hydroxylation Stereochemistry, Kinetic Deuterium Isotope Effects, and Rate-limiting Steps. *J Biol Chem* **280**:19596-19506.

Ku HY, Ahn HJ, Seo KA, Kim H, Oh M, Bae SK, Shin JG, Shon JH, and Liu KH (2008) The contributions of cytochrome P450 3A4 and 3A5 to the metabolism of the phosphodiesterase type 5 inhibitors sildenafil, udenafil, and vardenafil. *DMD* **36**:986-990.

Kuehl P, Zhang J, Lin Y, Lamba J, Assem M, Schuetz J, Watkins PB, Daly A, Wrighton SA, Hall SD, et al. (2001) Sequence diversity in CYP3A promoters and characterization of the genetic basis of polymorphic CYP3A5 expression. *Nat Genet* **27**:383-391.

Kushner DJ, Baker A, and Dunstall TG (1999) Pharmacological uses and perspectives of heavy water and deuterated compounds. *Can J Physiol Pharmacol* **77**:79-88.

Lamba JK, Lin YS, Scheutz EG, and Thummel KE (2002) Genetic contribution to variable human CYP3A-mediated metabolism. *Adv Drug Deliv Rev* **54**:1271-1294.

Leung L, Kalgutkar AS, and Obach RS (2012) Metabolic activation in drug-induced liver injury. *Drug Metab Rev* **44**:18-33.

Lewis, JH (2002) The rational use of potentially hepatotoxic medications in patients with underlying liver disease. *Expert Opin Drug Saf* **1**:159-172.

Lewis W, Day BJ, and Copeland WC (2003) Mitochondrial toxicity of NRTI antiviral drugs: an integrated cellular perspective. *Nat Rev Drug Discov* **2**:812-822.

Leyland-Jones (2009) Human epidermal growth factor receptor 2-positive breast cancer and central nervous system metastases. *J Clin Oncol* **27**:5278-5286.

Li, AP (2002) A review of the common properties of drugs with idiosyncratic hepatotoxicity and the "multiple determinant hypothesis" for the manifestation of idiosyncratic drug toxicity. *Chem Biol Interact* **142**:7-23.

Li X, Jeso V, Heyward S, Walker GS, Sharma R, Micalizio GC, and Cameron MD (2014) Characterization of T-5 N-oxide formation as the first highly selective measure of CYP3A5 activity. *Drug Metab Dispos* **42**:334-342.

Lin H, Zhang H, Medower C, Hollenberg PF, and Johnson WW (2011) Inactivation of cytochrome P450 (P450) 3A4 but not P450 3A5 by OSI-930, a thiophene-containing anticancer drug. *Drug Metab Dispos* **39**:345-350.

Lin NU, Carey LA, Liu MC, Younger J, Come SE, Ewend M, Harris GJ, Bullitt E, Van den Abbeele AD, Henson JW, et al. (2008) Phase II trial of lapatinib for brain metasteses in patients with human epidermal growth factor receptor 2-positive breast cancer. *J Clin Oncol* **26**:1993-1999.

Lin NU, Dieras V, Paul D, Lossignol D, Christodoulou C, Stemmler HJ, Roche H, Liu MC, Greil R, Ciruelos E, et al. (2009) Multicenter phase II study of lapatinib in patients with brain metastases from HER2-positive breast cancer. *Clin Cancer Res* **15**:1452-1459.

Lin YS, Dowling AL, Quigley SD, Farin FM, Zhang J, Lamba J, Scheutz EG, and Thummel KE (2002) Co-regulation of CYP3A4 and CYP3A5 and contribution to hepatic and intestinal midazolam metabolism. *Mol Pharmacol* **62**:162-172.

Loriot Y, Perlemuter G, Malka D, Penault-Llorca F, Boige V, Deutsch E, Massard C, Armand JP, and Soria JC (2008) Drug insight: gastrointestinal and hepatic adverse effects of molecular-targeted agents in cancer therapy. *Nat Clin Pract Oncol* **5**:268-278.

Lu Y, Hendrix CW, and Namandje NB (2012) Cytochrome P450 plays a prominent role in the oxidative metabolism of the anti-human immunodeficiency virus drug maraviroc. *Drug Metab Dispos* **40**:2221-2230.

Lübberstedt M, Müller-Vieira U, Mayer M, Biemel KM, Knöspel F, Knobeloch D, Nüssler AK, Gerlach JC, and Zeilinger K (2011) HepaRG human hepatic cell line utility as a surrogate for primary human hepatocytes in drug metabolism assessment in vitro. *J Pharmacol Toxicol Methods* **63**:59–68.

Luyendyk JP, Maddox JF, Cosma GN, Ganey PE, Cockerell GL, and Roth RA (2003) Ranitidine treatment during a modest inflammatory response precipitates idiosyncrasy-like liver injury in rats. *J Pharmacol Exp Ther* **307**:9-16.

Ma B, Prueksaritanont T, and Lin JH (2000) Drug interactions with calcium channel blockers: possible involvement of metabolite-intermediate complexation with CYP3A. *Drug Metab Dispos* **28**:125-130.

Maggs JL, Tingle MD, Kitteringham NR, and Park BK (1988) Drug-protein conjugates--XIV. Mechanisms of formation of protein-arylating intermediates from amodiaquine, a myelotoxin and hepatotoxin in man. *Biochem Pharmacol* **37**:303-311.

Martin AM, Nolan D, Gaudieri S, Almeida CA, Nolan R, Jamies I, Carvalho F, Phillips E, Christiansen FT, Purcell AW, McCluskey J, and Mallal S (2004) Predisposition to abacavir hypersensitivity conferred by HLA-B*5701 and a haplotypic Hsp70-Hom variant. *Proc Natl Acad Sci USA* **101**:4180-4185.

Matzinger P (1994) Tolerance, danger, and the extended family. *Annu Rev Immunol* **12**:991-1045.

Mayhew BS, Jones DR, and Hall SD (2000) An *in vitro* model for predicting *in vivo* inhibition of cytochromes P450 3A4 and 3A5 by metabolite-inhibitor complex-forming drugs. *Drug Metab Dispos* **28**:1031-1037.

McCune JS, Hawke RL, LeCluyse EL, Gillenwater HH, Hamilton G, Ritchie J, and Lindley C (2000) In vivo and in vitro induction of human cytochrome P4503A4 by dexamethasone. *Clin Pharmacol Ther* **68**:356-366.

McGill MR, Yan HM, Ramachandran A, Murray GJ, Rollins DE, and Jaeschke H (2011) HepaRG cells: a human model to study mechanisms of acetaminophen toxicity. *Hepatology* **53**:974-82.

McGinnity DF, Zhang G, Kenny JR, Hamilton GA, Otmani S, Stams KR, Haney S, Brassil P, Stresser DM, and Riley RJ (2009) Evaluation of multiple in vitro systems for assessment of CYP3A4 induction in drug discovery: human hepatocytes, pregnane X receptor reporter gene, and Fa2N-4 and HepaRG cells. *Drug Metab Dispos* **37**:1259-1268.

Melander L and Saunders WH Jr (1980) Reaction Rates of Isotopic Molecules. Wiley Interscience: New York, NY, USA. pp. 29-36.

Miyamoto G, Zahid N, and Uetrecht JP (1997) Oxidation of diclofenac to reactive intermediates by neutrophils, myeloperoxidase, and hypochlorous acid. *Chem Res Toxicol* **10**:414-419.

Moy B and Goss PE (2007) Lapatinib-associated toxicity and practical management recommendations. *Oncologist* **12**:756-765.

Mugundu GM, Sallans L, Guo Y, Shaughnessy EA, and Desai PB (2012) Assessment of the impact of CYP3A polymorphisms on the formation of α-hydroxytamoxifen and N-desmethyltamoxifen in human liver microsomes. *DMD* **40**:389-396.

Murray M (2000) Mechanisms of inhibitory and regulatory effects of methylenedioxyphenyl compounds on cytochrome P450-dependent drug oxidation *Curr Drug Metab* **1**:67-84.

Mutlib AE, Gerson RJ, Meunier PC, Haley PJ, Chen H, Gan LS, Daview MH, Gemzik B, Christ DD, Krahn DF, Markwalder JA, Seitz SP, Robertson RT, and Miwa GT (2000) The species-dependent metabolism of efavirenz produces a nephrotoxic glutathione conjugate in rats. *Toxicol Appl Pharmacol* **169**:102-113.

Navarro VJ and Senior JR (2006) Drug-related hepatotoxicity. *N Engl J Med* **354**:731-739.

Nelson SD, Garland WA, Mitchell JR, Vaishnav Y, Statham CN and Buckpitt AR (1978) Deuterium isotope effects on the metabolism and toxicity of phenacetin in hamsters. *Drug Metab Dispos* **6**:363-367.

Nelson SD and Trager WF (2003) The use of deuterium isotope effects to probe the active site properties, mechanism of cytochrome P450-catalyzed reactions, and mechanisms of metabolically dependent toxicity. *Drug Metab Dispos* **31**:1481-1498.

Njoku D, Laster MJ, Gong DH, Eger El 2nd, Reed GF, and Martin JL (1997) Biotransformation of halothane, enflurane, isoflurane, and desflurane to trifluoroacetylated liver proteins: association between protein acylation and hepatic injury. *Anesth Analg* **84**(1):173-178.

Njoku DB, Greenberg RS, Bourdi M, Borkowf CB, Dake EM, Martin JL, and Pohl LR (2002) Autoantibodies associated with volatile anesthetic hepatitis found in the sera of a large cohort of pediatric anesthesiologists. *Anesth Analg* **94**:243-249.

Omura T and Sato R (1964) The carbon monoxide-binding pigment of liver microsomes. Evidence for its hemoprotein nature. *J Biol Chem* **239**:2370-2378.

Ortiz de Montellano PR (2005) Cytochrome P450: Structure, Mechanism, and Biochemistry, 3rd Edn. Kluwer Academic/Plenum Publishers, New York, NY, USA.

Ostapowicz G, Fontana RJ, Schiodt FV, Larson A, Davern TJ, Han SH, McCashland TM, Shakil AO, Hay JE, Hynan L, et al. (2002) Results of a prospective study of acute liver failure at 17 tertiary care centers in the United States. *Ann Intern Med* **137**:947-954.

Paine MJ, McLaughlin LA, Flanagan JU, Kemp CA, Sutcliffe MJ, Roberts GC, and Wolf CR (2003) Residues glutamate 216 and aspartate 301 are key determinants of substrate specificity and product regioselectivity in cytochrome P450 2D6. *J Biol Chem* **278**:4021-4027.

Park BK, Boobis A, Clarke S, Goldring CEP, Jones D, Kenna JG, Lambert C, Laverty HG, Naisbitt DJ, Nelson SD, et al. (2011) Managing the challenge of chemically reactive metabolites in drug development. *Nature Rev* **10**:292-306.

Park BK, Kitteringham NR, Maggs JL, Pirmohamed M, and Williams DP (2005) The role of metabolic activation in drug-induced hepatotoxicity. *Annu Rev Pharmacol Toxicol* **45**:177-202.

Park BK, Kitteringham NR, Powell H, and Pirmohamed M (2000) Advances in molecular toxicology-towards understanding idiosyncratic drug toxicity. *Toxicology* **153**:39-60.

Park BK, Pirmohamed M, and Kitteringham NR (1998) Role of drug disposition in drug hypersensitivity: a chemical, molecular, and clinical perspective. *Chem Res Toxicol* **11**:969-988.

Pascussi JM, Drocourt L, Fabre JM, Maurel P, and Vilarem MJ (2000) Dexamethasone induces pregnane X receptor and retinoid X receptor-alpha expression in human hepatocytes: synergistic increase of CYP3A4 induction by pregnane X receptor activators. *Mol Pharmacol* **58**:361-372.

Pascussi JM, Drocourt L, Gerbal-Chaloin S, Fabre JM, Maurel P, and Vilarem MJ (2001) Dual effect of dexamethasone on CYP3A4 gene expression in human hepatocytes. Sequential role of glucocorticoid receptor and pregnane X receptor. *Eur J Biochem* **268**:6346-6358.

Paxil CR [Package insert] GlaxoSmithKline, Research Triangle Park, NC; December 2012. http://www.accessdata.fda.gov/drugsatfda_docs/label/2012/0290936s045lbl.pdf

Pearson JT, Wahlstrom JL, Dickmann LJ, Kumar S, Halpert JR, Wienkers LC, Foti RS, and Rock DA (2007) Differential time-dependent inactivation of P450 3A4 and P450 3A5 by raloxifene: a key role for C239 in quenching reactive intermediates. *Chem Res Toxicol* **20**:1778-1786.

Polli JW, Humphreys JE, Harmon KA, Castellino S, O'Mara MJ, Olson KL, John-Williams, LS, Koch KM, and Serabjit-Singh CJ (2008) The role of efflux and uptake transporters in [N-(3-chloro-4-[(3-fluorobenzyl)oxy]phenyl)-6-[5-({[2-(methylsulfonyl)ethyl]amino}methyl)-2-furyl]-4-quinazolinamine (GW572016, lapatinib) disposition and drug interactions. *Drug Metab Dispos* **36**:695-701.

Raucy JL, Lasker JM, Lieber CS, and Black M (1989) Acetaminophen activation by human liver cytochromes P450IIE1 and P450IA2. *Arch Biochem Biophys* **271**:270-283.

Roberts RA, Ganey PE, Ju C, Kamendulis LM, Rusyn I, and Klaunig JE (2007) Role of the Kupffer cell in mediating hepatic toxicity and carcinogenesis. *Toxicol Sci* **96**:2-15.

Rogue A, Lambert C, Spire C, Claude N, and Guillouzo A (2012) Interindividual variability in gene expression profiles in human hepatocytes and comparison with HepaRG cells. *Drug Metab Dispos* **50**:151-158.

Roth RA and Ganey PE (2010) Intrinsic versus idiosyncratic drug-induced hepatotoxicity – two villains or one? *JPET* **332**:692-697.

Roth RA, Luyendyk JP, Maddox JF, and Ganey PE (2003) Inflammation and drug idiosyncrasy--is there a connection? *J Pharmacol Exp Ther* **307**:1-8.

Rusnak DW, Affleck K, Cockerill SG, Stubberfield C, Harris R, Page M, Smith KJ, Guntrip SB, Carter MC, Shaw RJ, et al. (2001) The characterization of novel, dual ErbB-2/EGFR, tyrosine kinase inhibitors: potential therapy for cancer. *Cancer Res* **61**:7196-7203.

Russmann S, Jetter A, and Kullak-Ublick GA (2010) Pharmacogenetics of drug-induced liver injury. *Hepatology* **52**:748-761.

Russo MW, Galanko JA, Shrestha R, Fried MW, and Watkins P (2004) Liver transplantation for acute liver failure from drug induced liver injury in the United States. *Liver Transpl* **10**:1018-1023.

Ryken TC, McDermott M, Robinson PD, Ammirati M, Andrews DW, Asher AL, Burri SH, Cobbs CS, Gaspar LE, Kondziolka D, et al. (2010) The role of steroids in the management of brain metastases: a systematic review and evidence-based clinical practice guideline. *J Neurooncol* **91**:103-114.

Saeki M, Saito Y, Nakamura T, Murayama N, Kim SR, Ozawa S, Komamura K, Ueno K, Kamakura S, Nakajima T, et al. (2003) Single nucleotide polymorphisms and haplotype frequencies of CYP3A5 in a Japanese population. *Hum Mutat* **21**:653.

Schaid DJ, Spraggs CF, McDonnel SK, Parham LR, Cox CJ, Ejlertsen B, Finkelstein DM, Rappold E, Curran J, Cardon LR, and Goss PE (2014) Prospective Validation of HLA-DRB1*07:01 Allele Carriage As a Predictive Risk Factor for Lapatinib-Induced Liver Injury. *J Clin Oncol* [Epub ahead of print.]

Shao L and Hewitt MC (2010) The kinetic isotope effect in the search for deuterated drugs. *Drug News & Perspect* **23**:298-404.

Sharma AM, Klarskov K, and Uetrecht J (2013) Nevirapine bioactivation and covalent binding in the skin. *Chem Res Toxicol* **26**:410-421.

Sharma AM, Li Y, Novalen M, Hayes MA, and Uetrecht J (2012) Bioactivation of nevirapine to a reactive quinone methide: implications for liver injury *Chem Res Toxicol* **25**:1708-1719.

Sharma R, Strelevitz TJ, Gao H, Clark AJ, Schildknegt K, Obach RS, Ripp SL, Spracklin DK, Tremaine LM and Vaz AND (2012) Deuterium isotope effects on drug pharmacokinetics. I. System-dependent effects on specific deuteration with aldehyde oxidase cleared drugs. *Drug Metab Dispos* **40**:625-634.

Shen L, Fitzloff JF, and Cook CS (2004) Differential enantioselectivity and product-dependent activation and inhibition in metabolism of verapamil by human CYP3As. *Drug Metab Dispos* **32**:186-196.

Silverman RB. (1995) Mechanism-based enzyme inactivators. *Methods Enzymol* **249**:240-283.

Silverthorn DU (2004) *Human Physiology: An Integrated Approach, Third Edition* (Garrison CW, Illustrator) Pearson Benjamin Cummings, San Francisco, CA, USA: 682.

Slamon DJ, Clark GM, Wong SG, Levin WJ, Ullrich A, and McGuire WL (1987) Human breast cancer: correlation of relapse and survival with amplification of the HER-2/neu oncogene. *Science* **235**:177-182.

Soffietti R, Cornu P, Delattre JY, Grant R, Graus F, Grisold W, Heimans J, Hildebrand J, Hoskin P, Kalljo M, et al. (2006) EFNS Guidelines on diagnosis and treatment of brain metastases: report of an EFNS Task Force. *Eur J Neurol* **13**:674-681.

Spolarics Z (1998) Endotoxemia, pentose cycle, and the oxidant/antioxidant balance in the hepatic sinusoid. *J Leukoc Biol* **63**:534-541.

Spraggs CF, Budde LR, Briley LP, Bing N, Cox CJ, King KS, Whittaker JC, Mooser VE, Preston AJ, Stein SH, and Cardon LR (2011) HLA-DQA1*02:01 is a major risk factor for lapatinib-induced hepatotoxicity in women with advanced breast cancer. *J Clin Oncol* **29**:667-673.

Spraggs CF, Parham LR, Hunt CM, and Dollery CT (2012) Lapatinib-induced liver injury characterized by class II HLA and Gilbert's syndrome genotypes. *Clin Pharmacol Ther* **91**:647-652.

Stachulski AB, Baillie TA, Park BK, Obach RS, Dalvie DK, Williams DP, Srivastava A, Regan SL, Antoine DJ, Goldring CE, et al. (2013) The generation, detection, and effects of reactive drug metabolites. *Med Res Rev* **33**:985-1080.

Stamos J, Silwkowski MX, and Eigenbrot C (2002) Structure of the epidermal growth factor receptor kinase domain alone and in complex with a 4-anilinoquinazoline inhibitor. *J Biol Chem* **277**:46265-46272.

Stepan AF, Walker DP, Bauman J, Price DA, Baillie TA, Kalgutkar AS, and Aleo MD (2011) Structural alert/reactive metabolite concept as applied in medicinal chemistry to mitigate the risk of idiosyncratic drug toxicity: a perspective based on the critical examination of trends in the top 200 drugs marketed in the United States. *Chem Res Toxicol* **24**:1345-1410.

Stevens JC, Domanski TL, Harlow GR, White RB, Orton E, and Halpert JR (1999) Use of the steroid derivative RPR 106541 in combination with site-directed mutagenesis for enhanced cytochrome P-450 3A4 structure/function analysis. *JPET* **290**:594-602.

Takakusa H, Wahlin MD, Zhao C, Hanson KL, New LS, Chan EC, and Nelson SD (2011) Metabolic intermediate complex formation of human cytochrome P450 3A4 by lapatinib. *Drug Metab Dispos* **39**:1022-1030.

Tang W, Stearns RA, Bandiera SM, Zhang Y, Raab C, Braun MP, Dean DC, Pang J, Leung KH, Doss GA, et al. (1999) Studies on cytochrome P-450-mediated bioactivation of diclofenac in rats and in human hepatocytes: identification of glutathione conjugated metabolites. *Drug Metab Dispos* **27**:365-372.

Taylor RW and Turnbull DM (2005) Mitochondrial DNA mutations in human disease. *Nat Rev Genet* **6**:389-402.

Temple RJ and Himmel MH (2002) Safety of newly approved drugs: implications for prescribing. *JAMA* **287**:2273-2275.

Teng WC, Oh JW, New LS, Wahlin MD, Nelson SD, Ho HK, and Chan EC (2010) Mechanism-based inactivation of cytochrome P450 3A4 by lapatinib. *Mol Pharmacol* **78**:693-703.

Teo YL, Saetaew M, Chanthawong S, Yap YS, Chan EC, Ho HK, and Chan A (2012) Effect of CYP3A4 inducer dexamethasone on hepatotoxicity of lapatinib: clinical and in vitro evidence. *Breast Cancer Res Treat* **133**:703-711.

Therevet E, Anglicheau D, King B, Schlageter MH, Cassinat B, Beaune P, Legendre C, and Daly AK (2003) Impact of cytochrome p450 3A5 genetic polymorphism on tacrolimus doses and concentration-to-dose ratio in renal transplant recipients. *Transplantation* **76**:1233-1235.

Thummel KE and Wilkinson GR (1998) In vitro and in vivo drug interactions involving human CYP3A. *Annu Rev Pharmacol Toxicol* **38**:389-430.

Traxler PM (1997) Protein tyrosine kinase inhibitors in cancer treatment. *Exp Opin Ther Patents* **7**:571-588.

Traxler PM (1998) Tyrosine kinase inhibitors in cancer treatment (Part II) *Exp Opin Ther Patents* **8**:1599-1628.

Turpeinen M, Tolonen A, Chesne C, Guillouzo A, Uusitalo J, and Pelkonen O (2009) Functional expression, inhibition, and induction of CYP enzymes in HepaRG cells. *Toxicol in Vitro* **23**:748-753.

Uetrecht J (2007) Idiosyncratic drug reactions: current understanding. *Annu Rev Pharmacol Toxicol* **47**:513-539.

Uetrecht J (2008) Idiosyncratic drug reactions: past, present, and future. *Chem Res Toxicol* **21**:84-92.

Uetrecht JP (1999) New concepts in immunology relevant to idiosyncratic drug reactions: the "danger hypothesis" and innate immune system. *Chem Res Toxicol* **12**:387-395.

Uetrecht, JP (2000) Is it possible to more accurately predict which drug candidates will cause idiosyncratic drug reactions? *Curr Drug Metab* **1**:133-141.

Ulrich RG (2007) Idiosyncratic toxicity: a convergence of risk factors. *Annu Rev Med* **58**:17-34.

Vuilleumier N, Rossier MF, Chiappe A, Degoumois F, Dayer P, Mermillod B, Nicod L, Desmeules J, Hochstrasser D (2006) CYP2E1 genotype and isoniazid-induced hepatotoxicity in patients treated for latent tuberculosis. *Eur J Clin Pharmacol* **62**:423-429.

Walgren JL, Mitchell MD, and Thompson DC (2005) Role of metabolism in drug-induced idiosyncratic hepatotoxicity. *Crit Rev Toxicol* **35**:325-361.

Wang H, Dick R, Yin H, Licad-Coles E, Kroetz DL, Szklarz G, Harlow G, Halpert JR, and Correia MA (1998) Structure-function relationships of human liver cytochromes P450 3A: alflatoxin B1 metabolism as a probe. *Biochemistry* **37**:12536-12545.

Wang YH, Jones DR, and Hall SD (2005) Differential mechanism-based inhibition of CYP3A4 and CYP3A5 by verapamil. *Drug Metab Dispos* **33**:664-671.

Waring JF, Liquori MJ, Luyendyk JP, Maddox JF, Ganey PE, Stachlewitz RF, North C, Blomme EA, and Roth RA (2006) Microarray analysis of lipopolysaccharide potentiation of trovafloxacin-induced liver injury in rats suggests a role for proinflammatory chemokines and neutrophils. *J Pharmacol Exp Ther* **316**:1080-1087.

Wen B, Lampe JN, Roberts AG, Atkins WM, Rodrigues AD, and Nelson SD (2006) Cysteine 98 in CYP3A4 contributes to conformational integrity required for P450 interaction with CYP reductase. *Arch Biochem Biophys* **454**:42-54.

Wester MR, Yano JK, Schoch GA, Yang C, Griffin KJ, Stout CD, and Johnson EF (2004) The structure of human cytochrome P450 2C9 complexed with flurbiprofen at 2.0-A resolution. *J Biol Chem* **279**:35630-35637.

Williams PA, Cosme J, Vinkovic DM, Ward A, Angove HC, Day PJ, Vonrhein C, Tickle, IJ, and Jhoti H (2004) Crystal structures of human cytochrome P450 3A4 bound to metyrapone and progesterone. *Science* **305**: 683-686.

Wong M Balleine RL, Collins M, Liddle C, Clarke CL, and Gurney H (2004) CYP3A5 genotype and midazolam clearance in Australian patients receiving chemotherapy. *Clin Pharmacol Ther* **75**:529-538.

Wood ER, Truesdale AT, McDonald OB, Yuan D, Hassell A, Dickerson SH, Ellis B, Pennisi C, Horne E, Lackey K, Alligood KJ, Rusnak DW, Gilmer TM, and Shewchuk L (2004) A unique structure for epidermal growth factor receptor bound to GW572016 (lapatinib): relationships among protein conformation, inhibitor off-rate, and receptor activity in tumor cells. *Cancer Res* **64**:6652-6659.

Yano JK, Wester MR, Schoch GA, Griffin KJ, Stout CD, and Johnson EF (2004) The structure of human microsomal cytochrome P450 3A4 determined by X-ray crystallography to 2.05-A resolution. *J Biol Chem* **279**:38091-38094.

Yarden Y (2001) The EGFR family and its ligands in human cancer: signaling mechanisms and therapeutic opportunities. *Eur J Cancer* **37**:S3-S8.

Yarden Y and Sliwkowski MX (2001) Untangling the ErbB signaling network. *Nat Rev Mol Cell Biol* **2**:127-137.

Yun CH, Miller GP, and Guengerich FP (2000) Rate-determining steps in phenacetin oxidations by human cytochrome P450 1A2 and selected mutants. *Biochemistry* **39**:11319-11329.

Zanelli U, Caradonna NP, Hallifax D, Turlizzi E, and Houston JB (2012) Comparison of cryopreserved HepaRG cells with cryopreserved human hepatocytes for prediction of clearance for 26 drugs. *Drug Metab Dispos* **40**:104-110.

Zhang J, Huang W, Chua SS, Wei P, and Moore DD (2002) Modulation of acetaminophen-induced hepatotoxicity by the xenobiotic receptor CAR. *Science* **298**:422-424.

Zimmerman HJ (1976) Various forms of chemically induced liver injury and their detection by diagnostic procedures. *Environ Health Perspect* **15**:3-12.

Zimmerman HJ (1999) *Hepatotoxicity: The Adverse Effects of Drugs and Other Chemicals on the Liver.* Lippincott Williams and Wilkons, Philadelphia.

M I C H E L L E W A H L I N

11528 SAND POINT WAY NE, SEATTLE, WA 98125 • (360) 333-1050 • MICHELLE.WAHLIN@LAKESIDESCHOOL.ORG

EDUCATION

University of Washington, Seattle, WA
Ph.D.; Department of Medicinal Chemistry, School of Pharmacy — August 2014
Cumulative GPA: 3.55

University of San Diego, San Diego, CA
BA in Chemistry (Biochemistry Emphasis), Marine Science Minor — May 2007
Cumulative GPA: 3.92; Honors Program; First Honors; Summa Cum Laude

PROFESSIONAL EXPERIENCE

Science Teacher, General Chemistry and Pharmacology — Aug 2012 – Present
Lakeside Upper School — Seattle, WA

- Developed a project-based chemistry curriculum, including units on baking powder, Gatorade, and hypoxia from climbing Mt. Everest. Used a guided inquiry approach to promote curiosity and wonder, "thinking like a scientist," and the skills needed to be a life-long scientist and learner.
- Cultivate student ownership, problem-solving skills, laboratory techniques, and confidence via semi-structured and open-ended activities, labs, and projects.
- Give students time and space to take risks, fail, learn from their mistakes, and ultimately succeed in gaining a deep, intuitive understanding of the material.
- Integrated alternative assessment forms into the curriculum including lab practicums, infographic design, concept mapping, and design prototypes.

Research Associate — Sept 2007 – Aug 2012
University of Washington, Department of Medicinal Chemistry — Seattle, WA

- Contributed to enhancement of drug safety profiles through analysis of the mechanisms of liver toxicity caused by pharmaceutical agents and their structural analogues.
- Adapted and improved established methods and techniques in chemical synthesis, cell culture, nuclear magnetic resonance (NMR) and liquid chromatography mass spectrometry (LCMS) to enable application to the project at hand.
- Managed and oversaw lab activities including supply ordering, health and safety compliance, radioactivity requirements, waste disposal, and chemical inventory records.

Teaching Assistant — Sept 2008 – Dec 2010
University of Washington, School of Pharmacy — Seattle, WA

- Planned and led weekly discussion sections for Biochemistry and Medicinal Chemistry courses; wrote problem sets; proctored and graded exams.

Research Assistant — Mar 2004 – Jan 2007
Scripps Institution of Oceanography — La Jolla, CA

- Used state-of-the-art equipment to identify new chemical entities and drug candidates from marine natural products.

Hollings Scholar-Intern — May, 2006 – Aug 2006
NOAA, Coastal Protection and Restoration Division — Seattle, WA

- Completed a screening level risk assessment of PCBs and helped prioritize the clean up of hazardous waste sites.

Chemistry Intern — May 2005 – Aug 2005
Seattle Genetics — Bothell, WA

- Assisted in analytical development and analysis of monoclonal antibody drug candidates using established procedures while adhering to strict quality assurance standards and protocols in a structured environment

PUBLICATIONS

Hardy KD, **Wahlin MD**, Papageorgiou I, Unadkat JD, Rettie AE, Nelson SD. (2014) "Studies on the Role of Metabolic Activation in Tyrosine Kinase Inhibitor-Dependent Hepatotoxicity: Induction of CYP3A4 Enhances the Cytotoxicity of Lapatinib in HepaRG Cells." *Drug Metabolism and Disposition.* **42(1):**162-71.

Takakusa H, **Wahlin MD**, Zhao C, Hanson KL, New LS, Chan EC, Nelson SD. (2011) "Metabolic-Intermediate Complex Formation of Human Cytochrome P450 3A4 by Lapatinib." *Drug Metabolism and Disposition.* **31(6)**:1022-1030.

Teng WC, Oh JW, New LS, **Wahlin MD**, Nelson SD, Ho HK, Chan, EC. (2010) "Mechanism-Based Inactivation of Cytochrome P450 3A4 by Lapatinib." *Molecular Pharmacology.* **78(4):**693-703.

Michelle D. Leibrand Wahlin (2009). 87 Year History of G.W.I.S. New York: Anchor.

Plesniak LA, Botsch K, **Leibrand M,** Kelly M, Sem D, Adams JA, Jennings P. (2008) "Transferred NOE and STD NMR studies of novobiocin binding to EnvZ suggest binding mode similar to DNA gyrase." *Chem Bio & Drug Design* **71**:28-35.

POSTERS AND PRESENTATIONS

Wahlin MD, Hardy KD, Liu J, Harbeson S, Uttamsingh V, Tung R, and Nelson SD. "Metabolic activation by CYP3A4 plays a critical role in lapatinib-induced hepatocellular injury." Poster presentation at Society of Toxicology Conference, San Francisco, CA. March 2012.

Wahlin MD, Takakusa H and Nelson SD. "The role of CYP3A4 and CYP3A5 in reactive metabolite formation from lapatinib." Poster Presentation at Gordon Research Conference - Drug Metabolism. Holderness, NH. July 2011.

Wahlin MD. Understanding and Improving the Safety Profile of Lapatinib. *Interdepartmental Seminar*, UW*,* May 2011.

Wahlin MD. Mechanisms of Drug-Induced Liver Injury by Ximelagatran and Lapatinib**.** *Interdepartmental Seminar*, UW*,* Jan 2010.

Wahlin MD. NAD(P)H:quinone oxidoreductase 1 (NQO1): Possible Roles in Cancer**.** *Interdepartmental Seminar*, UW*,* Jan 2009.

ACADEMIC AWARDS AND HONORS

Klingenstein Summer Institute Fellow: Columbia University Teacher's College fellowship recipient.
Elmer M. Plein Endowed Research Fund: UW School of Pharmacy award for research supplies and materials.
Eli Lilly & Company Graduate Fellowship: Award for a living stipend during graduate school.
NOAA/Hollings Scholar: National scholarship to promote the goals and aims of NOAA.
Kyle O'Connell Memorial Scholarship: USD scholarship for involvement in cancer research.
AWIS San Diego Scholarship: Undergraduate scholarship for aspiring women in science.
UT Southwestern Medical Center McKnight Prize Finalist: Chemistry Department poster session presenter.
USD Trustee Scholarship: Most distinguished University of San Diego merit-based scholarship.

ADDITIONAL ACTIVITES

A.W.I.S. (Association for Women in Science) Board Member: Organization dedicated to advancing the careers of women in science and technology and to promoting the participation of girls in the sciences (Sept 2011 – Present).

GEMS (Girls in Engineering, Math and Science) Co-Chair: Program designed to encourage middle school girls in the Seattle School District to maintain and broaden their interest in science by providing mentoring, hands-on activities, field trips, and information pertaining to a variety of scientific fields. Responsibilities include general coordination and planning as well as writing, modifying, and implementing curriculum (Oct 2009 – Present).

Faculty Staff Academy: Taught a two-day course to Lakeside faculty and staff on soap-making (March 2013).

Graduate Women in Science: Chosen to compile and publish the 85-year history of the national organization dedicated to improving conditions for women in scientific disciplines (see publications).

PROFESSIONAL DEVELOPMENT

- Klingenstein Summer Institute: two-week training program for new independent school teachers at Columbia University, Teacher's College. Received four graduate-level credits from Columbia University. (June 2014)
- Lakeside summer technology workshops on Haiku (advanced), web-based presentation tools, and finding and evaluating digital resources
- Summer curriculum grants on women in STEM, incorporating statistics into the chemistry curriculum, and utilizing infographics in teaching and assessment.
- Teaching Certificate Program in Pharmacy Education, University of Washington School of Pharmacy (Spring 2010)